Electronic Theses and Dissertations

2013

Optimization of PHEV Power Split Gear Ratio to Minimize Fuel Consumption and Operation Cost

Yanhe Li

Follow this and additional works at: http://scholar.uwindsor.ca/etd

Recommended Citation

Optimization of PHEV Power Split Gear Ratio to Minimize Fuel Consumption and Operation Cost

by

Yanhe Li

A Thesis

Submitted to the Faculty of Graduate Studies

through Electrical and Computer Engineering

in Partial Fulfillment of the Requirements for

the Degree of Master of Applied Science at the

University of Windsor

Windsor, Ontario, Canada

2012

Optimization of PHEV Power Split Gear Ratio to Minimize Fuel Consumption and Operation Cost

by

Yanhe Li

APPROVED BY:

_____
Dr. Nader Zamani
Department of Mechanical Automotive & Material Engineering

_____
Dr. Xiang Chen
Department of Electrical and Computer Engineering

_____
Dr. Narayan C. Kar, Advisor
Department of Electrical and Computer Engineering

_____
Dr. Jonathan Wu, Chair of Defense
Department of Electrical and Computer Engineering

DECLARATION OF ORIGINALITY

I hereby certify that I am the sole author of this thesis and that no part of this thesis has been published or submitted for publication.

I certify that, to the best of my knowledge, my thesis does not infringe upon anyone's copyright nor violate any proprietary rights and that any ideas, techniques, quotations, or any other material from the work of other people included in my thesis, published or otherwise, are fully acknowledged in accordance with the standard referencing practices. Furthermore, to the extent that I have included copyrighted material that surpasses the bounds of fair dealing within the meaning of the Canada Copyright Act, I certify that I have obtained a written permission from the copyright owner(s) to include such material(s) in my thesis and have included copies of such copyright clearances to my appendix.

I declare that this is a true copy of my thesis, including any final revisions, as approved by my thesis committee and the Graduate Studies office, and that this thesis has not been submitted for a higher degree to any other University or Institution.

ABSTRACT

A Plug-in Hybrid Electric Vehicle (PHEV) is a vehicle powered by a combination of an internal combustion engine and an electric motor with a battery pack. The battery pack can be charged by plugging the vehicle to the electric grid and from using excess engine power. The research activity performed in this thesis focused on the development of an innovative optimization approach of PHEV Power Split Device (PSD) gear ratio with the aim to minimize the vehicle operation costs.

Three research activity lines have been followed:

- Activity 1: The PHEV control strategy optimization by using the Dynamic Programming (DP) and the development of PHEV rule-based control strategy based on the DP results.
- Activity 2: The PHEV rule-based control strategy parameter optimization by using the Non-dominated Sorting Genetic Algorithm (NSGA-II).
- Activity 3: The comprehensive analysis of the single mode PHEV architecture to offer the innovative approach to optimize the PHEV PSD gear ratio.

DEDICATION TO MY WIFE AND MY DAUGHTER

ACKNOWLEDGEMENTS

TABLE OF CONTENTS

NOMENCLATURE

List of Abbreviation

AERO   All Electric Operation Range

AHS   Allison Hybrid System

CAA   Clean Air Act

CAFÉ   Corporate Average Fuel Economy

CARB   California Air Resources Board

CD   Charge-Depleting

CS   Charge-Sustaining

CVT   Continuously Variable Transmission

DP   Dynamic Programming

ECM   Equivalent Fuel Consumption Minimization

ECMS   Equivalent Consumption Minimization Strategy

EIA   Energy Information Administration

EPA   Environmental Protection Agency

EV   Electric Vehicles

EVT   Electric Variable Transmission

GA   Genetic Algorithm

HEV   Hybrid Electric Vehicles

HWFET   Highway Fuel Economy Drive Schedule

LPG	Liquefied Petroleum Gas
NSGA	Non-dominated Sorting Genetic Algorithm
PHEV	Plug-in Hybrid Electric Vehicles
PMP	Pontryagin's Minimum Principle
PSD	Power Split Device
RESS	Rechargeable Energy Storage System
SOC	State of Charge
SQP	Sequential Quadratic Programming
THS	Toyota Hybrid System
UDDS	Urban Dynamometer Drive Schedule
ULEVs	Ultra Low Emission Vehicles
VTB	Virtual Test Bed
ZEVs	Zero Emission Vehicles

List of Symbols

A_F	Frontal area of vehicle
C_D	Coefficient of aerodynamic drag
F	PSD internal foce
F_{ad}	Aerodynamic drag force

F_g	Local gravitation force
F_r	Rolling resistance force
$F_{t,}$,	Force required at the vehicle wheel
H_{lv}	Lower heating value of fuel
i	Gear ratio between sun gear and carrier
I_c	Inertia of carrier
$i_{distance}$	Crowding distance
I_e	Inertia of engine
I_g	Inertia of generator
I_m	Inertia of motor
I_r	Inertia of ring gear
i_{rank}	Nondomination rank
I_s	Inertia of sun gear
$\dot{I}_e$	Combined inertia of engine
$\dot{I}_m$	Combined inertia of motor
$\dot{I}_g$	Combined inertia of generator
m	Vehicle mass

$\dot{m}_f$	Engine fuel mass flow rate
$O()$	Computation burden
P_{batt}	Battery power output
P_{fuel}	Fuel consumption rate in MJ in MJ/time step
$P_{electric}$	Power through the battery in MJ/time step
P_{dem}	Demanded power
P_{MG}	MG power
P_t	Population
Q	Battery capacity
Q_t	Population after selection, crossover, and mutation
R_{int}	Internal resistance
R_t	Combined population
R_{tire}	Radius of tire
SOC_{max}	Lowest desired battery SOC
SOC_{min}	Highest desired battery SOC
T_{brake}	Torque of hydraulic brake
T_c	Torque of carrier
T_d	Demanded torque

T_e	Engine torque
T_{e_dr}	Torque from engine to driveline
T_{e_max}	Engine maximum torque
$T_{e\_min\_opt}$	Engine optimal lower torque
T_{e_opt}	Engine optimal torque
T_{e_start}	Engine start torque
$T_{e\text{-}off}$	Engine shut off torque
T_f	Torque of final driveline
T_{MG}	MG torque
$T_{m\text{-}hi}$	Maximum motor driving torque
$T_{m\text{-}lo}$	Maximum motor driven torque
T_r	Torque of ring gear
T_{req}	Toque required on the wheel
T_s	Torque of sun gear
T_{wheel}	Wheel torque
$\boldsymbol{u}$	Normal vector of plane *A*
$\boldsymbol{v}$	Normal vector of plane *B*
V_{OC}	Open circuit voltage

Z_c	Tooth number of carrier
Z_f,	Final gear ratio
Z_r	Tooth number of ring gear
Z_s	Tooth number of sun gear
α	Gradient of road
$\alpha_{e\_opt\_high}$	Desired engine highest torque coefficient
$\alpha_{e\_opt\_low}$	Desired engine lowest torque coefficient
α_{g_charge}	Desired generator charge torque coefficient
$\alpha_{m\_discharge}$	Desired motor discharge torque coefficient
α_{fuel}	Fuel convert energy consumption in MJ/time step
$\alpha_{electric}$	Electricity convert energy consumption in MJ/time step
β	Energy price ratio
ω_{e_lau}	Engine Lowest speed
ω_e	Engine speed
ω_{MG}	MG speed
ω_s	Speed of sun gear
ω_r	Speed of ring gear
ω_c	Speed of carrier

$\dot{\omega}_s$	Acceleration of sun gear
$\dot{\omega}_r$	Acceleration of ring gear
$\dot{\omega}_c$	Acceleration of carrier
ω_{e_lau}	Engine launch speed
η_1	Engine directly driving efficiency
η_2	Motor directly driving efficiency
η_e	Engine efficiency at specified torque and speed
η_{MG}	MG efficiency at specified torque and speed
η_{Grid}	Charging efficiency
$\theta(A,B)$	Angle between plane A and B
ρ	Air density
$\prec_n$	Crowded-comparison operator

LIST OF TABLES

LIST OF FIGURES

CHAPTER 1

INTRODUCTION

1.1 Motivation

The automobile has been making great contribution to our civilization since it was invented over a century ago. It has become the necessary choice of transportation in our daily life. In most countries, the automotive industry also has become one of the most important segments. However, automobiles also are bringing the serious energy and environmental problems to our communities due to the large amount of green-house gas emissions accompany with the huge energy consumption. In the five major fuel consuming sectors contributing to CO_2 emission from fossil fuel combustion, 33% is from the transportation sector in 2009 [1].

Because of the recognition of the influence of automotive to the environment, most of the countries enacted the stringent emission standards. The European Union introduced the emission Directive 2005/55/EC and its implementing Directive 2005/78/EC as amended by 2006/51/EC, 2008/74/EC and 2011/582/EC and applies to all trucks, lorries and buses sold in the EU market. This Directive lays down limit values for emissions of gaseous and particulate pollutants and for the opacity of exhaust fumes from diesel, natural gas and liquefied petroleum gas (LPG) engines, known as Euro IV, Euro V and Euro VI. Table 1.1 is the Euro VI – 2011/582/EC which is the latest EU directive engine emission enacted by European Union. The application date of Euro VI is December 31, 2012.

The US emission standards were set by the Environmental Protection Agency (EPA), which was formed in 1970 to develop and enforce regulations to protect the environment. These standards focus on limiting the production of harmful tailpipe pollutants. Table 1.2 lists the heavy duty highway compression-ignition engines & urban buses exhaust emission standards. The standards adopted after 2007 are more stringent levels on NMHC, NO_x, and PM compared with those between 2004 and 2006.

At the same time, because of decreasing global crude oil supplies, the price of crude oil, according to the US Energy Information Administration (EIA) (2011) [2], is over 500% higher than ten years ago (Figure 1.1) and is likely to continue to surge in the future

Table 1.1. Euro VI – 2011/582/EC Engine Emission Standard

	CO	HC	NMHC	H4	NO_x [1]	NH_3	PM Mass	PM Number [2]
	mg/kWh					ppm	mg/kWh	#/kWh
WHSC (C.I.)	1500	130			400	10	10	8×10^{11}
WHTC (C.I.)	4000	160			460	10	10	6×10^{11}
WHTC (P.I.)	4000		160	500	460	10	10	[3]

Note: 1) Admissible level of NO_2 may be defined later

2) Measurement procedure to be introduced by Dec. 31, 2012

3) Particle number limit shall be introduced by Dec. 31, 2012

C.I. - Compression Ignition; P.I. - Positive Ignition

WHTC - World Heavy Duty Transient Cycle

WHSC - World Heavy Duty Steady State Cycle

Table 1.2. Heavy Duty Highway Compression-Ignition Engines & Urban Buses - Exhaust Emission Standards

Year	HC	NMHC	NMHC+NO$_x$	NO$_x$	PM	CO	Idle CO	Smoke	Useful Life	Warranty Period
			(g/bhp-hr)				(% exhaust gas flow)	(%)	(hrs/yrs/miles)	(yrs/miles)
2004-2006		-	2.4 (or 2.5 with a limit of 0.5 on NMHC)	-	0.05	15.5	0.5	20/15/50	LHDDE: -/10/110,000 MHDDE: -/10/185,000 HHDDE: 22,000/10/ 435,000	LHDDE: 5/50,000 All other HDDE: 5/100,000
2007+	-	0.14	2.4 (or 2.5 with a limit of 0.5 on NMHC)	0.2	0.01	15.5	0.5	20/15/50		

Note: HHDDE - Heavy Heavy-Duty Diesel Engines

MHDDE - Medium Heavy-Duty Diesel Engines

LHDDE - Light Heavy-Duty Diesel Engines

because of shrinking oil supplies. Although Corporate Average Fuel Economy (CAFE) was enacted by the US Congress in 1975 and sets fuel economy standards for cars and light trucks (trucks, vans, and sport utility vehicles) sold in the US. The discussion of reduction of fuel consumption is significant in the past fifteen years regarding shrinking oil supplies and increasing oil demands. Future legislation is focused on reducing fuel consumption and greenhouse gas emissions starting in 2013 based on EPA program announcement. The program will include a range of targets which are specific to the diverse vehicle types and purposes. Vehicles are divided into three major categories: combination tractors (semi-trucks), heavy-duty pickup trucks and vans, and vocational vehicles (like transit buses and refuse trucks). Within each of those categories, even more specific targets are laid out based on the design and purpose of the vehicle. This flexible

structure allows serious but achievable fuel efficiency improvement goals charted for each year and for each vehicle category and type. By the 2018 model year, the program is expected to achieve significant savings relative to current levels, across vehicle types. Certain combination tractors – commonly known as big-rigs or semi-trucks – will be required to achieve up to approximately 20 percent reduction in fuel consumption and greenhouse gas emissions by model year 2018, saving up to 4 gallons of fuel for every 100 miles traveled. For heavy-duty pickup trucks and vans, separate standards are required for gasoline-powered and diesel trucks. These vehicles will be required to achieve up to approximately 15 percent reduction in fuel consumption and greenhouse gas emissions by model year 2018. Under the finalized standards a typical gasoline or diesel powered heavy-duty pickup truck or van could save one gallon of fuel for every 100 miles traveled. Vocational vehicles – including delivery trucks, buses, and garbage trucks – will be required to reduce fuel consumption and greenhouse gas emissions by approximately 10 percent by model year 2018. These trucks could save an average of one gallon of fuel for every 100 miles traveled.

So the studies on fuel-saving and emission-reduction have been popular in recent years. Most of the auto makers are looking the solutions from the Hybrid Electric Vehicles (HEV), Plug-in Hybrid Electric Vehicles (PHEV), or Electric Vehicles (EV).

World oil prices move together due to arbitrage

World crude oil prices

dollars per barrel (real 2010 dollars, monthly average)

Legend: — WTI — Brent — Mars — Tapis — Dubai
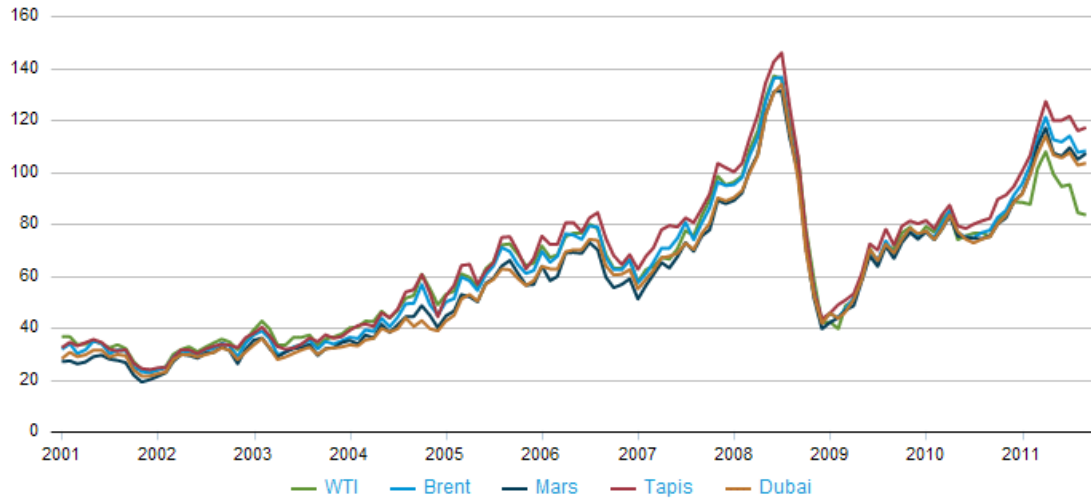
Sources: Bloomberg, Thomson Reuters. Published by: U.S. Energy Information Administration.
Updated: Monthly | Last Updated: 9/30/2011

Many types of crude oil are produced around the world. Variations in quality and location result in price differentials, but because oil markets are integrated globally, prices tend to move together.

Figure 1.1. World crude oil price have increased over 400% since 1998 (EIA, 2011)

Shortly after the US Congress adopted the 1990 Clean Air Act (CAA) Amendments, California state passed the "Low Emission Vehicle/Clean Fuel" program. California's emission limitation plan [3] was created by California Air Resources Board (CARB) and sets a more stringent emission standard for CO, NO_x, and formaldehyde. All the vehicles sold in California by a manufacturer in a given year must meet an overall "fleet average" emission requirement. The fleet average emissions requirement took effect in 1994 and declines each year until 2003. Fleet averaging allows automobile manufacturers flexibility to determine the volume and class of vehicle to manufacture and sell. The only mandatory vehicle requirement for fleet averaging is a sales quota for Zero Emission Vehicles (ZEVs). Two percent of all vehicles certified for sale in California must be

5

ZEVs in 1998, increasing to five percent in 2001 and to ten percent in 2003. Although the auto makers invested a large amount of the money to develop the ZEVs, the public did not show the enthusiasm to the pure battery powered vehicles. Honda announced to stop the manufacture the EV-plus after 2 years launch, and GMC also did not make the EV1 after 2000 because of the low market demands.

Because of the major barriers to the immediate introduction of the electric vehicle: insufficient battery capacity, lack of needed infrastructure, unresolved problems about the safety, consumer resistance, and significantly higher purchase prices than conventional automobiles, CARB revised the mandatory vehicle requirement for ZEVs and allowed 60% of the ZEVs can be replaced by the Ultra Low Emission Vehicles (ULEVs). Toyota successfully introduced its HEV car Prius on the Japanese, European, and US markets and proved that HEV is the new generation of the energy-saving vehicles and easy to be accepted by the customers. HEV sales in US is growing steadily (Figure 1.2) [4]. From 1999, the first HEV sold in US, to 2010, almost 2 millions HEV on US roads. Although there are still many unsolved challenges on the technologies and markets, the HEV, particularly PHEV seems to be the most promising short-term solutions to reduce the fuel consumption and emissions.

PHEVs with oversized batteries that can also be recharged using electric power from the grid, have recently become a hot topic in the automotive industrial because of the undoubted advantages in terms of emissions and fuel consumption deriving from the possibility to be driven for a relatively extended driving range using only electricity.
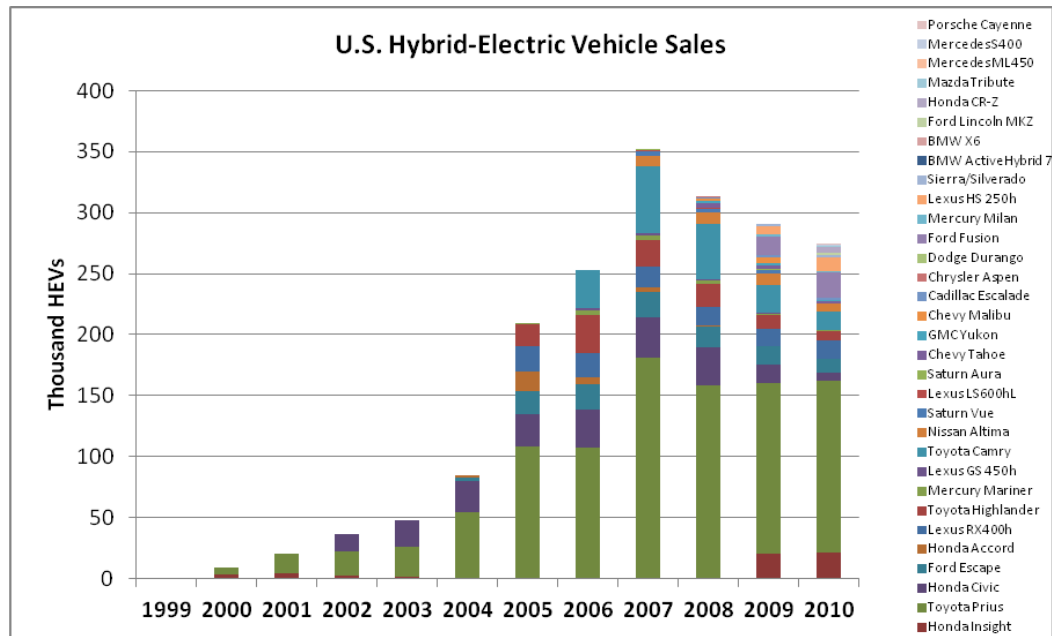
Figure 1.2. US HEV sales

General Motor (GM) introduced the first PHEV "Chevrolet Volt" in US market in 2011 although GM called it "Extended-range Electric Vehicle". However, PHEVs present some additional challenges for control and optimization, due to the necessity of accounting for the cost, energy depletion and pollution due to the use of electrical energy in place of the fuel.

1.2 HEV Technologies Introduction

Per SAE J1711, the definition of an HEV is "A road vehicle that can draw propulsion energy from both of the following sources of stored energy: 1) a consumable fuel and 2) a rechargeable energy storage system (RESS) that is recharged by an electric motor-generator system, an off-vehicle electric energy source, or both." The consumable fuel

that is covered in this study is limited to the gasoline. RESS that is covered in this study is the battery.

Comparing with the conventional vehicles, HEVs or PHEVs not only reduce the greenhouse gas emissions, but also have less fuel cost (Table 1.3) [5]. HEVs were categorized into serial and parallel HEV on the conventional concept. As the HEV development getting more and more attentions, various designs and technologies emerge and were applied to the production vehicles. The categorization and evaluation of HEV have been an important project to be studied to direct the HEV development and research [6-9]. Considering the HEV powertrain functions, architectures, and vehicle packages, the design of the HEV powertrain has a high level of degree of freedom. These designs can be categorized by their degrees of hybridization or their powertrain configurations.

Based on the degree of hybridization, the HEVs can be categorized full hybrid and mild hybrid. The hybridization always is determined into the ratio of the power of the propulsion motor to that of the engine. A full hybrid, sometimes also called a strong hybrid, is a vehicle that can run on just the engine, just the batteries, or a combination of both. The full HEV can be operated at different distinct regimes: electric mode, cruise mode, overdrive mode, battery charge mode, power boost mode, and negative split mode. Mild hybrids are essentially conventional vehicles with some degree of hybrid hardware, but with limited hybrid feature utilization. Typically they are a parallel system with start-stop only or possibly in combination with modest levels of engine assist or regenerative braking features. Unlike full hybrids, Mild hybrids generally cannot provide ICE-OFF

8

Table 1.3. Comparison of Emissions and Fuel Cost of X-vehicles

Emissions and Fuel Cost for a 100-Mile Trip		
Vehicle (compact sedans)	Greenhouse Gas Emissions (pounds of CO_2 equivalent)	Total Fuel Cost (U.S. Dollars)
Conventional	87 lb CO_2	$13.36
Hybrid Electric	57 lb CO_2	$8.78
Plug-in Hybrid Electric	62 lb CO_2	$7.10
All-Electric	54 lb CO_2	$3.74

all-electric propulsion. A plug-in hybrid electric vehicle is one of the full hybrids, able to run in electric-only mode, with larger batteries and the ability to recharge from the electric power grid. And can be parallel or series hybrid designs. They are also called gas-optional, or griddable hybrids. Their main benefit is that they can be gasoline-independent for daily commuting, but also have the extended range of a hybrid for long trips. Basically, the higher the hybridization the vehicle is, the more improvement of the fuel economy and emissions are. The hybridization of Honda Civic is 15.9% which is the mild hybrid. The hybridization of Toyota Prius is 62.3% which is the full hybrid.

Based on the powertrain system design, several kinds of hybrid electric vehicles have been conceived, usually distinguished by their architecture, which is related to the path that the power flow follows from the energy sources to the wheels. They are (see Figure 1.3): series hybrid, parallel hybrid, and power-split hybrid.

The series configuration is the simplest architecture in the hybrid electric vehicles. The engine directly drives the generator which transforms the mechanical power from engine

into the electric power and supplies the power to the power storage device through the inverter, or to the propulsion motor directly. The serial HEV is driven by the propulsion motor. The engine, as the auxiliary driving unit, extends the driving range of the vehicle. The motor power is supplied by either a power-storage device, or a generator, or the combination of both with a split ratio determined by the power management controller. Since the engine operation is independent of the vehicle speed and road condition, it is controlled to operate near its optimal condition most of the time. In addition, because the mechanical power transition path is eliminated, the energy loss due to the torque converter and the transmission is avoided. However, because of more processes to convert and transform, the energy from the engine to the wheels results in the lower efficiency. In addition, all of the serial elements, such as the engine, generator, and motor, need the extra stand-by powers to meet the vehicle dynamics requirements.

In a parallel configuration, the single electric motor and the engine are installed such that they can power the vehicle either individually or together. The engine mainly supplies the power to drive the vehicle. Meanwhile the motor works as the auxiliary power unit. The role of the motor is to assist the engine to operate efficiently and to capture regenerative braking energy. Comparing with the series HEV, the engine is larger and more powerful, while the motor is smaller and less powerful. The main advantage of the parallel hybrid vehicle is the relatively high efficiency. The engine power is directly transferred to the wheels and therefore no power conversion is needed. The main disadvantage of the parallel hybrid vehicle is the engine speed is directly coupled to the vehicle speed and road condition and therefore the engine can not be operated in the most economic point continuously.
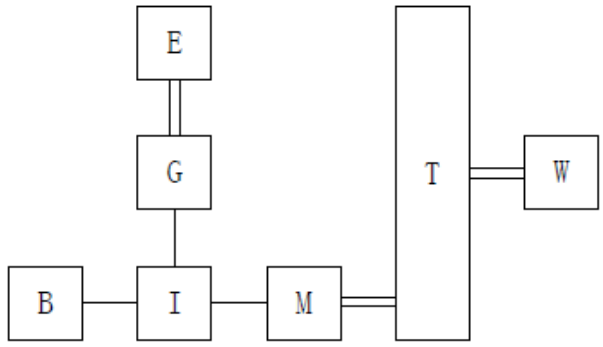
a) Series Hybrid

B: Battery

E: Engine

G: Generator

I: Inverter

M: Motor

T: Transmission

W: Wheel

-:   Electric Link

=:   Mechanical Link
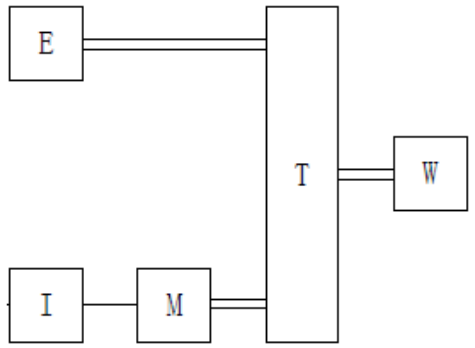
b) Parallel hybrid
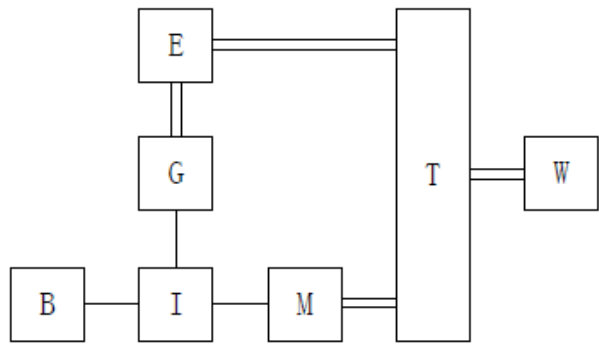
c) Power-split hybrid

Figure 1.3. HEV configurations

11

The power-split configuration (also called series-parallel HEV) combines the parallel and series powertrains. The power from the engine is split. One part of the power is transferred to the wheels through a mechanical path. The other part flows to the wheels via the electric path, which consists of the generator and the electric motor. A power split device (PSD), which is a planetary gear set, connects the engine, motor, and generator to work as a continuously variable transmission (CVT) and provides the advantage of adjusting the engine in the economic operation range. The generator is used to control the engine speed, the motor controls the engine torque. The generator is also used to convert excessive engine power to electric power that can be stored in the battery. The motor is operated for the power supply and for the recovery of energy during braking. Since only a small part of the engine power flows through the electric path, most of the power will be directly transferred to the wheels via a mechanical connection. This mechanical connection has a high efficiency. Therefore, the efficiency of the power-split configuration is high compared to the series.

1.3 Power Split Device Architecture Introduction

The earliest development of the power split mechanisms can be tracked back to 1969 [10]. But this power-split concept was not applied to passenger vehicles until the late 1990s. The first production power-split passenger vehicle is the Toyota Hybrid System (THS) [11] (Figure 1.4) which is known as the single mode PSD system. THS is vastly applied on the Toyota HEVs, such as Prius, and becomes the front-runner on the market. The advantage of the THS PSD is its relative simplicity and its increased performance over competing hybrid designs. However, the performance and fuel economy at high speeds and on steep grades is not outstanding due to the undersized engine and low efficiency at

12

high speed. This is common to many vehicle types, because actual driving conditions are different than the idealized conditions in the laboratory testing, such as faster accelerations and higher top speeds.

Another major design for power-split HEV on the market is the Allison Hybrid System (AHSII) (Figure 1.5) [12] which is invented by GM as a dual-mode PSD system in 2003. The main difference between single mode and dual mode PSD is the addition of clutches and/or brakes to create different transmission configurations. This increases the number of possible power flow paths through the transmission. The clutches are engaged and disengaged based on the system information such as the engine/motor efficiency maps, battery *SOC*, road load and driver demand to determine the operation mode. The dual-mode PSD system provides more efficient performance over a wider range of vehicle loads than that achieved by the single-mode design. However, the additional mechanical components will certainly increase both capital and maintenance costs.

Many other power split designs are developed by different companies. Bosch developed a power split transmission with circulating power for the hybrid electric vehicles [13] in 2004. GETRAG tested their democar with axle-split and torque-split hybrid transmissions to reduce the fuel consumption 24% and 35% respectively [14]. Ford Motor Company installed the power split transmission in Ford Escape Hybrid and brought to the market in 2004. Renault also developed a dual mode power split transmission [15].
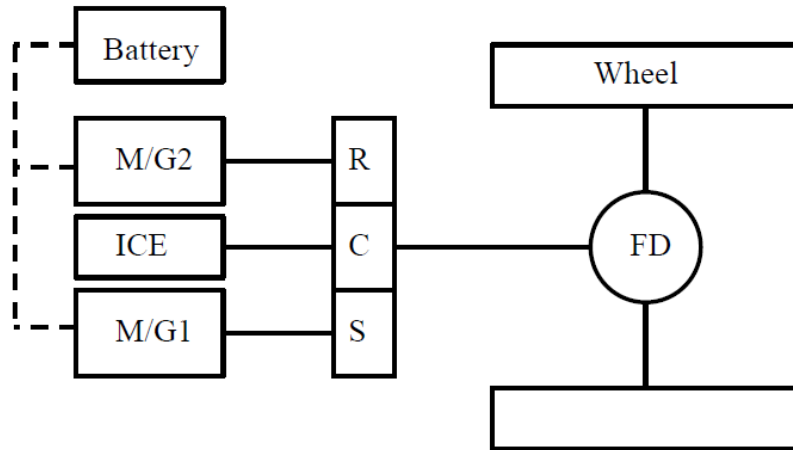
Figure 1.4. Single mode PSD system (Source: adapted from [13])
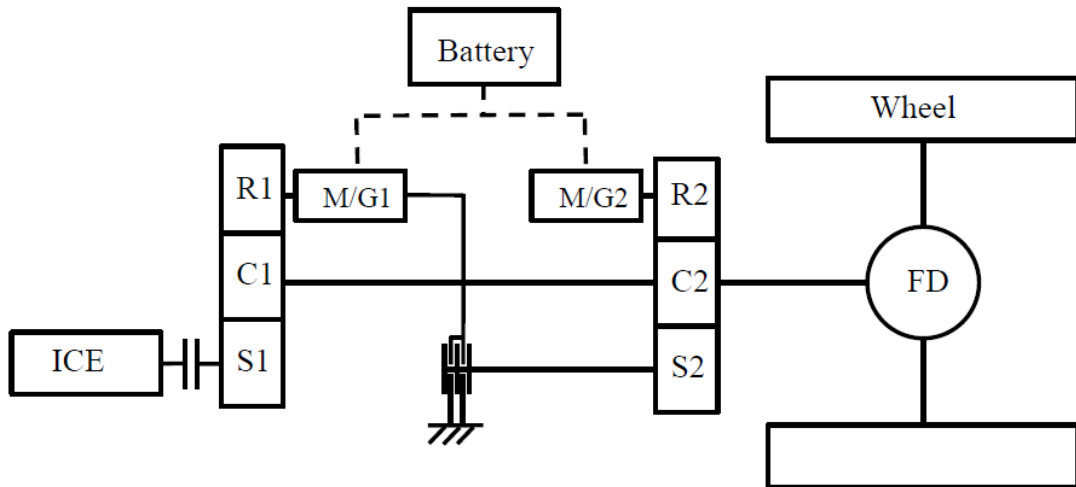
Figure 1.5. Dual mode PSD system (Source: adapted from [13])

1.4 Literature Review

1.4.1 Modeling power-split system

The proper modeling and simulation tools can shorten the vehicle development timing, reduce the development cost, validate the HEV control strategy, evaluate the vehicle performance, etc. in the early design and analysis stage. A considerable amount of work has

been done in the power split system modeling and simulation. A dynamic model (Zhang *et al.*) was created to evaluate an electric variable transmission (EVT) developed by Allison Transmission Division of General Motors [16]. The model is based on Kane's equations, and the concept of generalized velocity is used. The EVT performance was simulated by using the model. A mathematical model [17] of a vehicle with a power-split device based on the steady-state performance was presented by the researchers from Michigan Technological University (Rizoulis *et al.*). A math-based universal model [18] that presents different designs of power-split powertrains was created (Liu). This universal model presents the powertrain dynamics regardless of the various connections of engine-to-gear, motor-to-gear, and clutch-to-gear. A dynamic model (Zanasi *et al.*) of a planetary gear with internal elasticity [19] was presented. The model of the whole vehicle is given using the Power-Oriented Graphs approach. A dynamic model [20] of a multi-regime hybrid vehicle powertrain architecture (Wishart *et al.*) was presented to focus on the formulae governing the operation of the planetary gear systems in the powertrain and on the performance of a more complex heavy-duty vehicle with varying loading conditions.

1.4.2 Energy management optimization of power-split HEVs

The research of the energy management optimizations has been done on the different configuration of HEVs design. The global optimization and the local optimization of the HEV energy management are two major research directions. The typical represents of the global optimization are the Dynamic Programming (DP) [21]-[25] and Pontryagin's Minimum Principle (PMP) [26]-[29]. The typical example of the local optimization is Equivalent Fuel Consumption Minimization (ECM) [30]-[34]. Many papers about the power

split HEVs energy management optimization have been published. Banvait *et al*. [35] studied the energy control strategy of the plug-in hybrid electric vehicle with PSD using particle swarm optimization. Liu [36], [37] presented a stochastic dynamic programming method and the equivalent consumption minimization strategy to optimize the single mode power split HEV. Both approaches determine the engine power based on the overall vehicle efficiency and apply the electrical machines to optimize the engine operation. The performance of these two algorithms is assessed by comparing against the simulation results. Bole [23] also presented a dynamic programming method and the equivalent consumption minimization strategy to optimize the dual mode power split HEV. The optimization results of dynamic programming and equivalent consumption minimization compared with the developed rule-based control strategy simulation results. Moura [24] presented a dynamic programming method with consideration of trade-off of the fuel and electricity of usage and the fuel-to-electricity pricing to optimize the single mode PHEV energy management.

1.4.3 Control strategy of power-split HEVs

The supervisory control system represents the vehicle level controller that coordinates the sub-systems to satisfy certain performance targets. Control Strategy is the algorithm to make the controller to achieve the vehicle energy management and control the power systems. It is the vehicle "brain" and is the ultimate factor to determine the success or failure of a HEV development. So far, most of the research on the HEV control strategy is still on the computer simulation stage, particularly for the instantaneous optimal control strategy and the global optimal control strategy. It is difficult for them to be applied on the commercial

vehicles because of the heavy burden computation and very expensive high performance CPU. Although some vehicle OEMs, such as Toyota, GMC, Honda, are selling the HEVs with developed control strategies, those control strategies are companies' core technical secrets and can not be published.

Most of the early HEV control strategies are the speed – based control algorithms [38], [39] because it is simple and easy to be understood. The vehicle speed is the critical parameter in the control strategy. When the vehicle speed is lower then the threshold setup, the engine will be turned off. When the vehicle speed is higher then the threshold setup, the engine will be started. However, the disadvantage of the speed-based control strategy is that when the vehicle is driven at the high speed cruise, the engine may operate at the low efficiency zone.

The current control strategy is the torque-based control algorithm. The torque-based control strategy reasonably distributes the torque required by vehicle wheel between the engine, motor and generator to minimize the vehicle fuel consumption and emissions. The objective of the control strategy is to improve the vehicle fuel economy and reduce the emissions, so the rules to develop the control strategy are as follows:

- Control the engine to be operated at high efficiency zone.

- Keep the motor to be operated at high efficiency zone.

- Maintain the battery *SOC* to be within the specific range.

The current presented torque-base HEV control strategies include:

- Rule-based control strategy by adjusting the engine operation zone.

- Instantaneous optimal control strategy by real time calculating to determine the engine and motor/generator optimal operation points.

- Global optimal control strategy by applying the optimal control theory.

- Fuzzy logic or neural network intelligent control system.

Despite the early efforts, to my knowledge, the effects of the power-split planetary gear ratios to the vehicle fuel consumptions and operation costs do not yet exist in the literature. It is important and significant to optimize the PSD gear ratio to minimize the vehicle fuel consumptions and operation costs.

1.5 Contribution

This thesis focuses on the process of the single mode power-split PHEV (Figure 1.6) modeling, energy management optimization, ruled-based control strategy development,
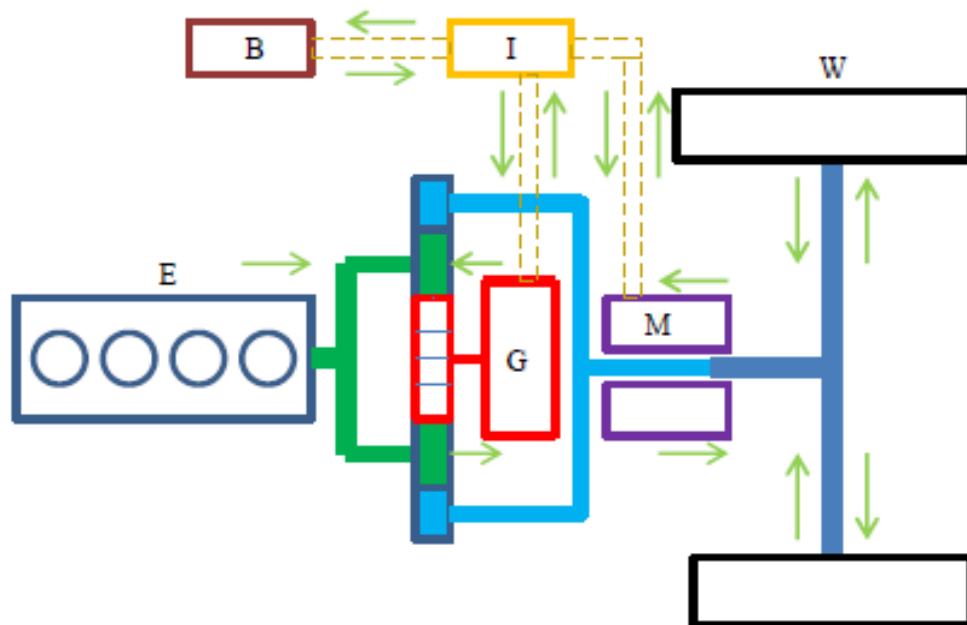
Figure 1.6. PHEV configuration and energy flow. (E– engine, G – generator, M – motor, W – wheel, I – Inverter, B - Battery).

and investigation of the effects of PSD gear ratios to the PHEV fuel consumptions and operation costs. A dynamic power-split PHEV simulation model is derived. By using this model, an optimal solution for the power-split PHEV with its benchmark performance is provided through the dynamic programming. The rule-based control strategy is then developed and the control strategy parameters are optimized by using the genetic algorithm. The effects of PSD gear ratios to the PHEV fuel consumptions and operation costs at the different driving cycles are finally discussed in this thesis. The main contributions of the thesis include the following:

- A backward-looking dynamic model of the power-split PHEV powertrain systems is created. The engine, power-split device, motor/generator, battery, and vehicle dynamics are integrated to perform a simulation. This simulation tool can be used to analyze the interaction between sub-systems and evaluate vehicle performance using measures such as fuel economy and operation costs.

- An optimal control design procedure based on dynamic programming (DP) is adopted in the power-split HEV fuel efficiency optimization study. DP is employed to find the optimal operation of the power-split system and achieve the benchmarks. The results are then applied to develop the real time control strategy designs.

- A rule-based control strategy based on the DP optimal results is developed. The comparisons between the rule-based control strategy and optimal benchmarks are discussed at different driving cycles. The developed rule-based control strategy is then applied to investigate the PSD gear ratios to PHEV fuel consumptions and operation costs at the different driving cycles.

19

- The rule-based control strategy parameters of the power-split PHEV are optimized by using non-dominated sorting genetic algorithm (NSGA-II). NSGA-II is employed to find the optimal control strategy parameters to minimize the vehicle fuel consumptions and operation costs. The results provide the engineers the fast and economic vehicle control strategy tunings.

- An innovative six-step approach to design the power split PHEV planetary gear ratio to minimize the fuel consumption and operation cost is presented.

1.6 Outline of the Thesis

The organization of this thesis is as follows. After the introduction in Chapter 1, the development of an integrated model for power-split plug-in hybrid electric vehicles is presented in Chapter 2. The optimal control by using dynamic programming is presented in Chapter 3. Chapter 4 presents the development of the rule-based control strategy for PHEV. Chapter 5 presents the optimization of rule-based control strategy parameters by using genetic algorithm NSGA-II. An innovative design approach to optimize the PSD gear ratio to minimize the vehicle fuel consumption and operation cost is developed in Chapter 6. Finally, a summary of this thesis and suggested future work are presented in Chapter 7.

CHAPTER 2

MODELING PHEV SYSTEMS

2.1 Introduction

Based on the level of details of the each modeled component, the vehicle model may be steady-state, quasi-steady, or dynamic. For example, the ADVISOR [40], [41] model can be categorized as a steady-state model, the PSAT [42] model as quasi-steady one, and PSIM [43] and Virtual Test Bed (VTB) [44] models as dynamic. On the other hand, based on the direction of calculation, vehicle models can be classified as forward-looking models or backward facing models [40] (See Figure 2.1 and Figure 2.2). In a forward-looking model, vehicle speed is controlled to follow a driving cycle during the analysis of fuel economy, thus facilitating the controller development.
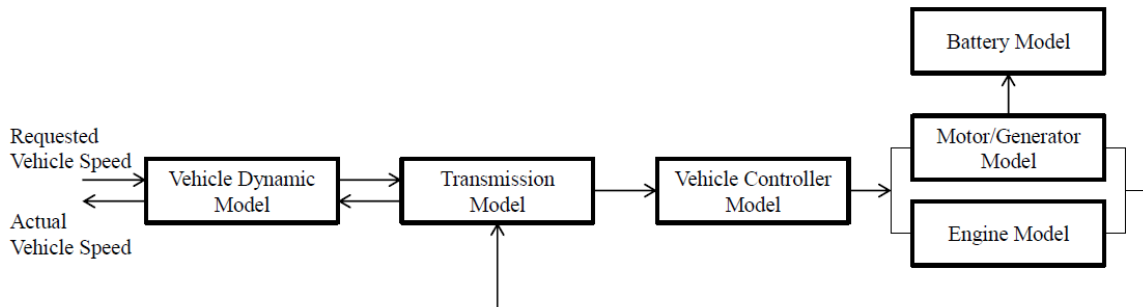
Figure 2.1. Flow diagram of the backward-looking model
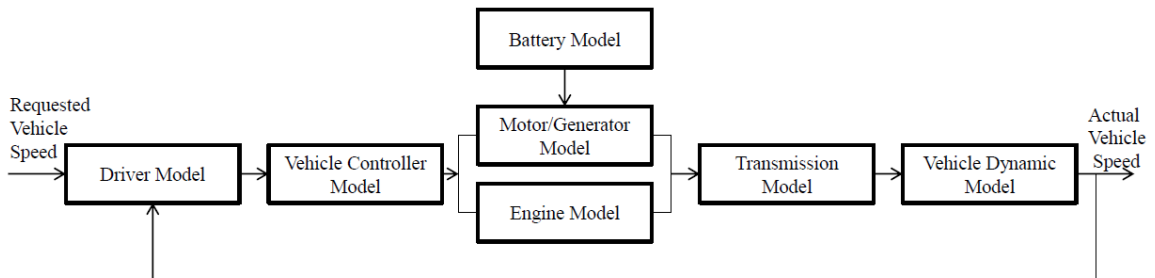
Figure 2.2. Flow diagram of the forward-looking model

When using backward-looking models, the control logic does not have to be considered complicated system constraints because the models calculate the exact torque or speed that a system requires and allow the controller to have only feasible control options. In contrast, in forward-looking models, the controller considers constraints and component losses and instantaneously makes decisions for the entire system. Therefore, the controller needs to collect the information required from the components and produces a control signal according to time-forward strategies. In this chapter, a backward-looking simulation model is developed for the power-split plug-in hybrid vehicles. The simulation model is implemented in the Matlab environment.

2.2 Engine Model

Figure 2.3 is the diagram of the inputs and outputs of the engine model. The inputs include the engine output torque and speed, and the outputs required are engine operation efficiency, fuel consumption rate, emissions, operation fuel cost. The inputs and outputs of the engine model are just considered during analysis the PHEV energy management. The theoretical engine model is not superior to the experimental engine model because of the accuracy caused by the many assumptions and the expensive computer operation cost. So the experimental engine model always used to simulate the HEV powertrain system.
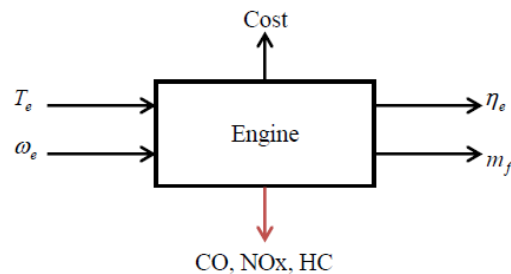
Figure 2.3. Inputs and outputs of the engine model

In order to support the computation over long driving cycles, a look-up table is used that provides torque as a function of engine speed and mass of fuel injected per cycle. The engine dynamics are ignored. The assumption is made that the working condition is at constant average level. The fuel consumption is evaluated by (2.1):

$$m_f = \int_0^t \dot{m}_f \, dt = \int_0^t f(T_e, \omega_e) \, dt = \sum_{t=0}^t \frac{T_e \omega_e}{\eta_e H_{lv}} \tag{2.1}$$

The fuel consumption map, in *g,* of the engine as function of the engine speed and engine torque is shown in Figure 2.4.

2.3 Motor/Generator Model

Figure 2.5 is the diagram of the inputs and outputs of the motor/generator model. The input is the motor/generator output speed. The model outputs include the motor/generator output torque, power, efficiency and electricity operation cost.
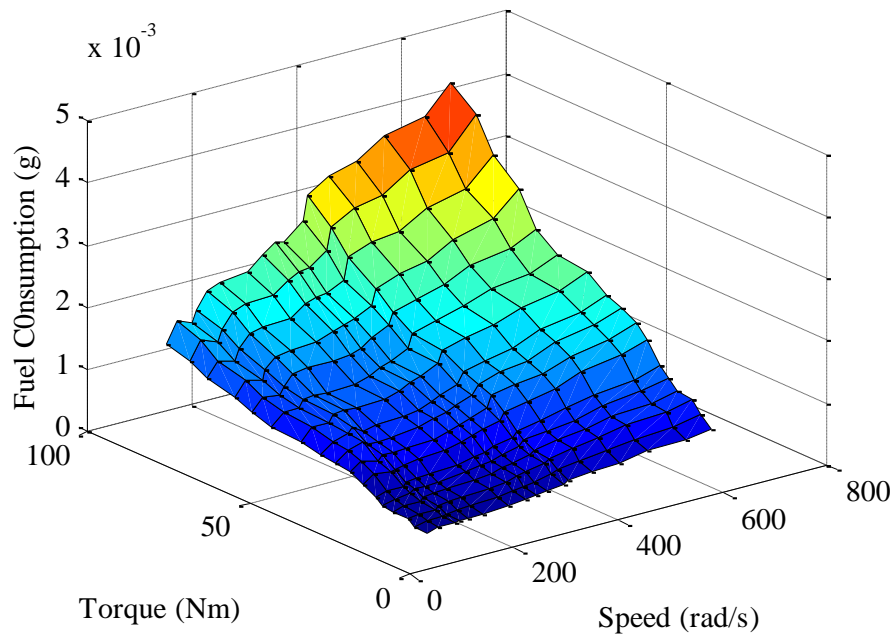
Figure 2.4. Engine fuel consumption map
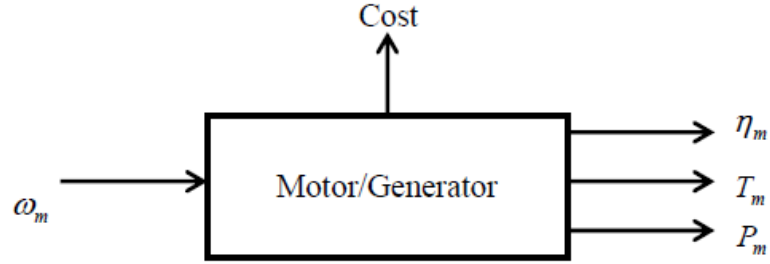
Figure 2.5. Inputs and outputs of the Motor/Generator model

Same as the engine model, the inputs and outputs of the motor/generator model are just considered during analysis the PHEV energy management. The look-up tables provide efficiency of the motor/generator as a function of the torque and speed. The motor/generator is the function of torque and speed, $\eta=f(T, \omega)$. When motor/generator consumes the energy, which means the power flows from battery to the motor/generator, the consumed power is represented by (2.2).

$$P_{MG} = {T_{MG}\, \omega_{MG}} \Big/ {\eta_{MG}} \qquad (2.2)$$

When the motor/generator generates electrical energy, which means the power flows from motor/generator to the battery pack, the generated power is represented by:

$$P_{MG} = T_{MG}\, \omega_{MG}\, \eta_{MG} \qquad (2.3)$$

Equations (2.2) and (2.3) will be used for the battery State-of-Charge (*SOC*) calculation. Figure 2.6 and Figure 2.7 are the efficiency maps for the Toyota Prius motor and generator which are at 15 kW and 35 kW respectively.
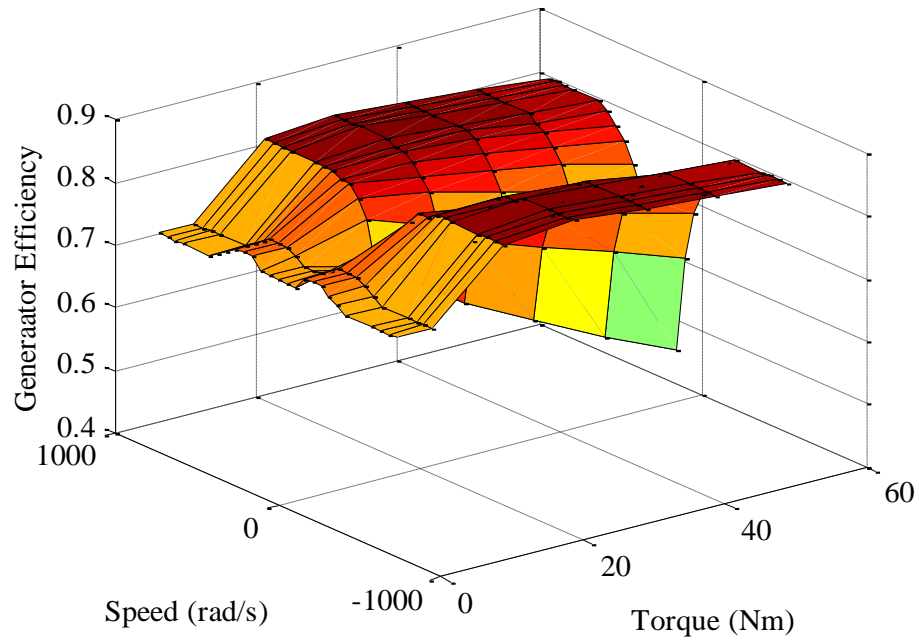
Figure 2.6. Generator efficiency map
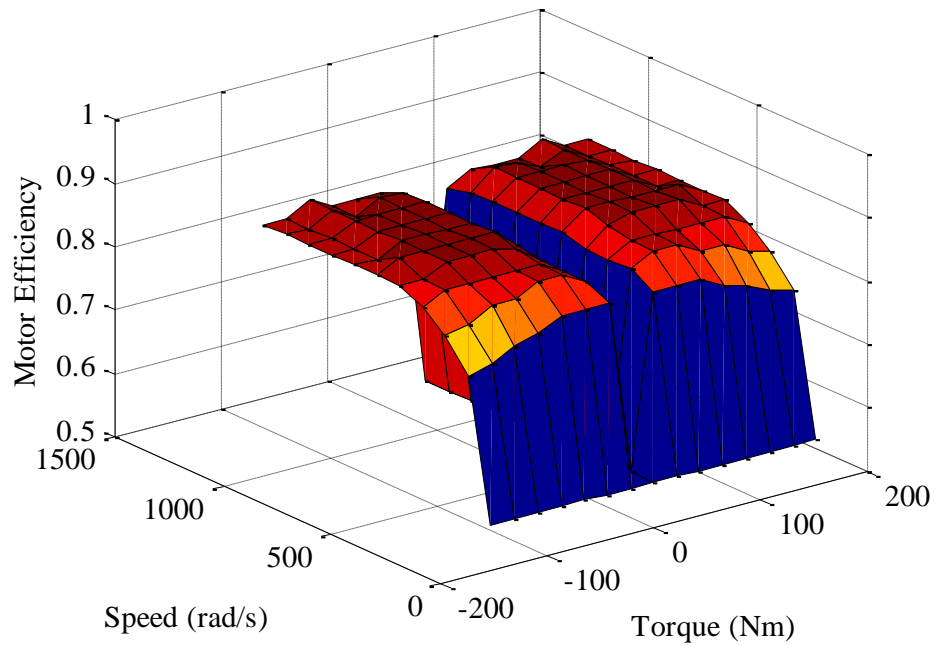
Figure 2.7. Electric motor efficiency map

2.4 Battery Model

Figure 2.8 is the relationship of the input and output of the battery model. The inputs include the battery capacity Q, internal resistance R_{int} , open circuit voltage V_{OC}, and battery power output P_{batt}. The output is the battery SOC. The battery model is represented by an equivalent circuit with an internal resistance, as shown in Figure 2.9. The battery R_{int} is the function of the SOC and the current direction I_{batt} (Figure 2.10):

$$R_{int} = f(SOC, I_{batt})$$
(2.4)

The battery SOC is the function of the V_{OC} (Figure 2.11):

$$SOC = f(V_{OC})$$
(2.5)

Both functions are obtained through the curve fitting based on the battery test results.
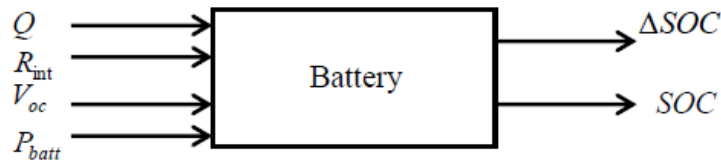
Figure 2.8. Inputs and outputs of the battery model
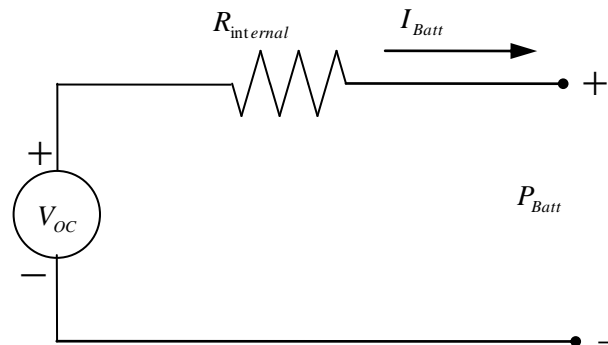
Figure 2.9. Battery electrical equivalent circuit
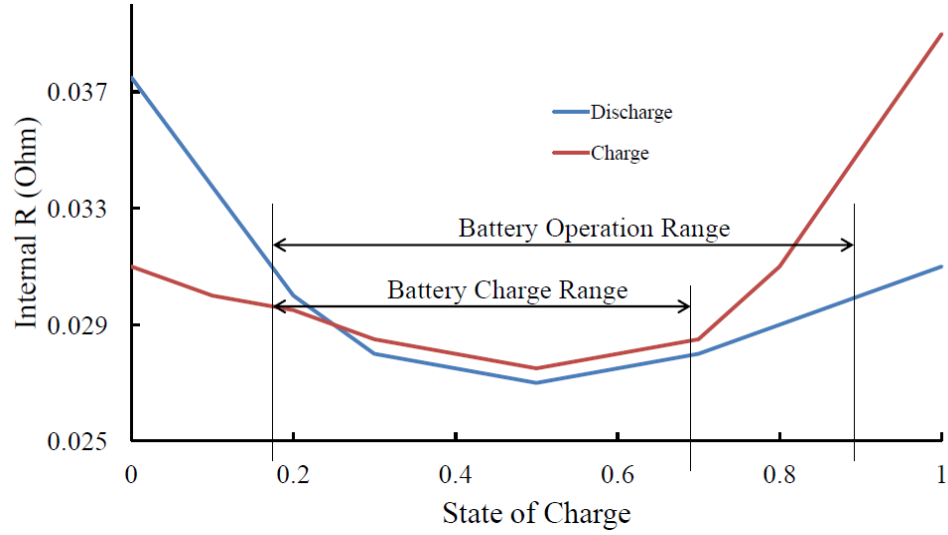
Figure 2.10 Battery internal resistance map with *SOC*
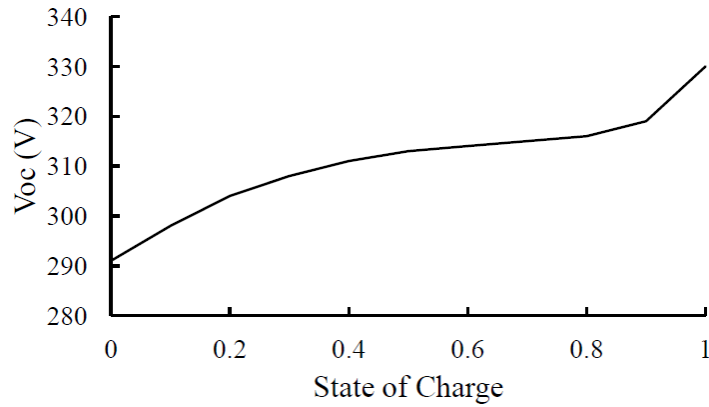
Figure 2.11. Battery open circuit voltage map with *SOC*

The battery pack dynamics are associated with *SOC*, and *SOC* depends on the equivalent battery capacity Q and the current flowing through the battery I_{Batt}:

$$S\dot{O}C = -I_{Batt} \big/ Q \tag{2.6}$$

The battery output power is a function of V_{OC}, I_{Batt}, and R_{int}:

$$P_{batt} = V_{OC} I_{Batt} - I_{Batt}^2 R_{int} \tag{2.7}$$

This expression may be written in terms of *SOC* and solved to obtain the equation for *SOC*:

$$S\dot{O}C = -\frac{V_{OC} - \sqrt{V_{OC}^2 - 4P_{Batt}R_{int}}}{2QR_{int}}$$

(2.8)

The power required from the battery will be:

$$P_{Batt} = \sum T_{MG}\omega_{MG}\eta_{MG}^k\eta_C^k$$

(2.9)

Where, $k=1$ when power flows to the battery and $k=-1$ when power flows away from the battery.

2.5 PSD Model

The planetary gear set is the core of the power split transmission as shown in Figure 2.12. The planetary gear set consists of a ring gear, a sun gear, a carrier, and pinion gears where the engine is connected to the carrier, the generator to the sun gear, and the motor to the ring gear and final driveline. The basic gear ratio of the planetary gear set follows:

$$\frac{\omega_s - \omega_c}{\omega_r - \omega_c} = -\frac{R_r}{R_s} = -k$$

(2.10)
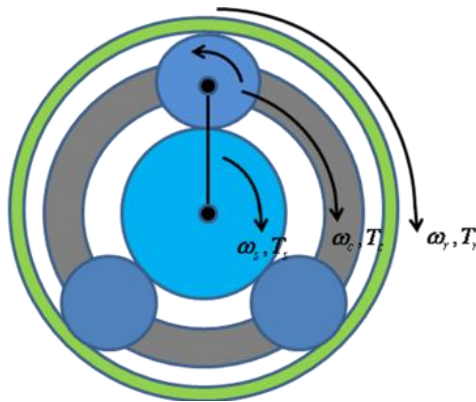
Figure 2.12. PHEV planetary gear set

28

The relationships between the torques are:

$$T_s = \frac{k}{k+1}T_c \tag{2.11}$$

$$T_f = T_r + \frac{T_c}{1+k} \tag{2.12}$$

Figure 2.13 shows the free body diagram of planetary gear set. The relationships between

the torques are:

$$\left.\begin{array}{l} I_r\dot{\omega}_r = FZ_r - T_r \\ I_c\dot{\omega}_c = T_c - F(Z_s + Z_r) \\ I_s\dot{\omega}_s = FZ_s - T_s \end{array}\right\} \tag{2.13}$$

2.6 Powertrain Dynamic Model

Figure 2.14 shows the free body diagram of the powertrain. The torques determine the

rotational speeds in the transmission. The powertrain dynamic equations are following:

$$\left.\begin{array}{l} I_e\dot{\omega}_e = T_e - T_c \\ I_g\dot{\omega}_g = T_g - T_s \\ (I_m + I_r)\dot{\omega}_r Z_f = (T_r + T_m)Z_f - T_d \end{array}\right\} \tag{2.14}$$

Combining equations (2.10)–(2.14), and only considering the vehicle dynamics along the

longitidinal direction which is the dominating factor for the fuel economic, the

powertrain dyamic model can be derived:

$$\begin{bmatrix} I_e + I_c & 0 & 0 & R_r + R_s \\ 0 & I_m + 2I_r & 0 & -R_r \\ 0 & 0 & I_g + I_s & -R_s \\ R_r + R_s & R_r & R_s & 0 \end{bmatrix} \begin{bmatrix} \dot{\omega}_e \\ \dot{\omega}_r \\ \dot{\omega}_s \\ F \end{bmatrix} = \begin{bmatrix} T_e \\ T_m - \dfrac{T_d}{Z_f} \\ T_g \\ 0 \end{bmatrix} \tag{2.15}$$

Where:

$$T_d = F_t R_{tire} \tag{2.16}$$
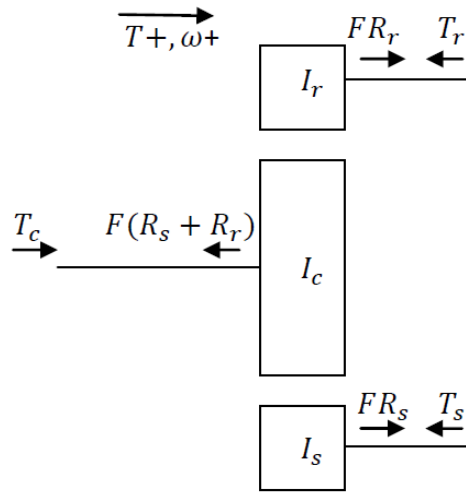
Figure 2.13. Free body diagram of planetary gear set
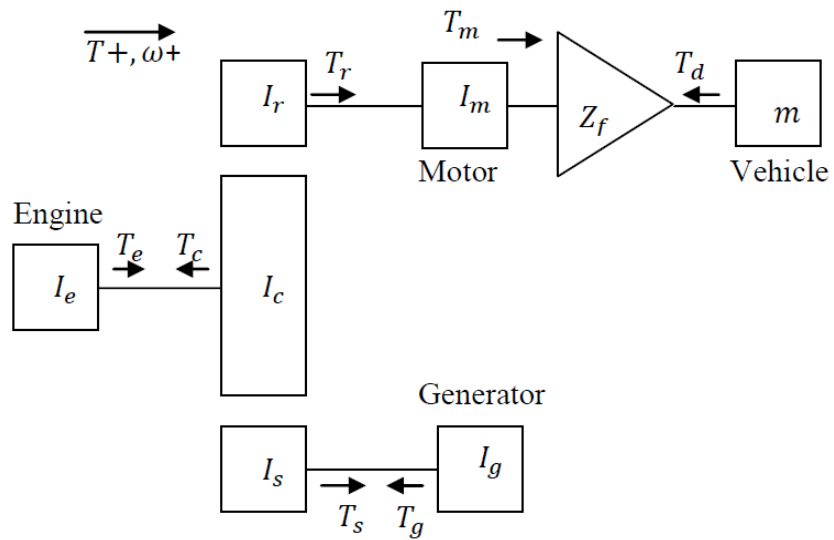
Figure 2.14. Free body diagram of powertrain

2.7 Vehicle Model
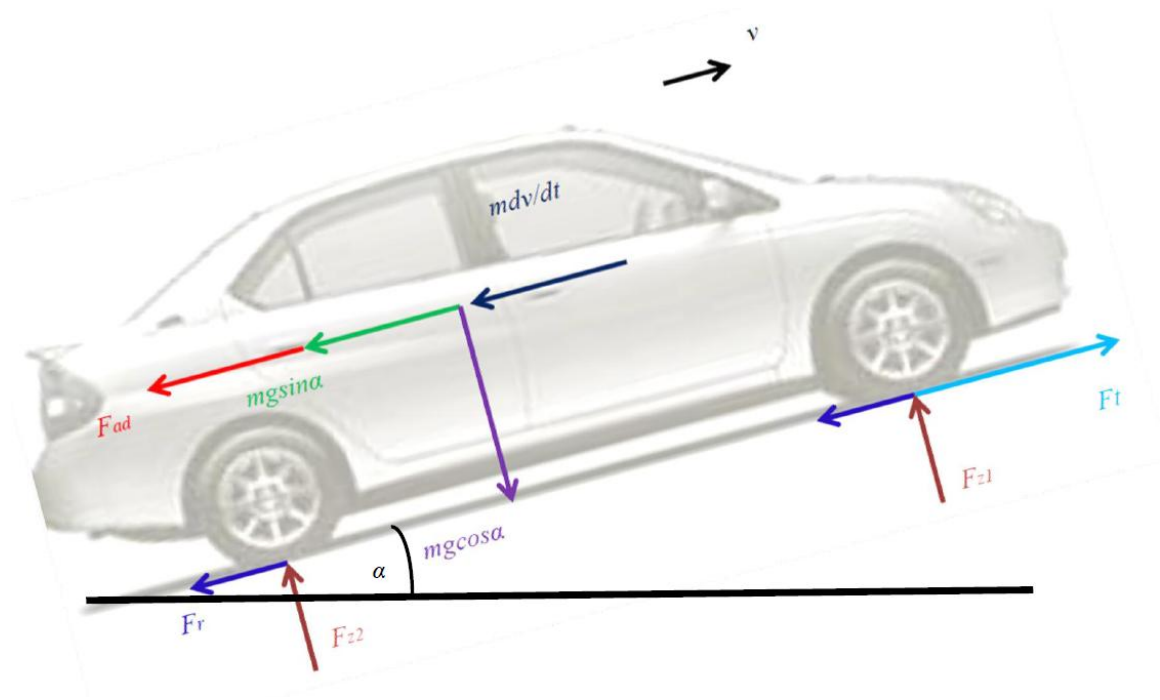
Figure 2.15. Vehicle free body diagram

The propulsion system produces mechanical energy that is stored in the vehicle. The amount of mechanical energy consumed while driving the vehicle depends on the following effects:

- The aerodynamic friction losses
- The uphill driving losses
- The rolling friction losses

The vehicle model is derived from the basic equation of solid-body motions (Figure 2.15):

$$m\frac{dv}{dt} = F_t - F_{ad} - F_g - F_r \qquad (2.17)$$

$$F_{ad} = 0.5\rho C_D A_F V^2 \qquad (2.18)$$

$$F_g = mg \sin \alpha \tag{2.19}$$

$$F_r = f_r mg \cos \alpha \tag{2.20}$$

2.8 Summary

The backward-looking model of PHEV was created in this chapter under Matlab environment. It provided the necessary platform to simulate the PHEV fuel consumption and study the control strategy. The main study in this chapter focused on following:

1. The look-up table based PHEV engine, motor/generator, and battery models were created. Those models represent the static state of the systems. However, the simulations will focus on the PHEV energy consumptions, so the model accuracy is enough.

2. The dynamic PSD and powertrain system models were created based on the system loads balances.

3. The vehicle model was created by applying the vehicle longitudinal dynamics.

CHAPTER 3

OPTIMAL CONTROL OF PHEV

3.1 Introduction

The optimal energy management of HEV is a global optimization problem whose objective is to determine the power split between the engine and the motor to minimize the vehicle fuel consumption and operation cost. Comparing with other optimal approaches, such as Pontryagin's Minimum Principle (PMP) [45], [46], the Equivalent Consumption Minimization Strategy (ECMS) [35], [46], the DP approach guarantees the global optimal results and the results are unbeatable under the given driving cycles. In this study, the DP approach was used to optimize the PHEV control strategy to minimize the fuel consumption and operation cost.

3.2 Mathematic Model of Optimal Control

Figure 1.4 shows the PHEV configuration in this study. From the Figure 2.12 and equation (2.14) and (2.15), the relationship of the torque on the wheels with the engine torque and motor/generator torque can be derived:

$$
\left[\frac{I_m(Z_r+Z_s)^2}{Z_r\dot{I}_e i_f} + \frac{I_m Z_s^2}{Z_r \dot{I}_g i_f} + Z_r\right]\dot{\omega}_r = \left[\frac{(Z_r+Z_s)^2}{Z_r\dot{I}_e} + \frac{Z_s^2}{Z_r\dot{I}_g}\right]T_m
$$
$$
+ \frac{(Z_r+Z_s)}{\dot{I}_e}T_e + \frac{Z_s}{\dot{I}_g}T_g - \left[\frac{(Z_r+Z_s)^2}{Z_r\dot{I}_e i_f} + \frac{Z_s^2}{Z_r\dot{I}_g i_f}\right]\frac{T_d}{\eta_f}
$$

(3.1)

The same routine to derive the relation of the engine speed and the engine torque:

$$\left[\frac{I_e Z_r^2 Z_f}{(Z_r + Z_s)\dot{I}_m} + \frac{I_e Z_s^2}{(Z_r + Z_s)\dot{I}_g} + (Z_r + Z_s) \right]\dot{\omega}_e =$$

$$\left[\frac{Z_r^2 Z_f}{(Z_r + Z_s)\dot{I}_m} + \frac{Z_s^2}{(Z_r + Z_s)\dot{I}_g} \right]T_e + \frac{Z_r Z_f}{\dot{I}_m}T_m - \frac{Z_s}{\dot{I}_g}T_g - \frac{Z_r}{\dot{I}_m}\frac{T_d}{\eta_f}$$

(3.2)

The relation of the motor speed and vehicle speed is written:

$$\omega_m = \frac{v}{R_{tire}Z_f}$$

(3.3)

The constrains of the components are as following:

$$T_{e,\min} \leq T_e \leq T_{e,\max}$$

(3.4)

$$\omega_{e,\min} \leq \omega_e \leq \omega_{e,\max}$$

(3.5)

$$T_{g,\min} \leq T_g \leq T_{g,\max}$$

(3.6)

$$\omega_{g,\min} \leq \omega_g \leq \omega_{g,\max}$$

(3.7)

$$\omega_{m,\min} \leq \omega_m \leq \omega_{m,\max}$$

(3.8)

$$T_{m,\min} \leq T_m \leq T_{m,\max}$$

(3.9)

For a given drive cycle, the vehicle speed at the given time is known. Considering equations (3.1) - (3.3), there are only two independent variables: motor torque T_m and generator torque T_g. The engine torque T_e can be derived from the motor torque T_m and generator torque T_g. The engine speed can be derived from the engine torque T_e.

The state variable of the PHEV is defined as following:

$$x(t) = [SOC(t)]$$

(3.10)

SOC(t) is the battery state of charge at the time *t*. it meets following constrain:

$$SOC_{min} \leq SOC \leq SOC_{max}$$

(3.11)

The control variables are determined:

$$u(t) = [T_m(t), T_g(t)]$$

(3.12)

And they meet the constrains of (3.4) to (3.9).

Given the driving cycle, the PHEV optimal control can be expressed: it is desired to determine a control law to minimize the performance measurement, from the initial state $x(0) = [SOC(0)]$ to the end of state $x(t_f) = [SOC(t_f)]$ at the driving cycle time t_f. The optimal function of the PHEV is:

$$J = \int_0^{t_f} L(x(t), u(t)) dt$$

(3.13)

For the PHEV, the fuel consumption function includes the fuel consumption and electricity consumption during the vehicle operation. The fuel consumption function can be described:

$$L(x(t), u(t) = fuel(t) + \alpha_{electric} electric(t)$$

(3.14)

3.3 Dynamic Programming

Dynamic Programming (DP) [47] which was developed by Bellman is a powerful tool to transform the complex decision-making problem to a series of sub-problems by the

global optimization. For a given driving cycle, the optimal operation strategy to minimize fuel consumption, or combined cost of fuel/electricity consumption can be obtained.

Due to the nonlinear characteristics of the hybrid powertrain, it is not possible to solve DP analytically. Instead, DP has to be solved numerically by some approximations. Equation (3.13) is a continuously operating system which can be approximated by a discrete system by considering N equally spaced time increments in the interval $0 \leq t \leq t_f$. Due to the fact that the system level dynamics are the main concern to evaluate fuel economy over a long driving cycle, dynamics that are much faster than 1 Hz could be ignored [48]. The sample time for the main-loop control problem is selected to be 1 second. The discrete-time model of PHEV can be described as:

$$x(k+1) = f[x(k), u(k)]$$ (3.15)

The state variable is SOC: $SOC(k+1) = SOC(k) + f[T_m(k), T_g(k)]$. (3.16)

The cost function of the PHEV powertrain can be expressed as:

$$J = \sum_{k=0}^{N-1}[L(x(k), u(k))]$$
$$= \sum_{k=0}^{N-1}\left[\beta\alpha_{fuel}P_{fuel} + \frac{\alpha_{electric}P_{Batt}}{\eta_{Grid}}\right]$$ (3.17)

Assume that the fuel price ratio is $\beta=0.65$, which is consistent with the energy price in the year 2010: \$2.77 USD per gallon of gasoline and \$0.1145 USD per kWh of electricity [49].

The optimization goal is to find the control variable, $u(k)$, to minimize the cost function. The optimization problem is subject to a set of inequality constraints arising from the component speed, torque and *SOC* characteristics. The constraints for state *X*:

$$SOC_{min} \leq SOC \leq SOC_{max}$$

$$P_{charge} \leq P_{battery} \leq P_{discharge}$$

$$\omega_{M,min} \leq \omega_M \leq \omega_{M,max}$$

$$\omega_{G,min} \leq \omega_G \leq \omega_{G,max}$$

$$T_{G,min} \leq T_G \leq T_{G,max}$$

The constraints for control *U*:

$$T_{M,min} \leq T_M \leq T_{M,max}$$

$$T_{e,min} \leq T_e \leq T_{e,max}$$

$$\omega_{e,min} \leq \omega_e \leq \omega_{e,max}$$

In addition, one equality constraint for optimization problem is imposed the drivability,

$$P_{dem} = P_e + P_M + P_G \tag{3.18}$$

Based on Bellman's principle, the DP algorithm is presented as follows:

$$J_{N-1}^* = \min_{u(N-1)} [L(x(N-1), u(N-1))] \tag{3.19}$$

Step *k*, for 0≤*k*<*N*-1:

$$J_k^*(x(k)) = \min_{u(N-1)} [L(x(k), u(k)) + J_{k+1}^*(x(k+1))] \tag{3.20}$$

and:

$$J_k^*(x(N)) = 0 \tag{3.21}$$

The dynamic programming process consists of two parts. The first part can be characterized as a backward procedure, because it travels through the states starting from the destination and finishing at the origin. The recursive equation is solved backwards from step N-1 to 0 in order to find the optimal control policy. Each of the minimizations is performed subject to the constraints above and the driving cycle. The optimal performance measurement $J_k^*(x(k))$ and optimal control $u(k)$ can be obtained at every step under the related state. Similarly, the second part is a forward procedure which traverses the states starting from the origin and moving towards the destination to determine the optimal control policy and optimal trajectory.

A standard way to solve equation (3.20) numerically is to use quantization and interpolation [50]-[52]. For continuous state space and control space, the state and control values are first discretized into finite grids. At each step of the optimization
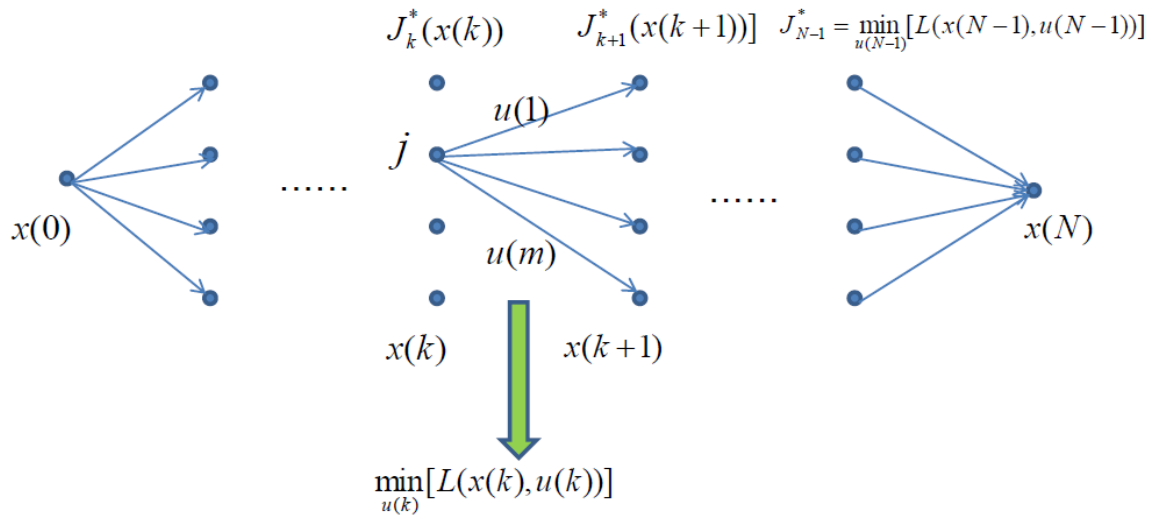
Figure 3.1. Numerical dynamic programming algorithm

search, the function is evaluated only at the grid points of the state variables. If the next state does not fall exactly on a quantized value, then the values of in equation (3.20) as well as in equation (3.19) are determined through linear interpolation.

3.4 Reduction of Dynamic Programming Grid Size

In order to reduce the computation burden of dynamic programming, the "limit trajectories" [53], [54] approach is used to reduce the grid size. If the initial state $x(0)$ is defined, it is possible to bound a region in the state space by means of the limit trajectories. Those state space trajectories obtained apply the extreme controls to the system equations. The only states to be explored are confined in the region defined by these trajectories and the constraints. Because the state variable is SOC, the SOC limit trajectories are determined as follows:

When the wheel torque $T_{wheel} > 0$, the maximum electricity consumption will be based on the maximum motor torque $T_{m\_hi}(k)$. $T_{m\_hi}(k)$ is the smallest of the following three:

1) $\dfrac{T_{wheel}(k)}{i}$;

2) The maximum motor torque provided by the motor;

3) The maximum output motor torque under the limitation of the battery discharge capacity;

When the wheel torque $T_{wheel} < 0$, the maximum electricity generated by the motor will be based on the maximum motor torque $T_{m\_lo}(k)$. $T_{m\_lo}(k)$ is the largest of the following three:

1) $\dfrac{T_{wheel}(k)}{i}$;

2) The maximum motor torque provided by the motor;

3) The maximum output motor torque under the limitation of the battery charge capacity;

Figure 3.2 shows the *SOC* limit trajectories. The state *SOC* will be explored in the limit trajectory boundaries. In this way, the calculation burden is greatly reduced.

3.5 Simulation Results

The DP optimal control is applied to PHEV in appendix I to calculate the vehicle fuel consumption. Figure 3.3 shows the *SOC* limit trajectories of UDDS driving cycle. Because the PHEV battery is charged before the operation, and considering the battery operation range, the highest *SOC* value is set to 0.9 and the lowest is set to 0.32. The grid size of the state variables and the control signals will directly influence the simulation accuracy and computational cost. Small grid sizes lead to longer computation time but more accurate optimization results and larger grid sizes save computational cost but may obtain
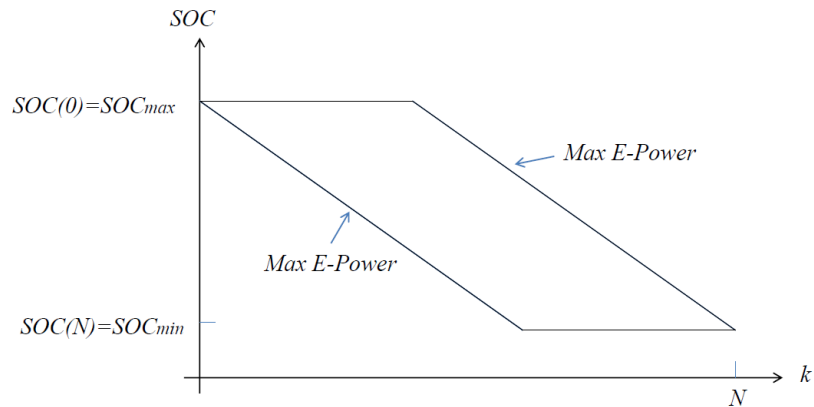
Figure 3.2. The limit trajectory boundaries

Table 3.1. The Selected Grid Points in DDP

States	
SOC	0.32:0.005:0.9
Controls Inputs	
Motor Torque [Nm]	-300:15:300
Generator Torque [Nm]	-55:5:55

inaccurate results. Also, the state and input grids need to be coherent. A state grid may not be reached by the control. The selected grid points are shown in Table 3.1.

Figure 3.4-3.6 are the simulation results of SOC, motor torque, engine torque and powers in two (2) driving cycles. The fuel consumption of 2 UDDS driving cycles is 273.93g (1.55L/100km) which is the best fuel economy that the PHEV can achieve. Any other control strategies can't compete this result.

3.6 Summary

The optimal control model of PHEV was created under the condition of given driving cycles to optimize the vehicle fuel consumption and operation cost in this chapter. The optimal control strategy was obtained by the DP approach. The optimal control strategy not only can evaluate the real time control strategy, but also direct the real time control strategy optimization. The purpose of this study is to determine the global optimal fuel consumption and operation cost as the benchmark of the real-time PHEV control strategy. The main study in this chapter focused on following:

- The optimal control model of PHEV was created. The state variable of the optimal control model is *SOC*, the control variables are the motor and generator

torques. In order to reduce the computation burden, the "limit trajectories" approach is used to reduce the grid size.

- The step was set to 1 second which was determined based on the given driving cycles. The assumption was made that the vehicle fuel consumption is constant within each steps, therefore changing the continuous optimal control to a series of sub-problems.

- The optimal results are the best PHEV fuel consumptions by using DP approach.
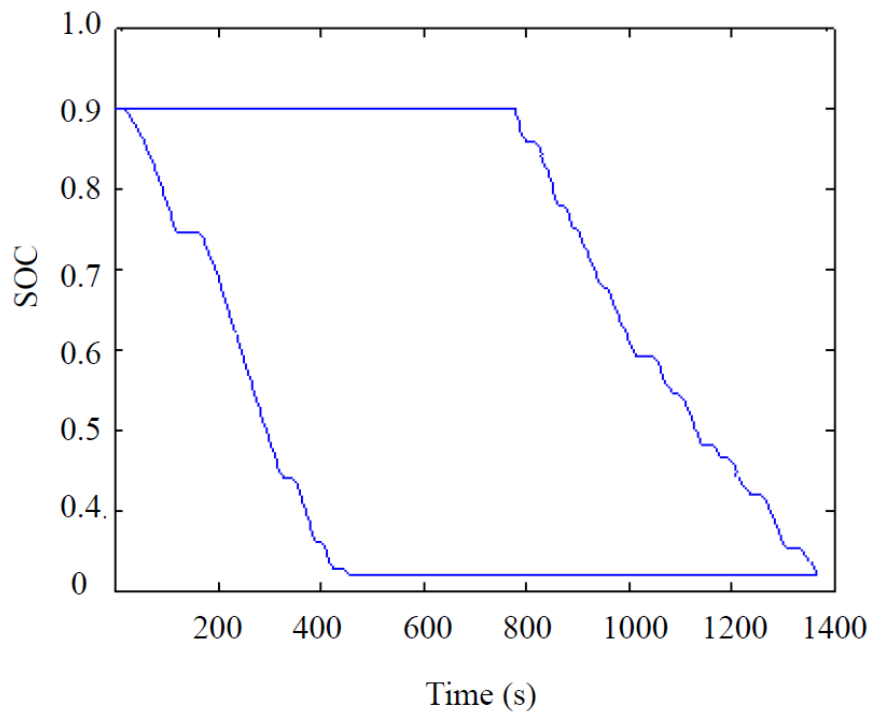
Figure 3.3. The limit trajectory boundaries for UDDS Driving cycle
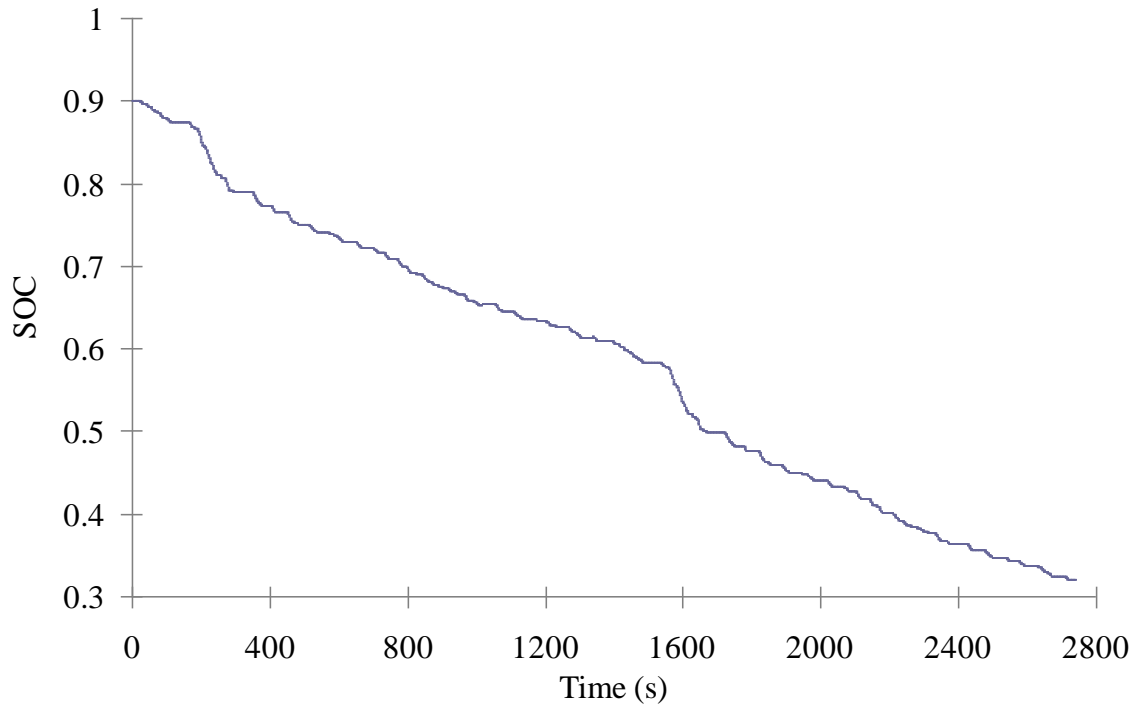
Figure 3.4. DP simulation results – SOC
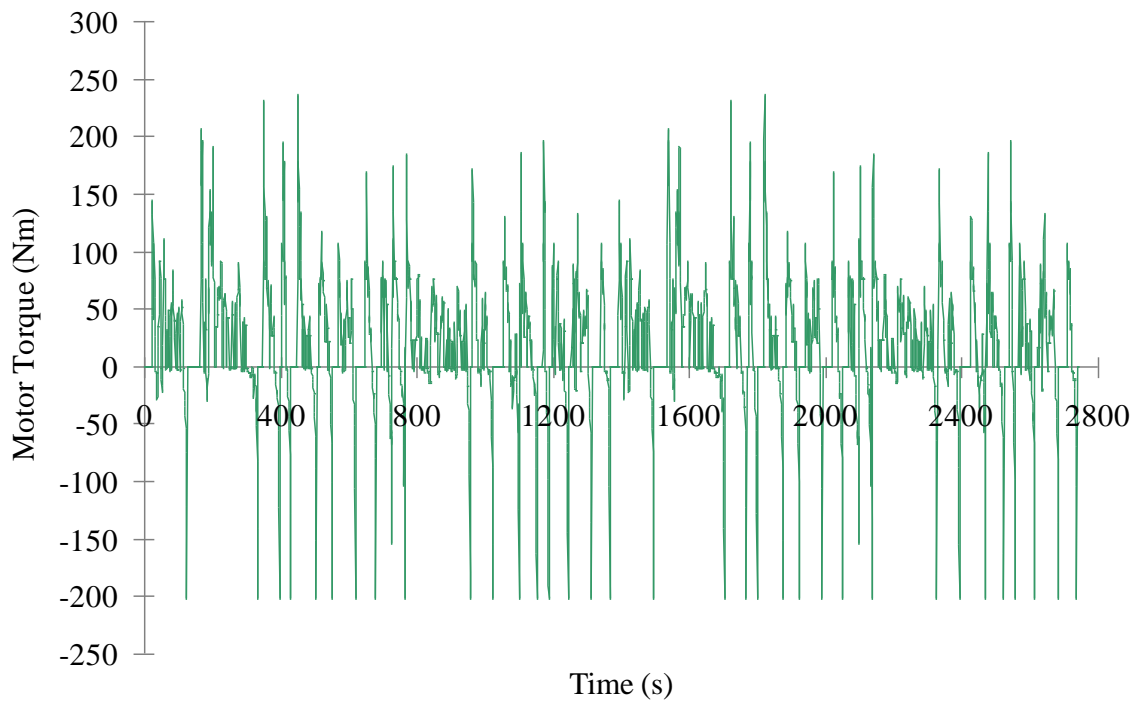
Figure 3.5 DP simulation results – Motor Torque
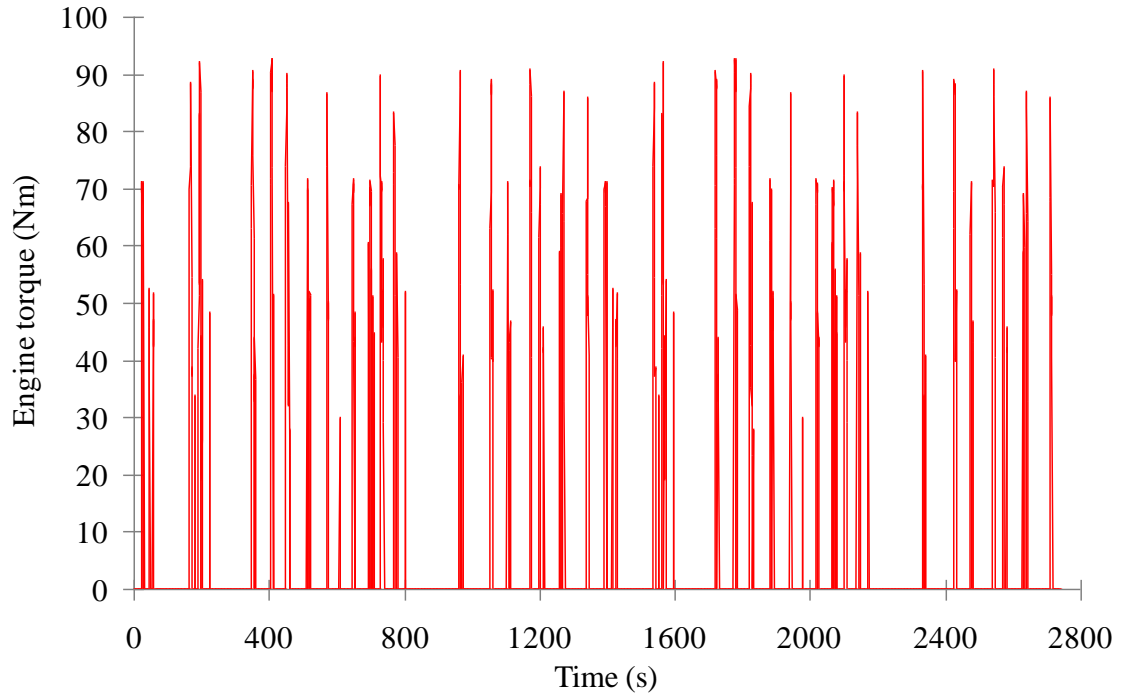
Figure 3.6. DP simulation results – Engine Torque
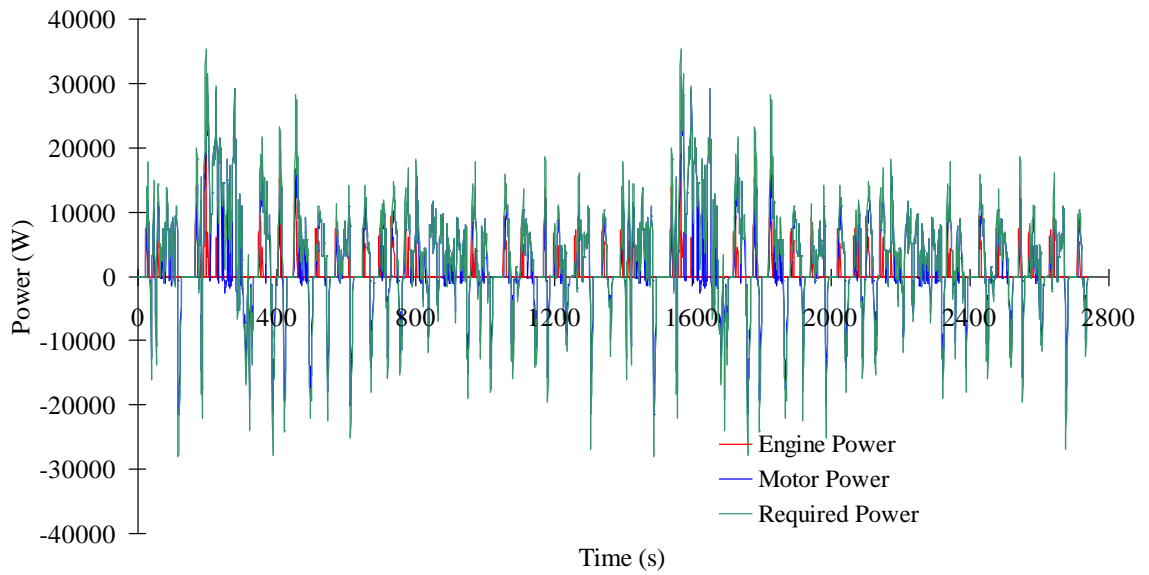
Figure 3.7. DP simulation results – Power

CHAPTER 4

PHEV RULE-BASED CONTROL STRATEGY

4.1 Introduction

Due to the multiple-power-source nature and the complex configuration and operation modes, the PHEV energy management is implemented by effectively controlling of the multiple power sources. The algorithm of the vehicle energy management and power systems control is called the control strategy. The PHEV control strategy and the vehicle controller are the vehicle nerve center and more complicated than that of an engine-only vehicle. The main function of the control strategy is the power management, i.e., the design of the high-level control algorithm that determines the proper power split between the motor and the engine to minimize fuel consumption and emissions, while satisfying constraints such as drivability, charge sustaining and component reliability.

The HEV control strategy studies mainly focus on the three areas: rule-based control strategy [55], [56], real time local optimization [57], [58], and fuzzy-logic/neural network intelligent control strategy [59], [60]. Because of the expensive computer operation cost of the real time local optimization, it currently cannot be applied on the commercial HEV. The popular control strategy used in the commercial vehicles is the rule-based control strategy [61], [62]. The fuzzy-logic/neural network intelligent control strategy has been applied in different engineering fields. The fuzzy logic control strategy is also used on the HEV.

In this chapter, a rule-based control strategy for PHEV will be developed based on the PHEV optimal control strategy created in Chapter III.

4.2 PHEV Torque Balance Control

From equation 2.16, the torque on the driveline is $T_d = F_t R_{tire}$. The energy management control strategy should meet the requirement of the torque demanded from vehicle wheels. The energy management control strategy will determine the power split ratio of the engine to the motor. When the torque on the driveline T_d is positive, then:

$$T_d = T_{e\_dr} + T_m \qquad (4.1)$$

$$T_e = T_{e\_dr} + T_g \qquad (4.2)$$

Where T_e, T_m, T_g are the torques of the engine, the motor and the generator. T_{e_dr} is the torque which is transferred from the engine to the driveline. The torque of the generator is always negative to adjust the engine torque based on the engine efficiency map. When the torque on the driveline T_d is negative, then:

$$T_d = T_m + T_{brake} \qquad (4.3)$$

Where T_m, T_{brake} are the torques of the motor and the hydraulic brake.

The goal of the control strategy is to choose an operating point that minimizes the engine's fuel consumption and emissions. The engine will be operated in the economic area which follows T_{e_opt} curve. When the engine torque falls below the limit T_{e_off} , the engine will be shut off. At the same time, the negative generator torque adjusts the engine always operate upper the $T_{e\_\min\_opt}$.

In order to determine the engine economic area, the engine directly driving efficiency and the motor driving efficiency would be compared, therefore determining $T_{e\_min\_opt}$ and T_{e_off}. The engine directly driving efficiency:

$$\eta_1 = \eta_e \eta_d \qquad (4.3)$$

The motor driving efficiency with the energy from the engine:

$$\eta_2 = \eta_{e\_opt} \eta_g \eta_{inv} \eta_m \eta_d \qquad (4.4)$$

If $\eta_1 < \eta_2$, then the engine operation point is not in the economic area. The engine should be shut off and the engine torque would be T_{e_off}. If just considering the battery charging, the minimum optimal engine torque $T_{e\_min\_opt}$ would be determined. However, the torques would be setup as the final control strategy parameters by optimization and calibration on the vehicle. The control strategy parameters optimization will be discussed in next chapter.

4.3 PHEV Operation Modes

Most of the rule-based control strategies are based on "IF-THEN" type of the control rules and perform the load balancing between the power sources. The typical PHEV control strategy is PSAT control strategy which is based on charge-depleting (CD) mode and charge-sustaining (CS) mode. The global energy management optimization of PHEV and PHEV control strategy testing show that the blended control strategy has better energy efficiency compared with the electric-only control strategy. The PHEV uses 6 operation modes to achieve the most efficient operation in response to the driving conditions based on the blended control strategy in this study.
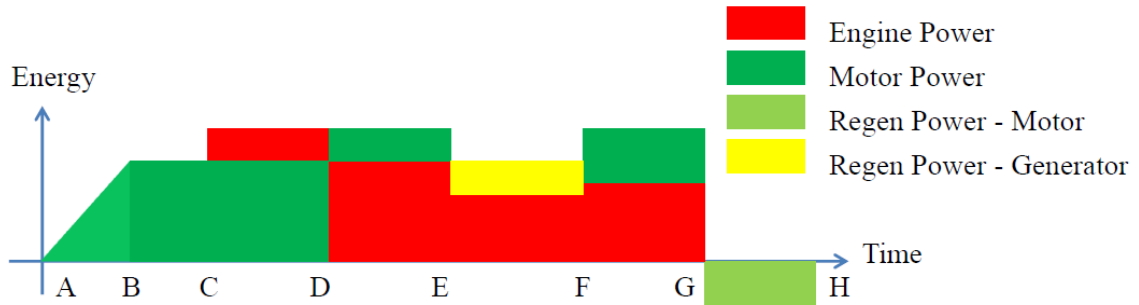
Figure 4.1. PHEV basic operation modes

Figure 4.1 represents the PHEV 6 basic operation modes:

1) AB, BC, and GH are all electric mode, including the driving and generation modes;

2) Point C is the engine start mode;

3) CD is the power boost mode;

4) DE is the low *SOC* normal driving and power boost mode;

5) EF is the battery charging mode;

6) FG is the negative power split mode.

Table 4.1 list the analysis of every operation modes and relationship of the torques.

4.4 Design of PHEV Energy Management Control Strategy

The important step of the PHEV rule-based control strategies based on "IF-THEN" is the determination of the control strategy parameters. Table 4.2 lists the parameters of the PHEV rule-based control strategy.

Table 4.1 PHEV Operation Mode Analysis
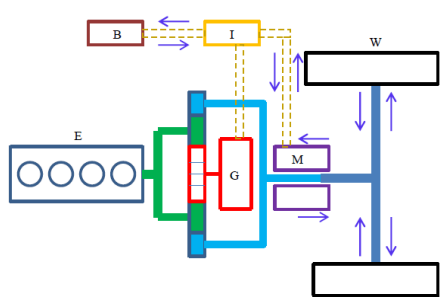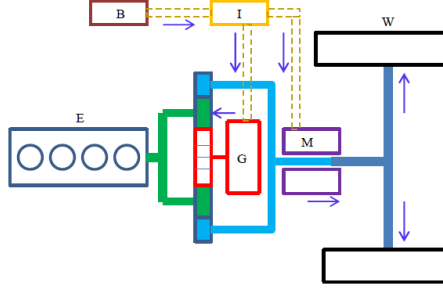
	Analysis and Description	Diagram
1	All electric model 1) Vehicle launch: low speed and low load. $T_d < T_{m\_max}$, $T_e = 0$, $T_g = 0$ 2) Vehicle normal operation and $SOC > SOC_{min}$, $T_d < T_{m\_max\_cont}$, $T_e = 0$, $T_g = 0$ 3) If $SOC > SOC_{max}$, $T_m = 0$; If $SOC < SOC_{max}$, Regenerative brake: $T_d < 0$, $T_e = 0$, $T_g = 0$, $T_m = T_{m\_gen}$ T_m is the maximum value as following: • T_d • The maximum motor torque provided by the motor; • The maximum output motor torque under the limit of the battery charge capacity;	
2	Engine Start Mode The engine is started by the generator, and the vehicle is driven by the motor. $T_m = T_d$ $T_g = T_{e\_start}$	

Table 4.1 PHEV operation mode analysis (Cont.)
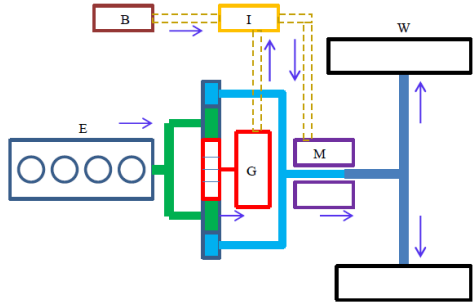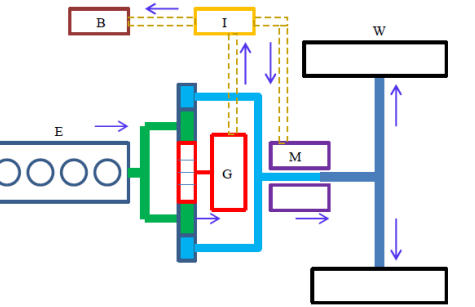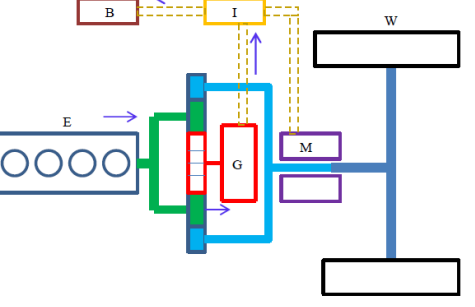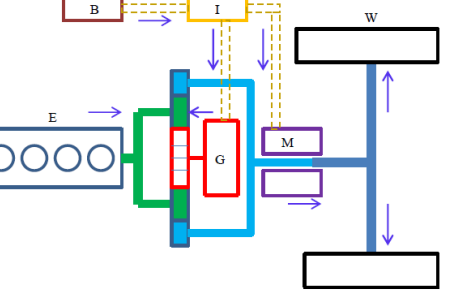
3	Power Boost Mode: Motor is main power source and engine is the power boost source High load and $SOC>SOC_{min}$: $T_d > T_{m\_max}$ $T_m = T_{m\_max}$ $T_{e\_dr} = T_d - T_m$ $T_g = T_e - T_{e\_dr}$	
4	Low SOC normal driving mode: Engine is main power source and motor is the power boost source, $SOC<SOC_{min}$: $0 < T_d < T_{e\_dr\_max}$ $T_d = T_{e\_dr}$, $T_m = 0$ $T_e = T_g + T_{e\_dr}$	
5	Battery charging mode: Vehicle speed $v=0$: $T_e = T_g$	
6	Negative power split mode: When $SOC>SOC_{min}$: $T_d > T_{e\_dr\_max} + T_{m\_max}$ $T_e = T_{e\_opt}$ $T_m = T_{m\_max}$	

Table 4.2 Parameters of the PHEV Rule-based Control Strategy

Item	Parameters	Descriptions
1	SOC_{min}	Highest desired battery SOC
2	SOC_{max}	Lowest desired battery SOC
3	α_{g_charge}	Desired generator charge torque coefficient
4	$\alpha_{m\_discharge}$	Desired motor discharge torque coefficient
5	$\alpha_{e\_opt\_low}$	Desired engine lowest torque coefficient
6	$\alpha_{e\_opt\_high}$	Desired engine highest torque coefficient
7	ω_{e_lau}	Engine Lowest speed

The baseline parameters of rule-based PHEV control strategy are determined based on the DP simulation results (Table 4.3). Combining the PHEV operation mode analysis, also considering that the engine can't be started in 2 seconds after it is shut down, the PHEV "IF-THEN" rule-based control strategy are listed in Table 4.4.

Table 4.3. Baseline Parameters of Rule–based PHEV Control Strategy

Item	Parameters	Baseline Values	Actual Values
1	SOC_{min}	0.3	-
2	SOC_{max}	0.9	-
3	α_{g_charge}	1	43 Nm
4	$\alpha_{m\_discharge}$	0.76	116 Nm
5	$\alpha_{e\_opt\_low}$	0.6	55 Nm
6	$\alpha_{e\_opt\_high}$	1	93 Nm
7	$\alpha_{\omega e\_lau}$	1	1,200 rpm

Table 4.4. PHEV "IF-THEN" Rule-based Control Strategy

Item	Condition	Engine	Motor	Generator
1	$0<T_d\leq T_{m\_discharge}$ & Engine ON Min Time Met & $SOC>SOC_{min}$	$T_e=0$	$T_m=T_d$	$T_g=0$
3	$0<T_d\leq T_{m\_discharge}$ & Engine ON Min Time NOT Met & $SOC>SOC_{min}$ & $T_{e\_opt\_low}>T_d$	$T_e=T_{e\_opt\_low}$	$T_m=0$	$T_g=T_{e\_opt\_low-Td}$
4	$0<T_d\leq T_{m\_discharge}$ & Engine ON Min Time NOT Met & $SOC>SOC_{min}$ & $T_{e\_opt\_low}<T_d<T_{e\_opt\_high}$	$T_e=T_{e\_dr}$	$T_m=0$	$T_g=T_{e\_g}$
5	$0<T_d\leq T_{m\_discharge}$ & $\omega_e<\omega_{e\_lau}$ & $SOC>SOC_{min}$	$T_e=0$	$T_m=T_d$	$T_g=0$
6	$T_d>T_{m\_discharge}$ & Engine OFF Min Time Met & $SOC_{min}<SOC<SOC_{max}$ & $\omega_e>\omega_{e\_lau}$	$T_e=T_{e\_opt\_low}$	$T_m=T_{m\_discharge}$	$T_g=T_{e\_opt\_low}-T_d+T_{m\_discharge}$
7	$T_{m\_discharge}<T_d<T_{m\_max}$ & Engine OFF Min Time NOT Met & $SOC_{min}<SOC<SOC_{max}$ & $\omega_e>\omega_{e\_lau}$	$T_e=0$	$T_m=T_d$	$T_g=0$
8	$T_d>T_{m\_max}$ & Engine OFF Min Time NOT Met & $SOC_{min}<SOC<SOC_{max}$ & $\omega_e>\omega_{e\_lau}$	$T_e=0$	$T_m=T_{m\_max}$	$T_g=T_{m\_max}-T_d$
9	$T_d<T_{e\_opt\_low}$ & $SOC<SOC_{min}$ & $\omega_e>\omega_{e\_lau}$	$T_e=\max(T_{e\_opt\_low}, T_d+T_{e\_g})$	$T_m=0$	$T_g=T_{e\_g}$
10	$T_{e\_opt\_low}<T_d<T_{e\_opt\_high}$ & $SOC<SOC_{min}$ & $\omega_e>\omega_{e\_lau}$	$T_e=\max(T_{e\_opt\_high}, T_{req}+T_{e\_g})$	$T_m=0$	$T_g=T_{e\_g}$
11	$T_d>T_{e\_max}+T_{m\_charge}$ & $SOC>SOC_{min}$ & $\omega_e>\omega_{e\_lau}$	$T_e=T_{e\_max}$	$T_m=T_{m\_discharge}$	$T_{g\_dr}=T_d-T_{de\_dr}-T_m$
12	$T_d<0$ & $SOC<SOC_{max}$	$T_e=0$	$T_m=\min(T_d,$ Battery limit)	$T_g=0$

4.5 Simulation Results

The PHEV rule-based control strategy was simulated in the Matlab environment. 2 UDDS driving cycles were used. The PSD gear ratio was set to 3.0. Figure 4.2 – Figure 4.5 show the simulation results.

From Figure 4.2, at second 1670 the *SOC* reduces to 0.32 which is set to minimum *SOC* value, the vehicle control strategy is changed from CD mode to CS mode. From Figure 4.3 and 4.4, the motor operation time reduces and the engine operation time increases. This is because the engine becomes the main power source after the second 1670.

Before the second 1670, the engine always operates around lower limit of the engine economy zone. After the second 1670, the engine always operates around higher limit of the engine economy zone. In this way, the engine not only can operate at the high efficiency zone, but also provide the power to charge the battery. Figure 4.5 shows the power relationship between the engine power, motor power and the required power. At some points, the engine power is larger than the required power after the second 1670.

The fuel consumption based on the rule-based control strategy is 309.53 g (1.75 L/100 km). Comparing with the fuel consumption based on the DP simulation results, the fuel consumption increases 12.98%.
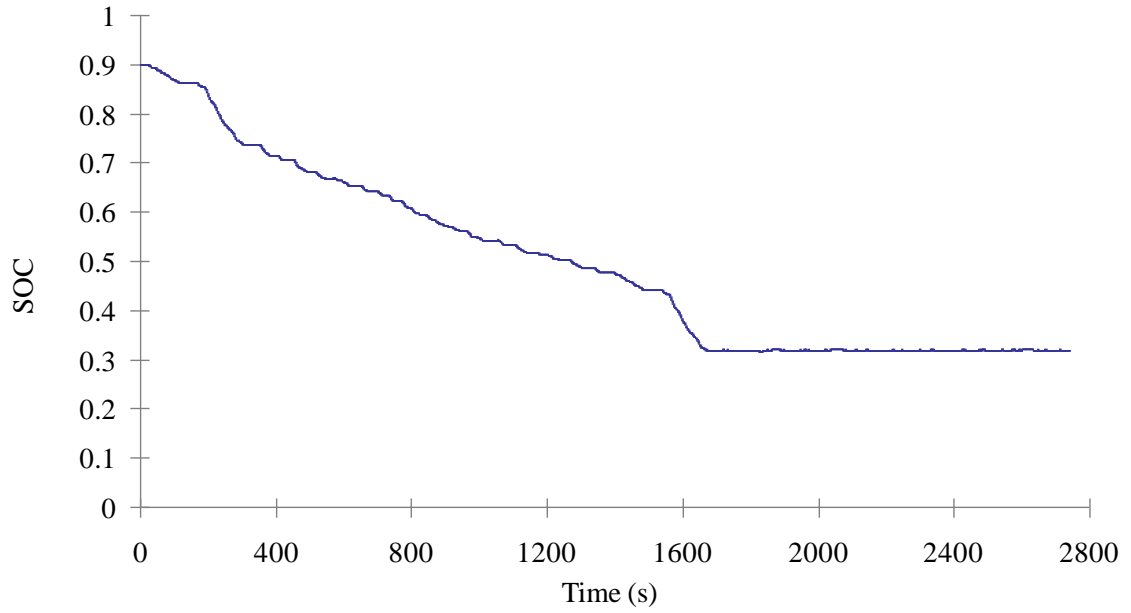
Figure 4.2. Rule-based control strategy simulation results – *SOC*
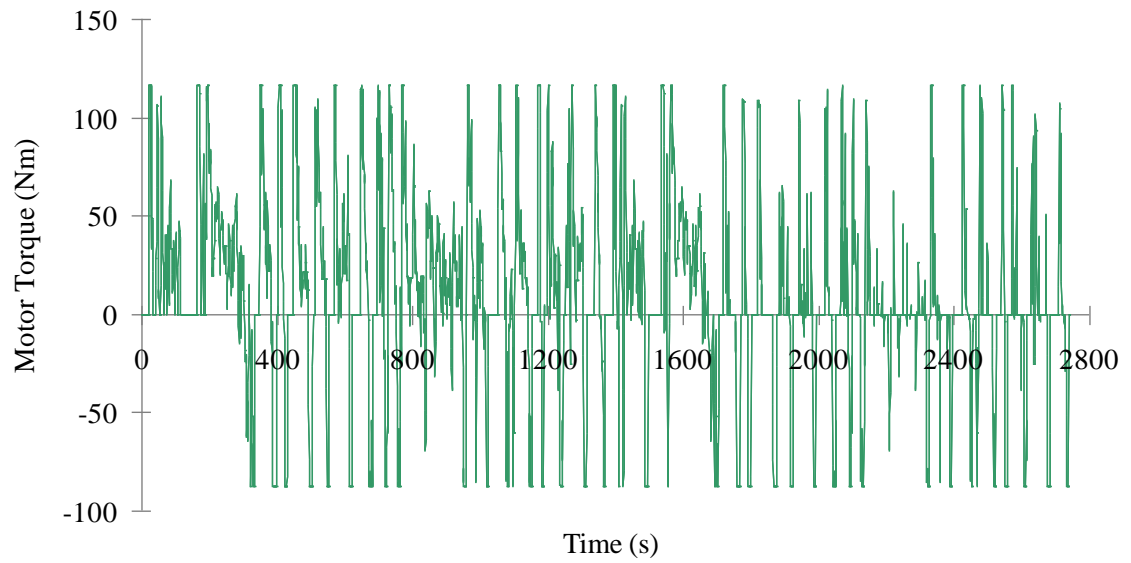
Figure 4.3. Rule-based control strategy simulation results – Motor Torque
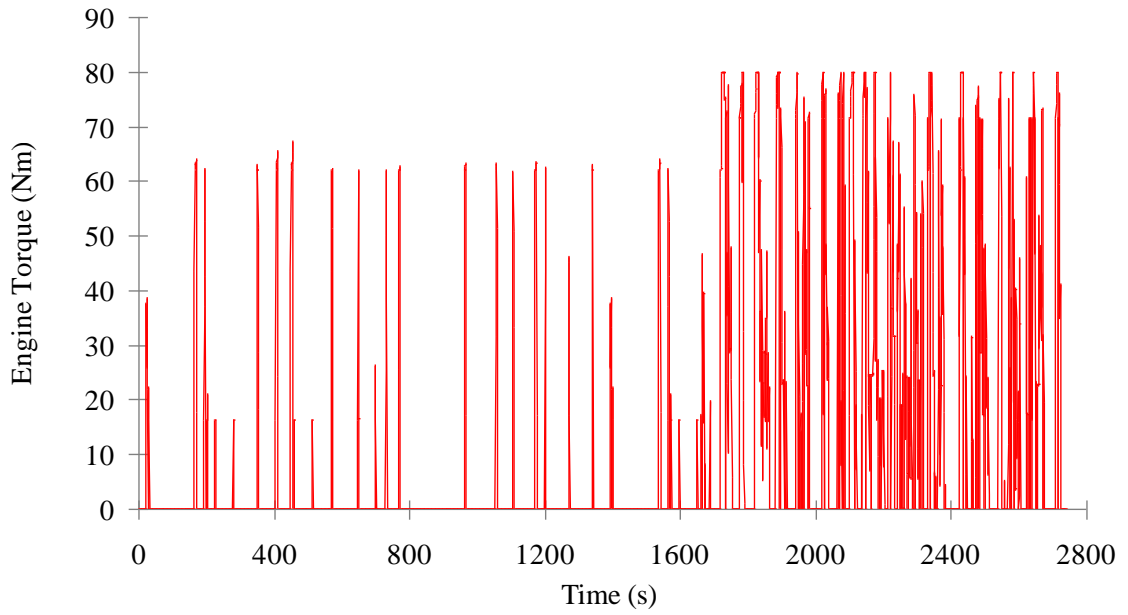
Figure 4.4. Rule-based control strategy simulation results – Engine Torque
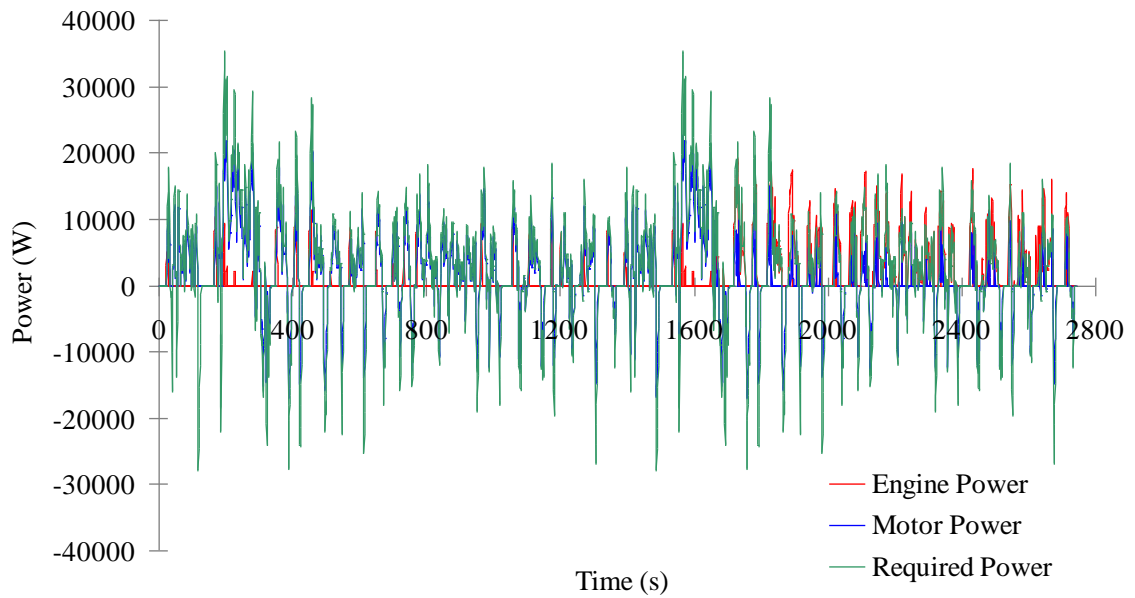
Figure 4.5. Rule-based control strategy simulation results – Power

4.6 Summary

The power split HPEV rule-based control strategy was studied in this chapter. Because it is difficult to create the accurate math models of the vehicle systems and components and complex to coordinate the operations between the vehicle systems, the rule-based is still the key method to design the control strategy. The main study in this chapter focused on following:

1. Analysed the power split PHEV energy management control strategy, determined the direction to minimize the PHEV fuel consumption is to control the engine to operate at the economy zone, defined the control strategy to ensure the engine operate at the economy zone is through the adjustment of the generator load.

2. Studied the vehicle operation modes and relationships between the loads to provide the base to create the rule-based control strategy.

3. Determined the rule-based control strategy parameters based on the vehicle system characteristics and DP simulation results.

4. Simulated the rule-based control strategy using the vehicle model created in Chapter II. The control strategy can coordinate and control the torque output of the engine, motor, and generator to ensure the fuel energy conversion efficiency as high as possible.

CHAPTER 5

RULE BASED CONTROL STRATEGY PARAMETERS

OPTIMIZATION

5.1 Introduction

The common problem during the design of the control strategy is the optimization of control strategy parameters. The general method to determine the parameters is to initially set up the parameters, then validate by trail-and-error. If trail-and-error is implemented on the vehicle, the parameters calibration cycle is around 30 minutes, including the parameters adjustment and driving cycle vehicle running. This method spends a lot of time and money to get the final parameters, but also has difficulty searching for the optimal solution. The improved method is to introduce the gradient-based Sequential Quadratic Programming (SQP) to optimize the control strategy parameters [63], [64]. However, for the HEV system objective function, it is difficult to make the assumptions, such as continuity, differentiability, and satisfaction of the Lipschitz condition etc. to determine the objective function gradients.

Genetic algorithm (GA), as a powerful and broadly applicable stochastic search and optimization technique, has turned much of its attention to optimization problems in industrial engineering, resulting in a fresh body of research and applications. Recently, GA is also widely applied in the optimization of HEV control strategy parameters [65]-[68]. Because HEV has a number of control strategy parameters, as well as multiple objective functions, which are conflicting, the optimization of HEV control strategy

parameters can be formulated to multi-objective constrained nonlinear optimization problem.

Multiple-objective optimization models have been solved by many researchers. The classical optimization methods convert multi-objective optimization into a single objective optimization by allocating weights to each of the objective functions which reflect their importance in the overall problem and focusing on a particular optimal solution at one time [69]. In fact, it is always difficult to find the suitable weights capable of accurately indicating the actual situation. Adopting such procedures does not only entail repetition of the same process many times to find multiple solutions, but also lacks quality solutions. Therefore, this method has been replaced by the multi-objective evolutionary algorithms (MOEAs) Pareto optimal solutions in a single simulation run.

Non-dominated Sorting Genetic Algorithm (NSGA) [70] is one of MOEAs and a popular non-domination based genetic algorithm for multi-objective optimization. It is a very effective algorithm but has been generally criticized for its computational complexity, lack of elitism and for choosing the optimal parameter value for sharing parameter σ_{share}. An improved version of NSGA, utilizing parameter less elitist approach named NSGA-II, was proposed by Deb *et al*. [71]. NSGA-II has a better sorting algorithm, incorporates elitism and does not require a sharing parameter to be chosen *a priori*.

In this paper, the rule-based control strategy parameters based on the blended operation are optimized by using NSGA-II.

5.2 GA Terminology and Definition

Chromosome* :** A solution vector $\mathbf{x} \in \mathbf{X}$ is called an individual, or ***Chromosome.

Genes : Chromosomes are made of discrete units called ***Genes***. Each gene controls one or more features of the chromosome.

Encoding : Normally, a chromosome corresponds to a unique solution $\mathbf{x}$ in the solution space. This requires a mapping mechanism between the solution space and the chromosomes. This mapping is called an ***encoding***. In fact, GA works on the *encoding* of a problem, not on the problem itself.

Population : GA operates with a collection of chromosomes, called a *population*. The population is normally randomly initialized.

Crossover and ***Mutation*** : GA use two operators to generate new solutions from existing ones: ***crossover*** and ***mutation***.

Parents and ***Offspring*** : In crossover, generally two chromosomes, called *parents*, are combined together to form new chromosomes, called *offspring*.

Fitness Function : ***Fitness Function*** is the function to be optimized.

Definition 1: ***Dominating***: A feasible solution x is said to dominate another feasible solution y ($x \prec y$), if and only if, $f_k(x) \leq f_k(y)$ for k=1, 2 … p, and $f_m(x) \leq f_m(y)$ for least one objective function m.

Definition 2: ***Pareto optimal***: A solution is said to be *Pareto optimal* if it is not dominated by another solution in the solution space.

5.3 NSGA-II Description

Without loss of generality, a multiple-objective optimization problem can be represented formally as follows:

$$\min y = \{f_1(x), f_2(x), f_3(x), ..., f_p(x)\}$$
$$s.t.$$
$$g_i(x) \geq 0, i = 1,2,...m \tag{5.1}$$
$$x_{min}^j \leq x^j \leq x_{max}^j, j = 1,2,...,n$$

where:

$f(x) \in R^p$ is a vector of p objective functions, $x \in R^n$ is a vector of n decision variables, $g(x)$ is m inequality constrain functions. The set of Pareto optimal solutions forms a Pareto front P (Figure 5.1). Where Y is the solution space (possible solution area); P is the Pareto front; f_1, f_2 are the objective functions; A, B, C, D are the optimal solutions for the corresponding objective functions.
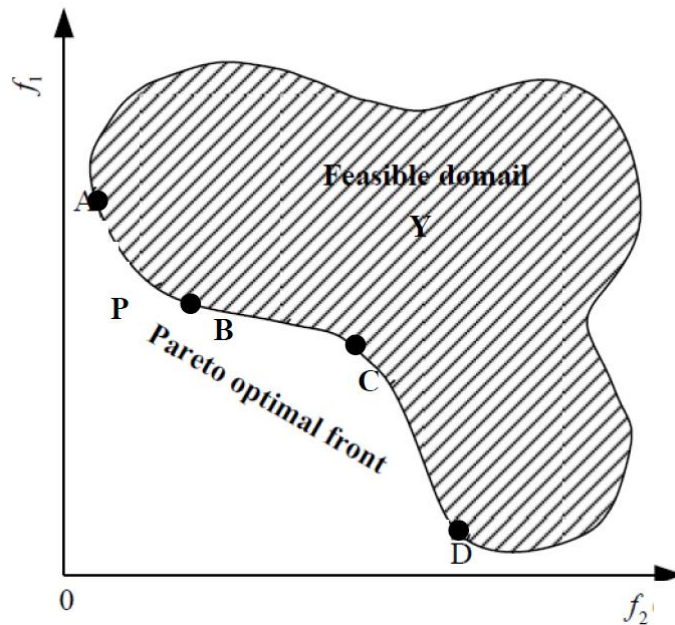
Figure 5.1. Pareto optimal front

The ultimate goal of a multi-objective optimization algorithm is to identify solutions in the Pareto optimal set. However, identifying the entire Pareto optimal set, for many multi-objective problems, is practically impossible due to its size. In addition, for many problems, especially for combinatorial optimization problems, proof of solution optimality is computationally infeasible. Therefore, a practical approach to multi-objective optimization is to investigate a set of solutions (*the best-known Pareto set*) that represent the Pareto optimal set as much as possible. With these concerns in mind, a multi-objective optimization approach should achieve the following three conflicting goals:

1. The best-known Pareto front should be as close possible as to the true Pareto front. Ideally, the best-known Pareto set should be a subset of the Pareto optimal set.

2. Solutions in the best-known Pareto set should be uniformly distributed and diverse over of the Pareto front in order to provide the decision maker a true picture of trade-offs.

3. In addition, the best-known Pareto front should capture the whole spectrum of the Pareto front. This requires investigating solutions at the extreme ends of the objective function space.

In order to maintain sustainable diversity in a population with appropriate setting of its associated parameters, the density-estimation metric and the crowded-comparison operator are used in NSGA-II.

1) Density Estimation: To get an estimate of the density of solutions surrounding a particular solution in the population, we calculate the average distance of two points on either side of this point along each of the objectives. This quantity $i_{distance}$ serves as an estimate of the perimeter of the cuboid formed by using the nearest neighbors as the vertices (call this the *crowding distance*). In Figure 4.2, the crowding distance of the *i*th solution in its front (marked with solid circles) is the average side length of the cuboid (shown with a dashed box). The crowding-distance computation requires sorting the population according to each objective function value in ascending order of magnitude. Thereafter, for each objective function, the boundary solutions (solutions with smallest and largest function values) are assigned an infinite distance value. All other intermediate solutions are assigned a distance value equal to the absolute normalized difference in the function values of two adjacent solutions. This calculation is continued with other objective functions. The overall crowding-distance value is calculated as the sum of individual distance values corresponding to each objective. Each objective function is normalized before calculating the crowding distance. The algorithm as shown at the bottom of the page outlines the crowding-distance computation procedure of all solutions in an nondominated set I.

After all population members in the set I are assigned a distance metric, we can compare two solutions for their extent of proximity with other solutions. A solution with a smaller value of this distance measure is, in some sense, more crowded by other solutions. This is exactly what we compare in the proposed crowded-comparison operator, described below. Although Figure 5.2 illustrates the crowding-distance computation for two objectives, the procedure is applicable to more than two objectives as well.
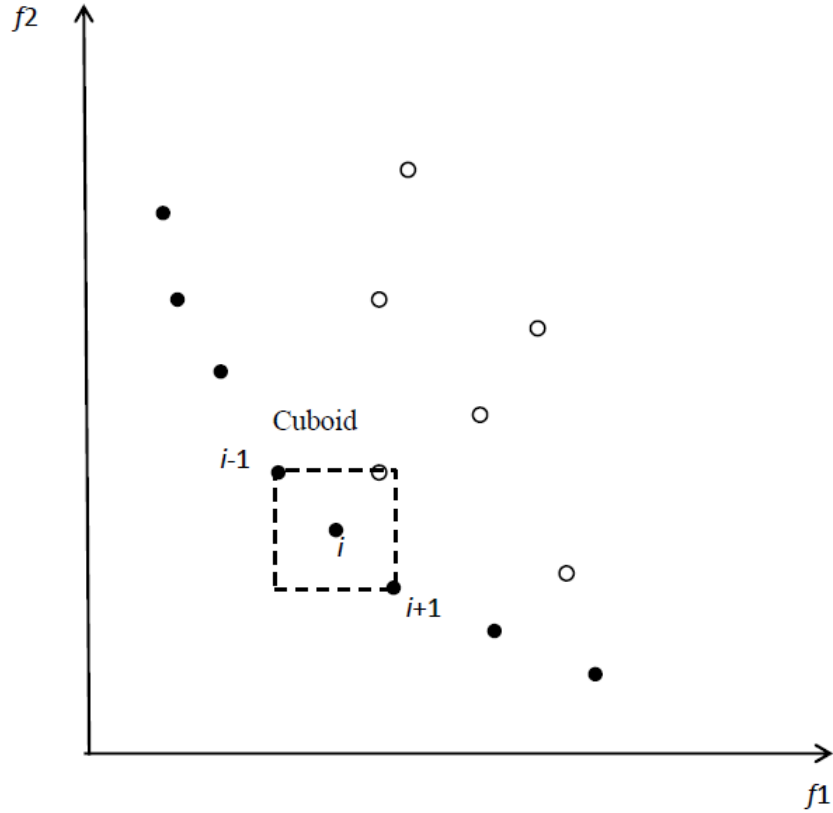
Figure 5.2. Crowding-distance calculation. Points marked in filled circles are solutions of the same nondominated front

2) Crowded-Comparison Operator: The crowded-comparison operator ($\prec_n$) guides the selection process at the various stages of the algorithm toward a uniformly spread-out Paretooptimal front. Assume that every individual i in the population has two attributes:

    1) nondomination rank (i_{rank});

    2) crowding distance ($i_{distance}$).

We now define a partial order $\prec_n$ as

    $i \prec_n j$ if ($i_{rank} < j_{rank}$)

    Or (($i_{rank} = j_{rank}$) and ($i_{distance} > j_{distance}$))

That is, between two solutions with differing nondomination ranks, we prefer the solution with the lower (better) rank. Otherwise, if both solutions belong to the same front, then we prefer the solution that is located in a lesser crowded region.

In NSGA-II, the initialized population is sorted based on non- domination. Each solution is assigned fitness equal to the level of non-domination (Level 1 is the best level, Level 2 is the next best Level and so on). In this manner, minimization of fitness is assumed. An offspring population, Q_0, of size N is created, using binary tournament selection, crossover, and mutation. Since the elitism is introduced by comparing current populations with previously found best non-dominated solutions, the procedure is different after the first generation, and onwards. The NSGA-II procedure is known in Figure 5.3. Table 5.1 describes the NSGA-II algorithm.
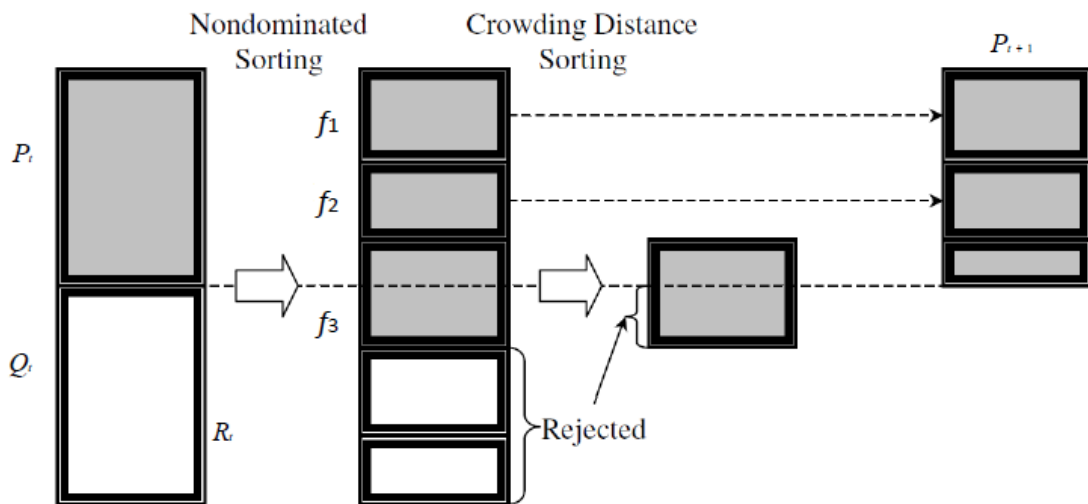
Figure 5.3. NSGA-II procedure

Table 5.1. NSGA-II Elitism Procedure

$R_t = P_t \cup Q_t$
f=fast-nondomimated-sort(R_t)
P_{t+1} =0 and i=1
Until $|P_{t+1}| + |f_i| \le N$
   Crowding-distance-assignment(f_i)
   $P_{t+1} = P_{t+1} \cup f_i$
   i=i+1
sort($f_i, \prec_n$)
$P_{t+1} = P_{t+1} \cup f_i[1:(N - |P_{t+1}|)]$
Q_{t+1} =make-new-pop(P_{t+1})
t=t+1

The NSGA-II algorithm is simple and straightforward. First, a combined population $R_t = P_t \cup Q_t$ is formed. The population R_t is of size 2N. Then, the population R_t is sorted according to nondomination. Since all previous and current population members are included in R_t, elitism is ensured. Now, solutions belonging to the best nondominated set f_1 are of best solutions in the combined population and must be emphasized more than any other solution in the combined population. If the size of f_1 is smaller then N, we definitely choose all members of the set f_1 for the new population P_{t+1}. The remaining members of the population P_{t+1} are chosen from subsequent nondominated fronts in the order of their ranking. Thus, solutions from the set f_2 are chosen next, followed by solutions from the set f_3, and so on. This procedure is continued until no more sets can be accommodated. Say that the set f_k is the last nondominated set beyond which no other set can be accommodated. In general, the count of solutions in all sets from f_1 to

f_k would be larger than the population size. To choose exactly *N* population members, we sort the solutions of the *last* front f_k using the crowded-comparison operator $\prec_n$ in descending order and choose the best solutions needed to fill all population slots. The new population P_{t+1} of size *N* is now used for selection, crossover, and mutation to create a new population Q_{t+1} of size *N*. The individuals are selected by using a binary tournament selection with crowed-comparison-operator. Real-coded GAs use Simulated Binary Crossover (SBX) operator for crossover and polynomial mutation. Figure 5.4 shows the flow chart of the NSGA-II algorithm.

Comparing with NSGA, the overall complexity of the algorithm and the computation burden of NSGA-II has reduced from $O(pN^3)$ of NSGA to $O(pN^2)$, which is governed by the nondominated sorting part of the algorithm.

5.4 NSGA-II Objective Functions

The power split PHEV rule-based control strategy optimization is a multi-objective problem which has two major objectives under the constraints. The mathematical description of the multi-objective optimization problems is as follows:

Optimization objectives of the PHEV powertrain are to reduce the fuel consumption cost and the electricity cost. Two functions about the fuel consumption cost and the electricity cost can be expressed as:
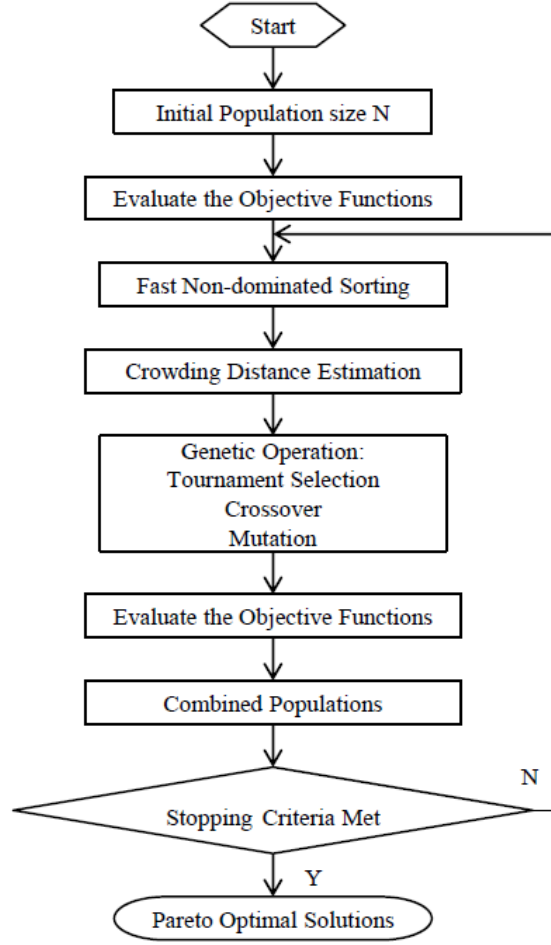
Figure 5.4. The flowchart of multi-objective optimization algorithm of NSGA-II

$$f_{fuel} = \min \sum_{k=0}^{N-1} \beta \alpha_{fuel} P_{fuel}$$

$$f_{elec} = \min \sum_{k=0}^{N-1} \frac{\alpha_{electric} P_{Batt}}{\eta_{Grid}} \tag{5.2}$$

where,

$$f_{fuel}, f_{elec} = f(SOC_{min}, SOC_{max}, \alpha_{g\_charge},$$

$$\alpha_{m\_discharge}, \alpha_{e\_opt\_low}, \alpha_{e\_opt\_high}, \omega_{e\_lau}) \tag{5.3}$$

Generally, the constraints of multi-objective problems for the power split PHEV include the vehicle performance, such as accelerating ability and gradeability, and energy balance between energy sources and sinks of PHEV. This study mainly focuses on the PHEV energy management and operation cost, so the constraint considered in this study is as follows:

$$P_{dem} = P_e + P_M + P_G \tag{5.4}$$

The optimization parameters of multi-objective problems for the power split PHEV in Table II have a critical influence over PHEV fuel economy and operation cost. The parameters of PHEV and their range are listed follows:

$$0.3 \leq SOC_{min} \leq 0.6$$

$$0.7 \leq SOC_{max} \leq 0.9$$

$$0.7 \leq \alpha_{g\_charge} \leq 1.1$$

$$0.7 \leq \alpha_{m\_discharge} \leq 0.8$$

$$0.4 \leq \alpha_{e\_opt\_low} \leq 0.7$$

$$0.9 \leq \alpha_{e\_opt\_high} \leq 1.1$$

$$1010 \leq \omega_{e\_lau} \leq 1250$$

In this study, the population N is initially set to 20. The initialized population is sorted based on non-domination. The total generation of NSGA-II algorithm is set to 100. The crossover probability is 0.9 and the mutation probability is 0.01. When the generation meets the criteria, the final populations and related objectives will be obtained.

5.5 Simulations

This section presents the rule-based control strategy parameters optimization results through the different driving cycles and the PSD ratios effects to the vehicle operation cost based on the optimization results. Two typical driving cycles - UDDS and HWFET driving cycles are used in the simulation. Two driving cycles specification can be found in appendix B. The influence of different numbers of the driving cycles on the rule-based control strategy parameters are studied through the simulations. Following are driving cycles schedule during the simulation to evaluate the driving cycle numbers effects to the operation costs including fuel consumptions and electricity costs:

CASE I: UDDS – 1, 2, 3 driving cycles.

CASE II: HWFET – 1, 2, 3 driving cycles.

5.5.1. Baseline simulation

The baseline of the PHEV rule-based control strategy parameters is shown in Table 4.3. The fuel consumptions and total operation costs for 1 UDDS driving cycle, 2 UDDS driving cycles, 3 UDDS driving cycles, 1 HWFET driving cycle, 2 HWFET driving cycles and 3 HWFET driving cycles are listed in Table 5.2.

5.5.2. Objective optimization for PSD gear ratio =3.0

The PHEV control strategy parameter optimization is carried out according to the parameters setting given in Chapter 4.4. The PSD gear ratio is set to 3.0. Table 5.7 only shows the optimization results of 3 HWFET driving cycles. The Pareto optimal results for

1 UDDS driving cycle, 2 UDDS driving cycles, and 3 UDDS driving cycles are shown in Figure 5.5. The Pareto optimal results for 1 HWFET driving cycle, 2 HWFET driving cycles and 3 HWFET driving cycles are shown in Fig 5.6.

The purpose of NSGA-II is to find a bunch of trade-off solutions which are termed *optimal*. However, there also exist a number of poor schemes that can be substituted by other superior ones whose objectives are non-inferior to, and at least one objective better than theirs. From Table 5.3, the total costs of all of the Pareto optimal solutions are less than 0.898 (USD) which is the baseline total cost. 17 Pareto optimal solutions have the better fuel consumptions than 661.25 g, which is the baseline fuel consumption. This means that most of the Pareto solutions are better than the baseline. *Better* here means both of the objectives are smaller than the baseline. Though this fact cannot sufficiently demonstrate that the 20 solutions are true Pareto solutions, it does demonstrate that the solutions are at least better than the baseline.

The range of each objective in the Pareto set for 3 HWFET driving cycles is as follows:

Fuel Consumption: [510, 655] g.

Total operation cost: [0.6606, 0.7414] (USD).

Figure 5.5 and 5.6 show the relationships between the fuel consumption and electricity cost as the distribution of the Pareto optimal solutions with the different driving cycles, when PSD is 3.0. A set of alterative optimal PHEV parameter solutions can be obtained. In order to compare with the baseline, the best total operation cost and best fuel

70

consumption of the Pareto results for the UDDS and HWFET driving cycle with the different numbers of driving cycles are listed in Table 5.4 and 5.5, respectively.

For the UDDS driving cycles, when considering the best operation cost solution only, the operation costs reduce 2.98%, 2.82%, and 2.74%, respectively, for 1 UDDS driving cycle, 2 UDDS driving cycles, 3 UDDS driving cycles. The fuel consumption increases 5.35% and 3.58% for 2 UDDS driving cycles and 3 UDDS driving cycles, although it reduces 27.12% for 1 UDDS driving cycle. When considering the best fuel consumption solution only, both fuel consumption and the operation cost reduce for 1 UDDS driving cycle, 2 UDDS driving cycles, and 3 UDDS driving cycles. The fuel consumptions reduce 27.12%, 3.53%, and 3.62%. The operation costs reduce 2.98%, 1.94%, and 2.53%, respectively, for 1 UDDS driving cycle, 2 UDDS driving cycles, and 3 UDDS driving cycles.

For the HWFET driving cycles, when considering the best operation cost solution only, the operation costs reduce 24.22%, 25.04%, and 26.5%, respectively, for 1 HWFET driving cycle, 2 HWFET driving cycles, and 3 HWFET driving cycles. The fuel consumption increases 797.25% and 4.9% for 1 HWFET driving cycle and 2 HWFET driving cycles, although it reduces 11.17% for 3 HWFET driving cycles. When considering the best fuel consumption solution only, both fuel consumption and the operation costs reduce for 1 HWFET driving cycle, 2 HWFET driving cycles, and 3 HWFET driving cycles. The fuel consumptions reduce 6.07%, 21.64%, and 22.87%. The operation costs reduce 0.00%, 11.58%, and 18.26%, respectively, for 1 HWFET driving cycle, 2 HWFET driving cycles, and 3 HWFET driving cycles.

Based on the analysis above, the conclusion can be made that the fuel consumption is the critical objective to determine which Pareto optimal solutions will be chosen as the final setting parameters.

5.5.3. Control strategy parameters optimization for PSD gear ratio =3.0

Although the optimal control strategy parameters are different with the different driving cycles, the trends to setup the parameters still can be obtained.

For HWFET driving cycles, in order to get the best fuel consumptions, the ranges between maximum *SOC* and minimum *SOC* are 0.6, 0.599, and 0.552, respectively for 1 HWFET driving cycle, 2 HWFET driving cycles, and 3 HWFET driving cycles. However, in order to have the best total operation cost, the ranges between maximum *SOC* and minimum *SOC* are 0.212, 0.208, and 0.233, respectively. The desired generator charge torque will be higher to get the best fuel consumption, compared to the torque for the best total operation cost. However, the desired motor discharge torque and the desired engine lowest torque will be lower to get the best fuel consumption. The engine's lowest speed is almost same for the best operation cost and the best fuel consumption.

For the UDDS driving cycles, the best operation cost and the best fuel consumption achieve the best simultaneously for 1 UDDS driving cycle. But for 2 UDDS driving cycles and 3 UDDS driving cycles, the optimal control strategy parameters have the same trend as the HWFET driving cycles.

Most researchers only used 1 driving cycle to optimize the control strategy parameters of HEV by using GA, because they assume that the number of driving cycles will not affect the control strategy parameters. But for PHEV, the number of driving cycles will obviously influence the control strategy parameters. When determining the control strategy parameters, at least three driving cycles should be considered based on the battery capacity in this study.

Table 5.2. PHEV Operations Costs and Fuel Consumptions with Baseline Rule–based Control Strategy

Item	1 UDDS	2 UDDS	3 UDDS	1 HWT.	2 HWT.	3 HWT.
Baseline Total Cost($)	0.235	0.568	0.949	0.289	0.587	0.898
Baseline Fuel(g)	46.13	309.53	714.81	14.16	330.65	661.25

Table 5.3. Objectives of the Output – 20 Tradeoff Solutions for 3 HWFET Driving Cycles

| No.	SOC_{max}	SOC_{min}	α_{g_charge}	$\alpha_{m\_discharge}$	$\alpha_{e\_opt\_low}$	$\alpha_{e\_opt\_high}$	$\alpha_{\omega e\_lau}$	Fuel Cons.(g)	Elec. Cost($US)	Total Cost($US)
1	0.8931	0.3415	0.7000	0.7267	0.5655	1.0915	0.8622	587.4029	0.2546	0.7344
2	0.7000	0.6000	0.7123	0.7808	0.6262	1.0012	0.8500	617.2907	0.0464	0.7133
3	0.7000	0.4673	0.7195	0.7000	0.7000	1.0547	0.8509	604.2579	0.1079	0.6606
4	0.7000	0.5996	0.7113	0.7772	0.6221	1.0027	0.8500	628.7101	0.0471	0.6801
5	0.8752	0.3719	0.7061	0.7000	0.5449	1.1000	0.8500	672.7689	0.2324	0.7399
6	0.8318	0.5050	0.7196	0.7552	0.6212	1.0994	0.8509	651.4669	0.1513	0.6844
7	0.8215	0.5084	0.7201	0.7626	0.6224	1.0993	0.8500	655.2454	0.1450	0.6903
8	0.8422	0.4036	0.7084	0.7028	0.6158	1.0975	0.8532	639.8811	0.2026	0.7150
9	0.7003	0.5230	0.7511	0.7004	0.6921	1.0582	0.8752	566.531	0.0822	0.6843
10	0.8088	0.4172	0.7158	0.7047	0.6128	1.0961	0.8549	667.3826	0.1810	0.7077
11	0.7044	0.5766	0.7510	0.7000	0.7000	1.0811	0.8774	616.8726	0.0593	0.6872
12	0.7039	0.5133	0.7105	0.7028	0.6995	1.0614	0.8637	579.6275	0.0882	0.6798
13	0.8324	0.4088	0.7083	0.7035	0.6161	1.1000	0.8531	559.7747	0.1958	0.7121
14	0.8691	0.3432	0.7001	0.7305	0.5602	1.0935	0.8618	559.4005	0.2426	0.7414
15	0.7000	0.4952	0.7112	0.7402	0.6680	1.1000	0.8500	548.7519	0.0953	0.6761
16	0.7050	0.5599	0.7304	0.7005	0.6734	1.0508	0.8689	708.7293	0.0673	0.6802
17	0.7000	0.4676	0.7193	0.7000	0.7000	1.0533	0.8509	544.5978	0.1078	0.6763
18	0.8107	0.4154	0.7159	0.7046	0.6122	1.0949	0.8549	510.0097	0.1827	0.7090
19	0.7003	0.4679	0.7194	0.7000	0.7000	1.0534	0.8518	539.349	0.1078	0.6882
20	0.7050	0.5603	0.7298	0.7005	0.6724	1.0503	0.8688	530.1569	0.0671	0.6836
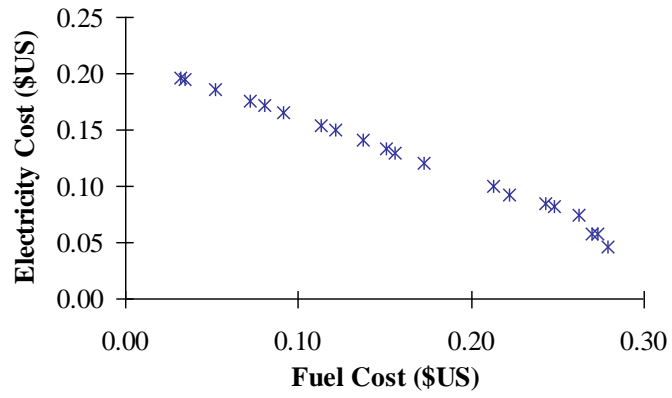
(a)
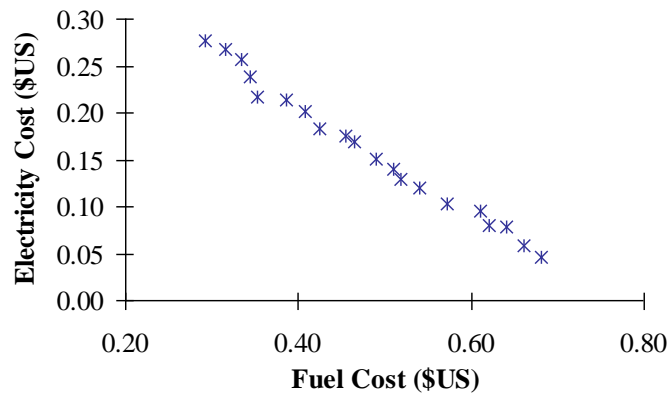
(b)
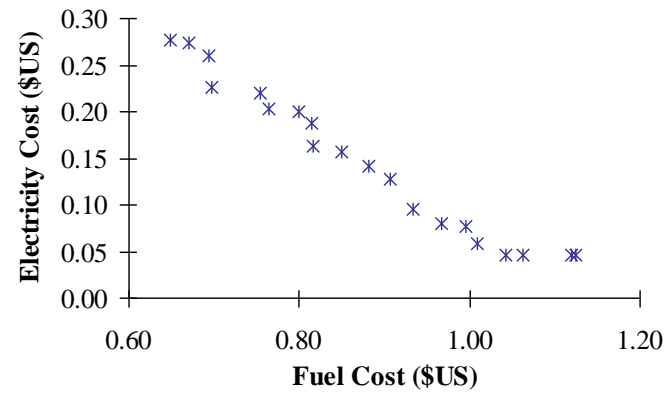
(c)

Figure 5.5. NSGA-II Pareto optimal results for UDDS. (a) 1 UDDS driving cycle. (b) 2 UDDS driving cycles. (c) 3 UDDS driving cycles.
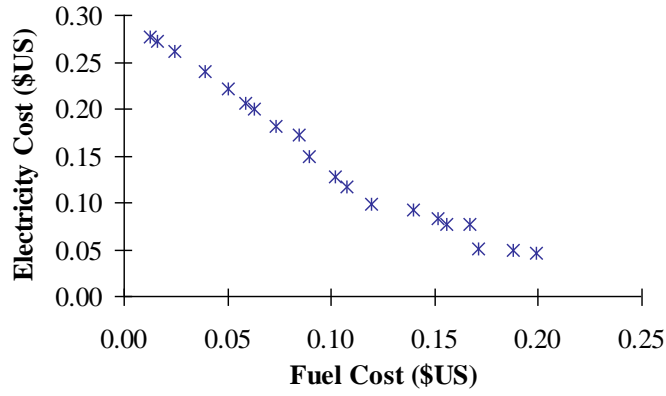
(a)
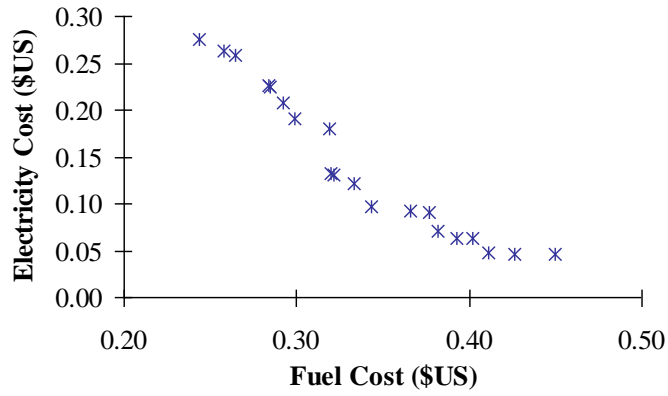
(b)
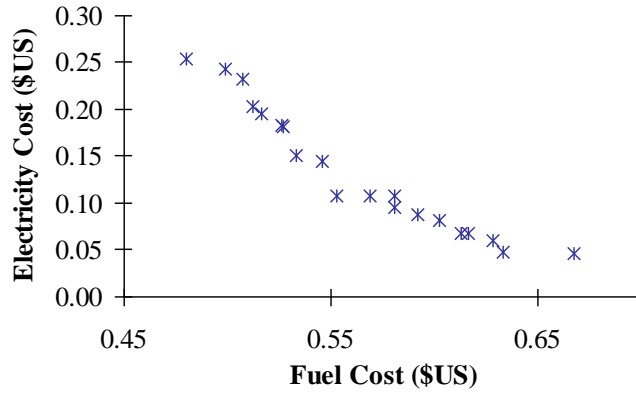
(c)

Figure 5.6. NSGA-II Pareto optimal results for HWFET: (a)1 HWFET driving cycle. (b)

2 HWFET driving cycles. (c) 3 HWFET driving cycles.

Table 5.4. PHEV NSGA-II Simulation Results in UDDS Driving Cycles – Control Strategy Parameters and Operations Costs

Item	Best Total Costs			Best Fuel Consumptions		
	1 UDDS	2 UDDS	3 UDDS	1 UDDS	2 UDDS	3 UDDS
SOC_{max}	0.869	0.894	0.863	0.869	0.900	0.900
SOC_{min}	0.443	0.364	0.373	0.443	0.300	0.300
α_{g_charge}	0.794	0.877	0.920	0.794	0.867	0.998
$\alpha_{m\_discharge}$	0.800	0.799	0.794	0.800	0.710	0.800
$\alpha_{e\_opt\_low}$	0.561	0.572	0.700	0.561	0.668	0.644
$\alpha_{e\_opt\_high}$	1.095	1.049	1.064	1.095	0.901	1.100
$\alpha_{\omega e\_lau}$	0.850	0.851	0.951	0.850	1.100	0.917
Tot. Cost ($)	0.228	0.552	0.923	0.228	0.557	0.925
Cost Comparison	2.98%	2.82%	2.74%	2.98%	1.94%	2.53%
Fuel (g)	33.62	326.1	740.4	33.62	298.60	688.9
Fuel Comparison	27.12%	-5.35%	-3.58%	27.12%	3.53%	3.62%

Table 5.5. PHEV NSGA-II Simulation Results in HWFET Driving Cycles – Control Strategy Parameters and Operations Costs

Item	Best Total Costs			Best Fuel Consumptions		
	1 HWT.	2 HWT.	3 HWT.	1 HWT.	2 HWT.	3 HWT.
SOC_{max}	0.717	0.791	0.700	0.900	0.899	0.893
SOC_{min}	0.505	0.583	0.467	0.300	0.300	0.341
α_{g_charge}	0.916	0.729	0.720	1.036	0.942	0.700
$\alpha_{m\_discharge}$	0.800	0.799	0.700	0.745	0.789	0.727
$\alpha_{e\_opt\_low}$	0.700	0.693	0.700	0.615	0.648	0.566
$\alpha_{e\_opt\_high}$	1.100	1.100	1.055	0.906	1.036	1.091
$\alpha_{\omega e\_lau}$	0.850	0.852	0.851	0.850	0.852	0.862
Tot. Cost ($)	0.219	0.440	0.660	0.289	0.519	0.734
Cost Comparison	24.22%	25.04%	26.50%	0.00%	11.58%	18.26%
Fuel (g)	127.05	346.85	587.40	13.30	259.09	510.01
Fuel Comparison	-797.25%	-4.90%	11.17%	6.07%	21.64%	22.87%

5.6 Summary

The PHEV rule-based control strategy parameter optimization based on the genetic algorithm NSGA-II was studied in this chapter. It will save the vehicle controller calibration time and reduce the development cost to apply this approach as off-line optimization. The main study in this chapter focused on following:

- The NSGA-II objective functions were created based on the PHEV rule-based control strategy vehicle model. The constrains of the rule-based control strategy parameters were determined by evaluating the performance of the components and systems. The total generation of NSGA-II algorithm is set to 100. The crossover probability is 0.9 and the mutation probability is 0.01.

- The simulations of the baseline vehicle (PSD gear ratio = 3.0) for 1, 2, and 3 UDDS and HWFET driving cycles were implemented and the optimal simulations of the baseline vehicle at the different driving cycles also were discussed. Comparing the optimal simulation results with the baseline, the best fuel consumptions are improved at all of the driving cycles. However, the best total cost only are improved at 1 UDDS driving cycle and 3 HWFET driving cycles.

CHAPTER 6

OPTIMAL DESIGN OF PSD GEAR RATIO

6.1 Introduction

The HEVs perfectly combine the advantages of the conventional vehicles and electric vehicles. The power split HEVs are the highlight in the HEV family. Same as the other vehicles, the power split device (Transmission – e-CVT) design is one of the most important parts during the development of the power split HEV. The power split device gear ratio is one of the most critical parameters. The basic power split device gear ratio design is based on the vehicle performance requirements [72]. The gear ratio should ensure the vehicle to meet the acceleration, gradeability, maximum top speed requirements. With the development of the HEV study, the optimal methods [73], [74] are implemented to optimize the planetary gear parameters to lower the fuel consumption. However, because of the condition of assembly of planetary gear set, the series gear ratios are not continuous. The simulation results cannot meet the practice requirements.

An innovative six step design approach to optimize the PSD gear ratio to minimize the fuel consumption and operation cost is presented in this chapter. Figure 6.1 shows the flow chart of the design procedure. The related study from step 2 to step 5 has been discussed in Chapter 2 to Chapter 5. This chapter will focus on step 1 and step 6.
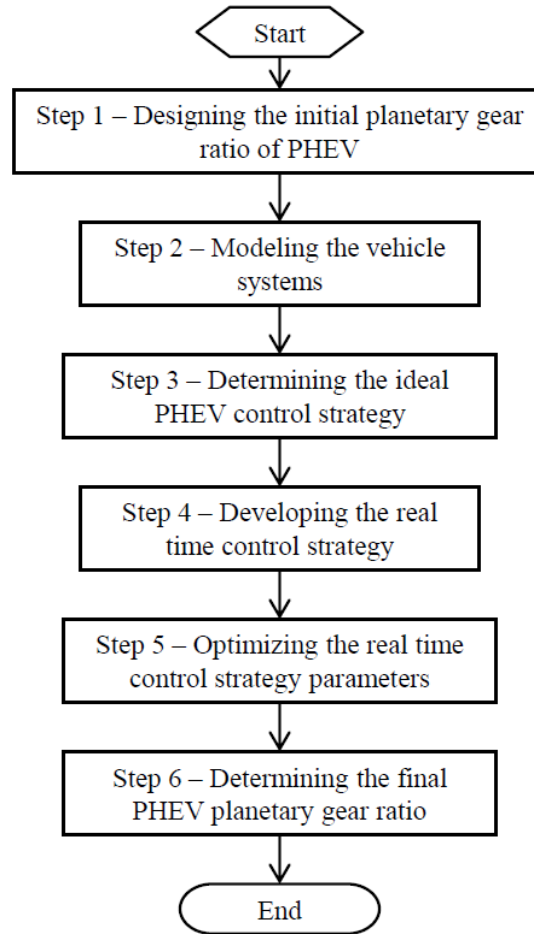
Figure 6.1. Flow chat of six-step approach to design PHEV PSD gear ratio

6.2 Determination of Initial PSD Gear Ratio

Rearranging (2.10) to express the speed function of planetary gear components as following:

$$\omega_s + k\omega_r = (1+k)\omega_c \qquad (6.1)$$

(6.1) is a plane equation, which is called the Characteristic Speed Plane (CSP), in the Cartesian Coordinate System, ω_r, ω_c, ω_s represented by the x, y and z axes, respectively (Figure 6.2).

Figure 6.2. Relationship between characteristic speed plane with maximum vehicle performance plane

The CSP shows the working range of the planetary gear. The plane *A* in Figure 6.2 represents the CSP, where A_1A_2 is located at plane *abcd,* which is parallel to the plane *xy,* and represents the speed relationship between the carrier and the ring gear when the sun gear is running a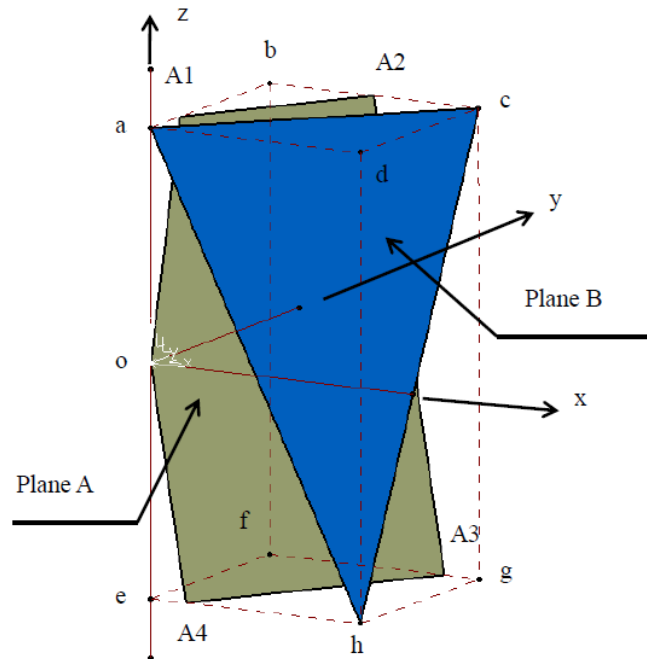t highest speed. A_2A_3 is located at plane *bcgf,* which is parallel to the plane *xz,* and represents the speed relationship between the sun gear and the ring gear when the carrier gear is running at highest speed. A_3A_4 is located at plane *cdgh,* which is parallel to the plane *yz,* and represents the speed relationship between the carrier and the sun gear when the ring gear is running at highest speed. Plane *B* was created when $\omega_r = \omega_{r,max}$, $\omega_c = \omega_{c,max}$ and $\omega_s = \omega_{s,max}$. The normal vector of plane *A* and *B* are $\boldsymbol{u} = [k, -(k+1), 1]$ and $\boldsymbol{v} = (2/\omega_{r,max}, -2/=\omega_{c,max}, 1/=\omega_{s,max})$.

In order to have better vehicle performance, the engine and motor should have a wider range of speed regulation. This means the smaller the angle between plane A and B is the better the vehicle performance will be. The angle between plane A and B can be calculated as follows:

$$\theta(A, B) = \cos^{-1} \frac{\vec{u} \cdot \vec{v}}{|\vec{u}||\vec{v}|} \tag{6.2}$$

6.3 PSD Planetary Gear Ratio Numerical Analysis

6.3.1. Initial planetary gear ratio

From (6.2), the analyses to the planetary gear ratio variation with the maximum speeds of the traction motor, the engine and the generator/motor are illustrated in Figures 6.3, 6.4 and 6.5. The optimal planetary gear ratio affects the maximum speeds of the engine, the traction motor and the generator/motor. The optimal planetary gear ratio will be decreased with the increase of the designed maximum traction motor speed (Figure 6.3), the decrease of the designed maximum engine speed (Figure 6.4), and the decrease of the designed maximum generator/motor speed (Figure 6.5).

Based on the vehicle information of Appendix I, the curve of the angle between plane A and B with the planetary gear ratio was determined in Figure 6.6. The minimum angle is 0.03 (rad) at $k=3.08$. The gear ratios from 2.6 to 3.4 were considered for the further simulation.
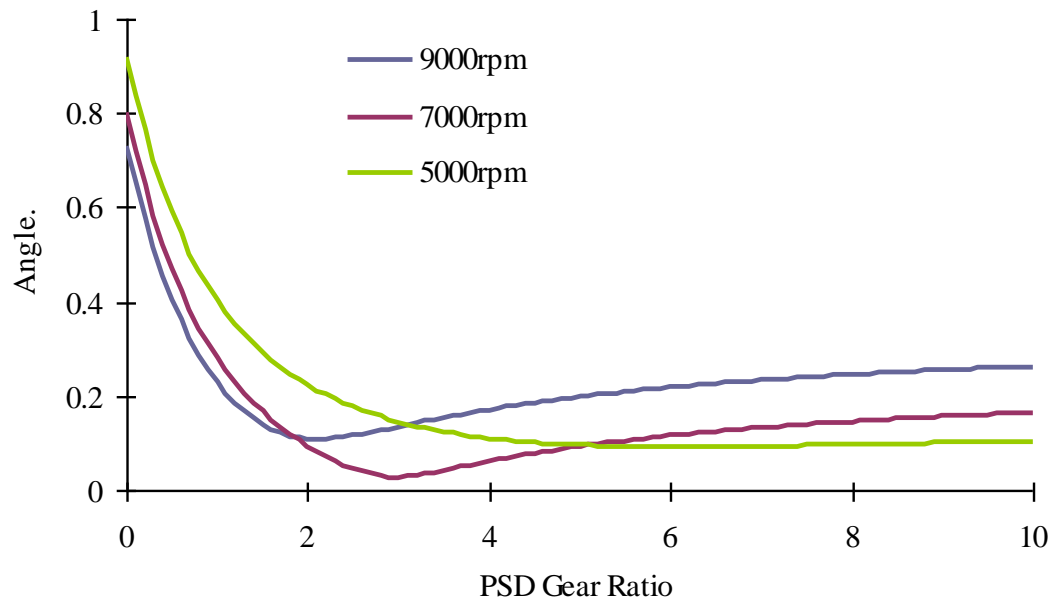
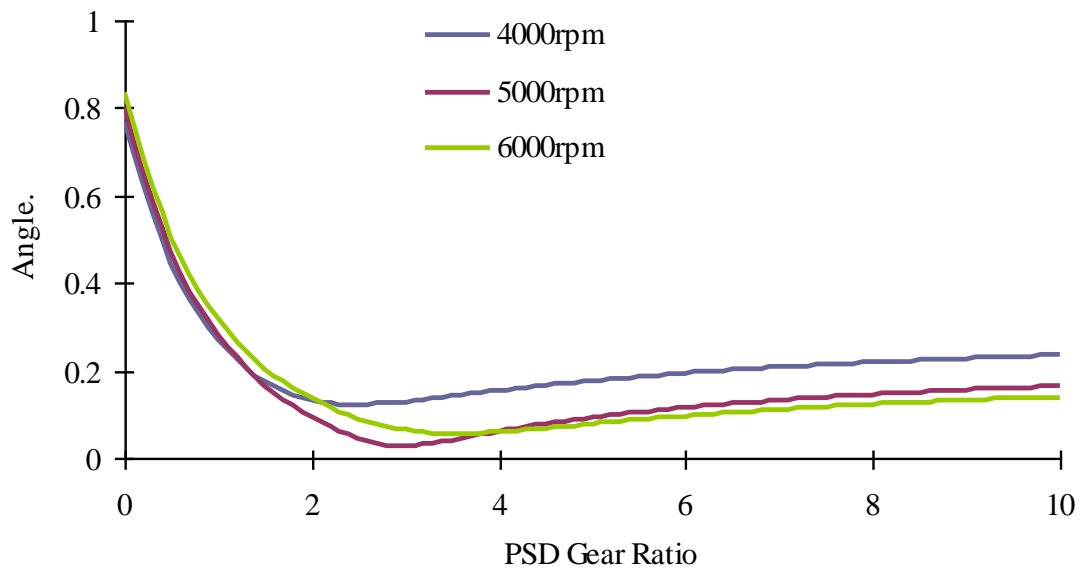Figure 6.3. Planetary gear ratio versus maximum ring gear speed ($\omega_{r,max}$)

Figure 6.4. Planetary gear ratio versus maximum carrier speed ($\omega_{c,max}$)
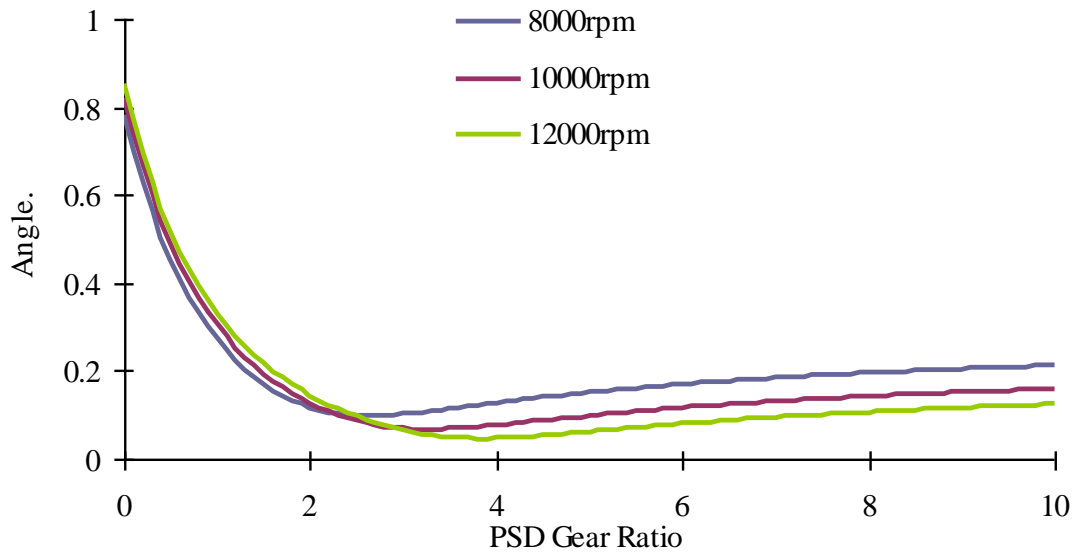
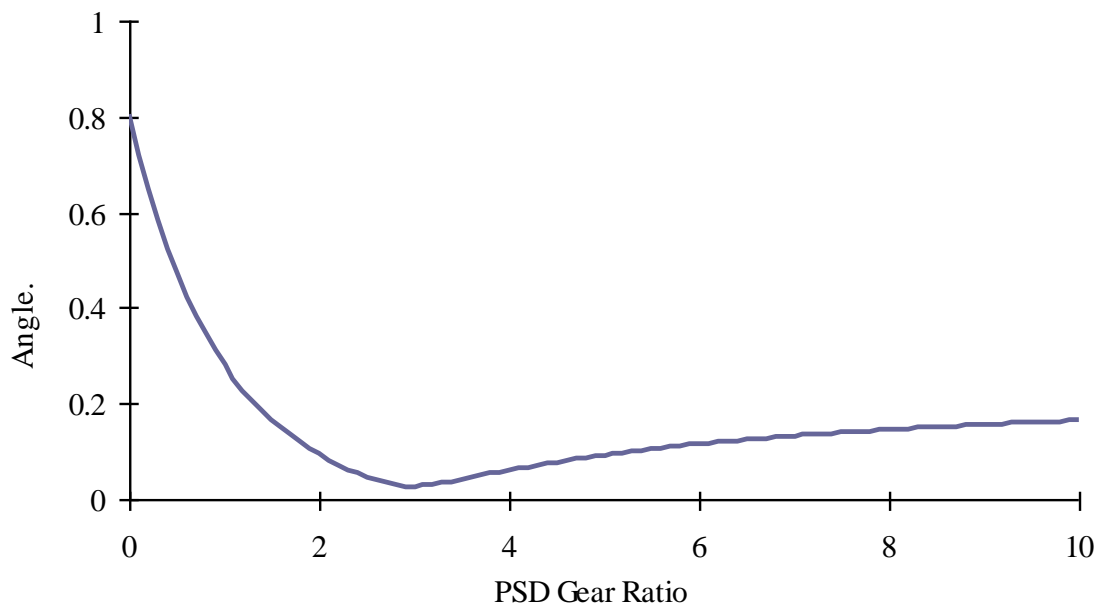Figure 6.5. Planetary gear ratio versus maximum sun gear speed ($\omega_{s,max}$)

Figure 6.6. Initial PSD gear ratio

6.4 Planetary Gear Condition of Assembly

Consideration of the condition of assembly [75], the determination of the tooth number of the planetary gear train will be based on the gear ratio. Assuming that the ring gear is fixed when designing the tooth number of the planetary gear train, the sun gear is the driving gear, and the carrier is the driven component. From equation (2.10), the gear ratio between the sun gear and the carrier i is:

$$i=1+k \tag{6.3}$$

The relationship between the tooth number of planetary gear train – Z_s, Z_r, and Z_c – is:

$$Z_c = \frac{Z_r - Z_s}{2} = \frac{i-1}{2} Z_s \tag{6.4}$$

Based on the condition of assembly:

$$\frac{Z_r + Z_s}{n} = C \tag{6.5}$$

Combining the equations from (6.3) to (6.5):

$$Z_s : Z_c : Z_r : C = 1 : \frac{i-2}{2} : (i-1) : \frac{i}{n} \tag{6.6}$$

Table 6.1. shows all of the gear ratio which meet the equation (6.6) from $k=2.6$ to $k=3.4$.

Table 6.1. The Tooth Number Which Meet the Condition of Assembly From Gear Ratio 2.6 to 3.4

k	C	Z_a	Z_b	Z_c
2.60	24	20	52	16
2.75	20	16	44	14
2.90	26	20	58	19
3.00	24	18	54	18
3.20	28	20	64	22
3.25	34	24	78	27
3.40	22	15	51	18

6.5. PSD Gear Ratio Optimization Design

The optimization simulations of the power split PHEV at different gear ratios are carried out through NSGA-II for the UDDS and HWFET driving cycles. The different numbers of the driving cycles are used in the simulations to evaluate the influence on the rule-based control strategy parameters. Following are driving cycles used during the simulation to evaluate the driving cycle numbers effects to the operation costs including fuel consumptions and electricity costs at different planetary gear ratios between 2.6 to 3.4:

CASE I: UDDS – 1, 2, 3 driving cycles.

CASE II: HWFET – 1, 2, 3 driving cycles.

Based on the driving cycle numbers and the gear ratios from 2.6 to 3.4, the simulation matrix is set up. Figure 6.7- Figure 6.12 show the simulation results.

For 1 UDDS driving cycle, both fuel consumptions and operation costs decrease with the increase of gear ratios. For 2 UDDS driving cycles, the fuel consumptions decrease with the increase of the gear ratios. However, both of the lowest operation costs and fuel consumptions still are at gear ratio 3.4. For 3 UDDS driving cycles, the lowest economy fuel consumption and operation cost can be found at gear ratio 2.9.

For 1 HWFET driving cycle, both fuel consumption and operation costs have the same trend as the UDDS driving cycles, as they decrease with the increase of the gear ratio. For 2 and 3 UDDS driving cycles, the economy fuel consumption can be found at gear ratio 3.0 and 3.2, respectively. The economy operation costs are shown at gear ratio 3.25 or 3.4.

Table XI shows the differences of the maximum and minimum optimal fuel consumptions between gear 2.6 and 3.4. When the number of driving cycles increases, the difference also increases. This is because the vehicle was run at CD mode at the first or first and a half driving cycle, and CS mode at the third driving cycle.

From the simulation results above, the designed all electric operation range (AEOR) will influence the PSD gear ratio selection. In other word, the battery capacity will influence the PSD gear ratio selection. If the designed AERO is larger and the more battery capacity will be chosen, the higher PSD gear ratio will be selected. If the designed AERO is lower and the less battery capacity will be chosen, the lower PSD gear ratio will be selected.

However, the PSD planetary gear design is a trade-off process. When designing a power split PHEV planetary gear, not only are the fuel consumption and operation costs considered, but also the vehicle performance, emission, gear weight, strength, standards etc.

Table 6.2. The Differences of the Maximum and Minimum Fuel consumptions at Gear Ratio 2.6 to 3.4

# of Driving Cycle	1	2	3
UDDS	3.40	11.35	25.89
HWFET	2.54	27.85	62.28
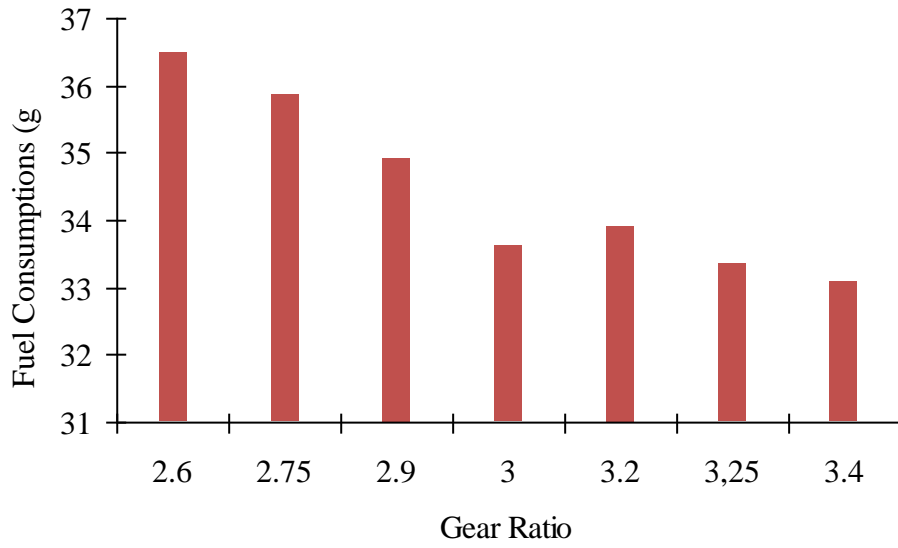
(a)
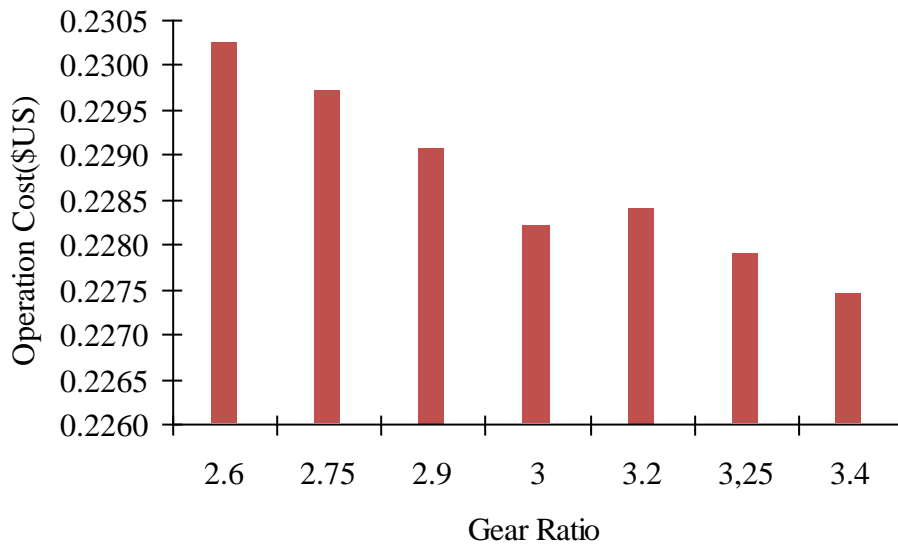
(b)

Figure 6.7. Fuel consumption and operation cost for 1 UDDS driving for various PSD gear ratios. (a) Best fuel consumptions. (b) Best operation costs.

(a)

(b)

Figure 6.8. Fuel consumption and operation cost for 2 UDDS driving cycle for various PSD gear ratios. (a) Best fuel consumptions. (b) Best operation costs.

(a)

(b)

Figure 6.9. Fuel consumption and operation cost for 3 UDDS driving cycles for various PSD gear ratios. (a) Best fuel consumptions. (b) Best operation costs.

(a)

(b)

Figure 6.10. Fuel consumption and operation cost for 1 HWFET cycle for various PSD gear ratios. (a) Best fuel consumptions. (b) Best operation costs.

(a)
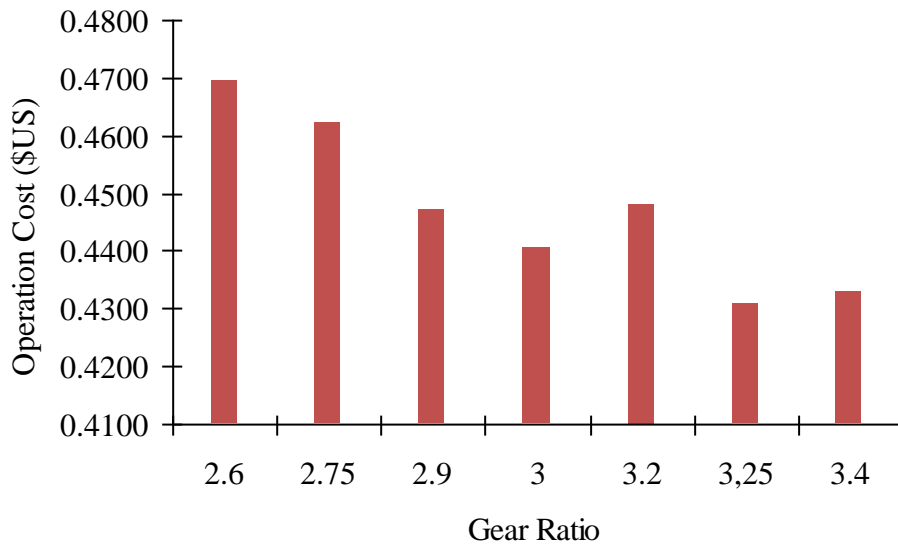
(b)

Figure 6.11. Fuel consumption and operation cost for 2 HWFET driving cycles for various PSD gear ratios. (a) Best fuel consumptions. (b) Best operation costs.
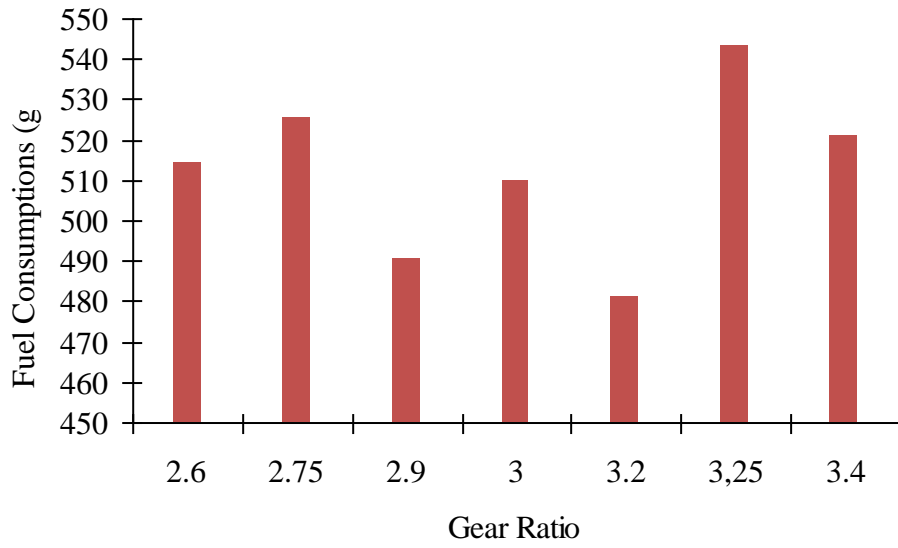
(a)
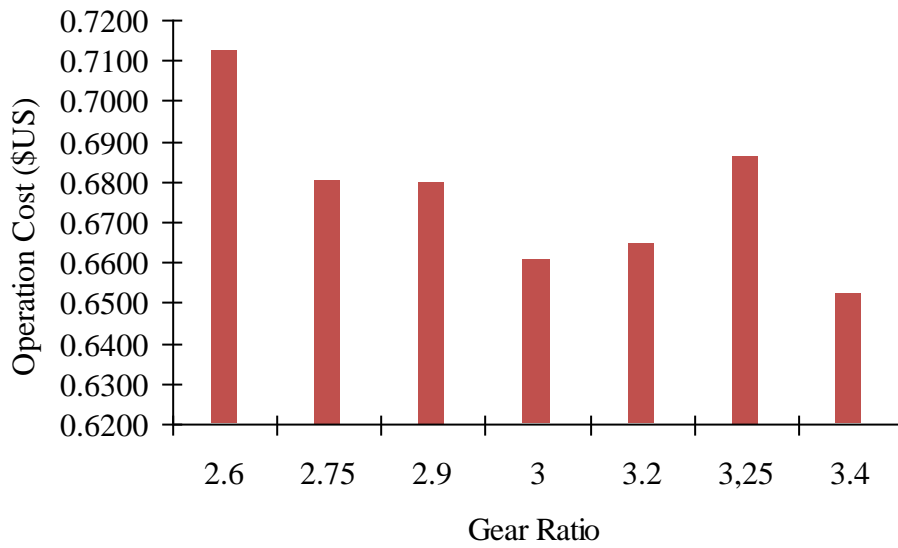
(b)

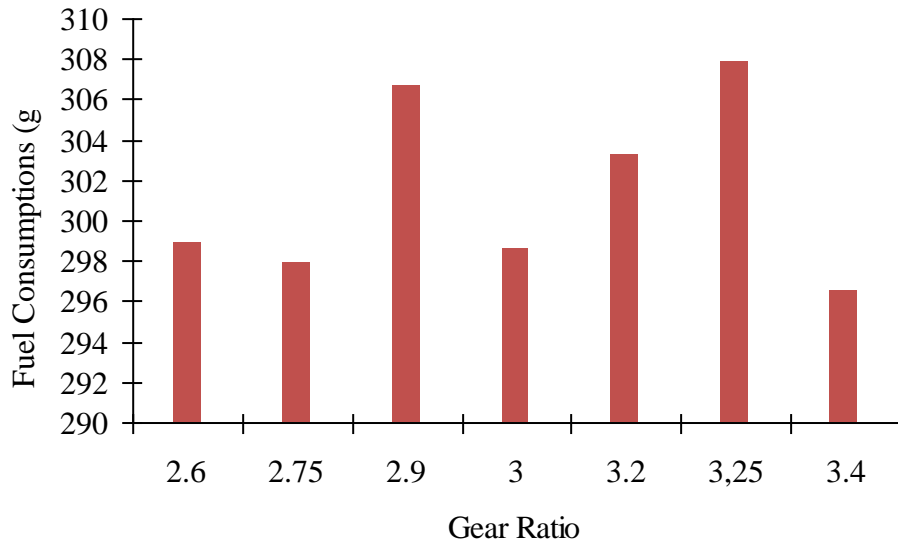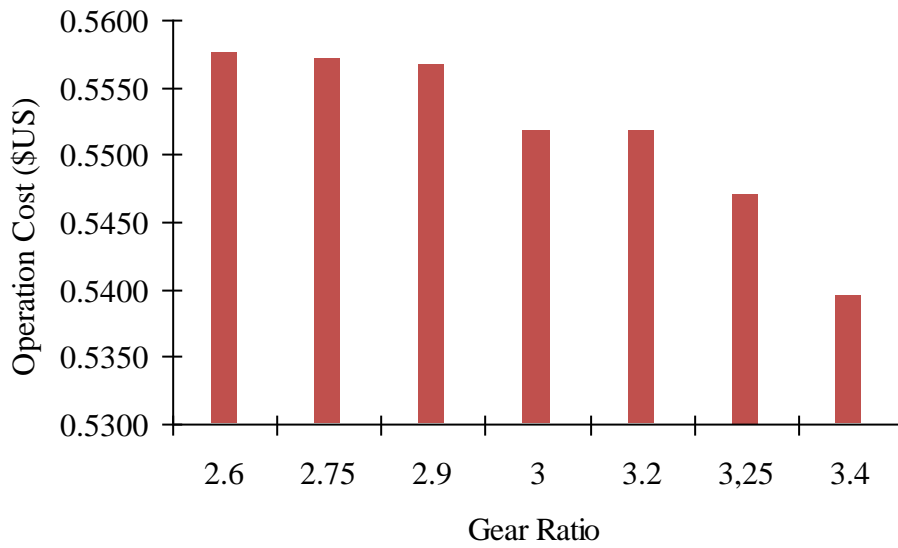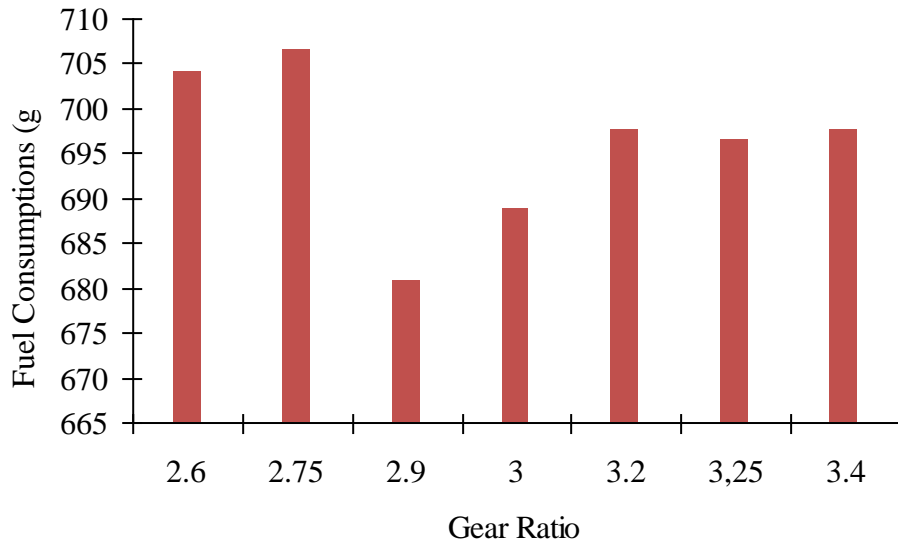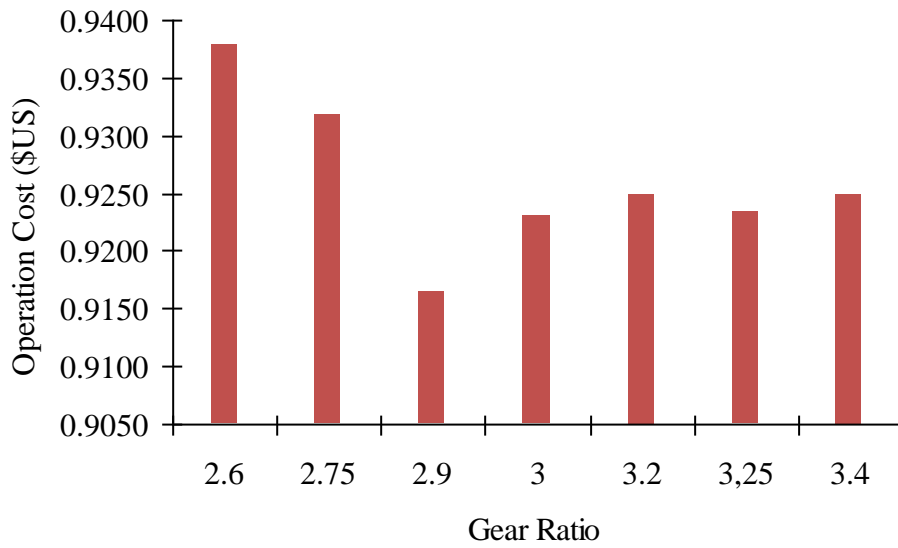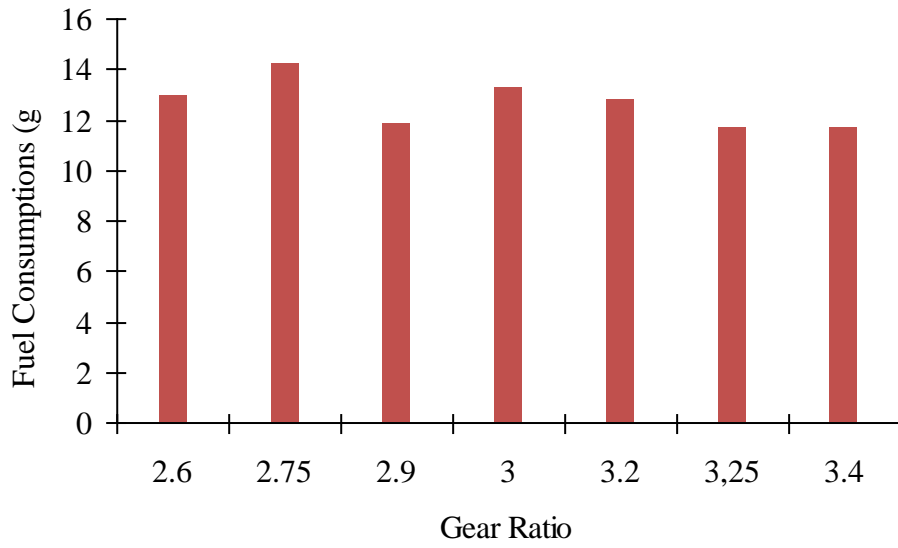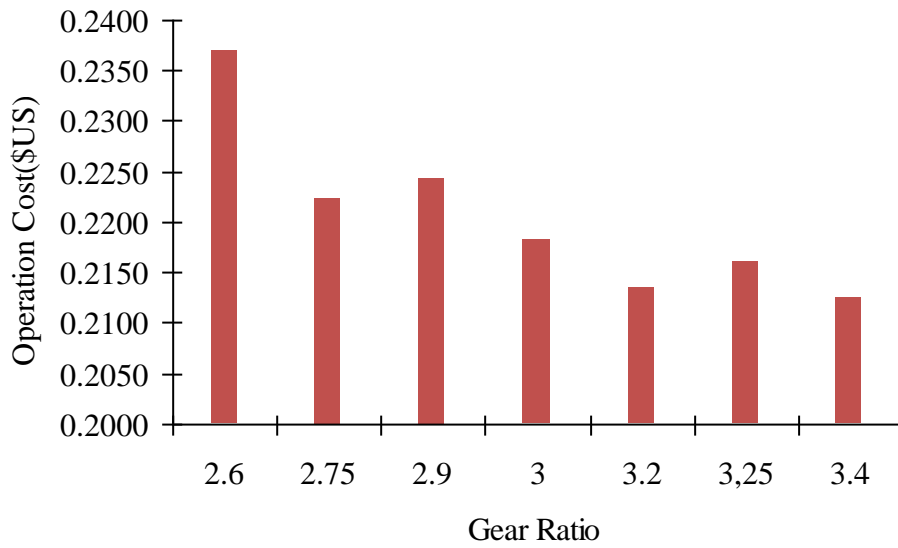Figure 6.12. Fuel consumption and operation cost for 3 HWFET driving cycles for various PSD gear ratios. (a) Best fuel consumptions. (b) Best operation costs.
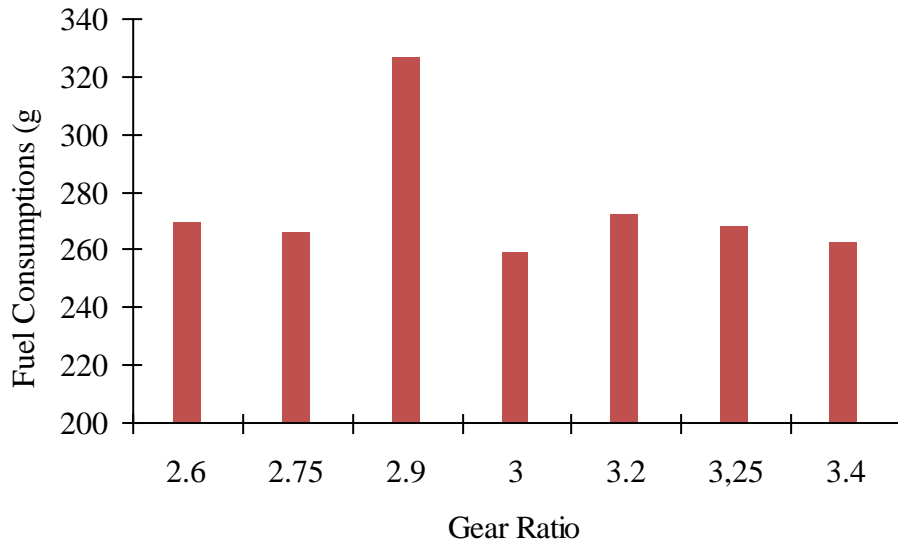
6.6 Summary

An innovative PSD gear ratio design approached of the single mode power split PHEV was presented in this chapter. The NSGA-II algorithm was used to optimize the rule-based control strategies parameters at the different diving cycles and different gear ratios. An important conclusion obtained is that the designed AEOR is the key parameter to determine the PSD gear ratio. The main study in this chapter focused on following:

- The initial PSD gear ratio determination was presented. It was based on the main power sources maximum speed to ensure the engine and motor to have the wider operation ranges.

- The condition of assembly of PSD planetary gear was discussed and the available gear ratios were analysed at a reasonable range.

- The fuel consumptions and operation costs were simulated by NSGA-II, therefore determining the best PSD gear ration to minimum the PHEV fuel consumption and operation cost.

From the above chapters discussed, the innovative PSD gear ratio design approached of the single mode power split PHEV can be summarized as following :

- Step 1 – Designing the initial planetary gear ratio of PHEV: the gear ratio range was be determined based on the vehicle performance requirements.

- Step 2 – Modeling the vehicle systems: the dynamic PSD and powertrain models were used for the PHEV energy management simulations.

- Step 3 – Determining the ideal PHEV control strategy: DP was employed to optimize the control strategy.

- Step 4 – Developing the real time control strategy: the rule based control strategy was developed based on DP simulation results:

- Step 5 – Optimizing the rule-based control strategy parameters: NSGA-II was used to optimize the rule-based control parameters.

- Step 6 – Determining the final PHEV planetary gear ratio: two typical driving cycles - the UDDS and HWFET - were used to determine the PSD gear ratio.

CHAPTER 7

CONCLUSIONS AND FUTURE WORKS

7.1 Summary and Conclusion

The main objective of this study was to present an innovative design approach to optimize the single mode power split PHEV PSD gear ratio to minimize the vehicle fuel consumption and operation cost in this thesis.

The works that have been done on this research and main conclusions are summarized as follows:

- The backward-looking power split PHEV model was effectively created under the Matlab environment based on the power source testing results. It provided a simulation platform for the vehicle control strategy development. The interaction between the sub-systems can be analyzed, the vehicle performance, such as fuel economy and drivability, can be evaluated, the components size also can be studied by using this vehicle model. The model accurate is enough for the energy consumption simulations. It also laid the solid foundation for the close-loop forward looking vehicle model simulation.

- The DP optimal control model of PHEV was created under the condition of given driving cycles to optimize the vehicle fuel consumption and operation cost. The state variable of the optimal control model is *SOC*, the control variables are the motor and generator torques. The step was determined based on the given driving cycles. The assumption was made that the vehicle consumption is constant within each steps, therefore changing the continuous optimal control to a series of sub-

problems. The optimal control strategy was obtained by the DP approach. The purpose of this study is to determine the global optimal fuel consumption and operation cost as the benchmark of the real-time PHEV control strategy.

- The rule-based PHEV control strategy was developed by studying the vehicle operation modes. The control strategy parameters were determined based on the engine, motor, battery internal resistance, and the DP simulation results. Comparing with the fuel consumption based on the DP simulation results, the fuel consumption increases 12.98%.

- The multi-objective optimal model for the PHEV rule-based control strategy parameters was presented based on the non-dominated sorting genetic algorithm (NSGA-II). The control strategy parameters were optimized by using the backward looking vehicle model to calculate the objectives and constrains. The simulation results show that the optimized rule-based control strategy can reduce the vehicle fuel consumption 3.53% for 2 UDDS driving cycles and 21.64% for 2 HWFET driving cycles.

- An innovative design method for the single mode power split PHEV PSD gear ratio was discussed. The purpose of this study is to find an approach to design the PSD gear ratio by considering the vehicle performance and fuel consumptions. The significant of this method is not only improve vehicle performance and fuel consumptions, but also to reduce the vehicle PSD development time and save the cost.

7.2 Future Works

The PHEV technology is still a new area for the automotive industry. There are many problems to be solved in the future. For this study, the further research is as following:

- Forward-looking vehicle model development: In order to describe the vehicle operate in the real conditions, the forward looking vehicle model should be developed. The forward looking vehicle model is a close loop control system, including the driver model to simulate the actions of brake and acceleration pedals. The model should include the transient characteristics of the sub-system, such as clutches on and off. Some sub-system model should be improved. The engine emission did not consider in this study. The future work should consider the engine fuel consumption and emissions.

- Adaptive control strategy study: Because the driver operations and road conditions are random, it is difficult to apply the specific driving cycle optimal control strategy to the actual vehicle. In order to simulate the random driver operations and road conditions, the fuzzy control logic or neural network can be used. The real time on line recognition function to the driver intention, driving cycle characteristic parameters should be considered in the control strategy.

APPENDIX A   PHEV Vehicle Specification

Table A.1. PHEV Vehicle Specification

Vehicle Mass [kg]	Coefficient of Aerodynamic Drag	Frontal Area of Vehicle [m^2]
1,250	0.30	2.52
Wheel Radius [m]	Coefficient of Rolling Resistance	Air Density [kg/m^3]
0.287	0.015	1.184
Engine		
Max Power [kW]	Max torque [Nm]	Max Speed [rpm]
57 @ 4,500 rpm	111 @ 4,200 rpm	5,000
Motor I		
Rated Power [kW]	Rated Torque [Nm]	Max Speed [rpm]
35 @ 940 to 2,000 [rpm]	305 @ 0 to 940 [rpm]	7,000
Motor II		
Rated Power [kW]	Rated Torque [Nm]	Max Speed [rpm]
15	60	11,000
Battery		
Voltage [V]	Capacity [Ah]	
312	13	

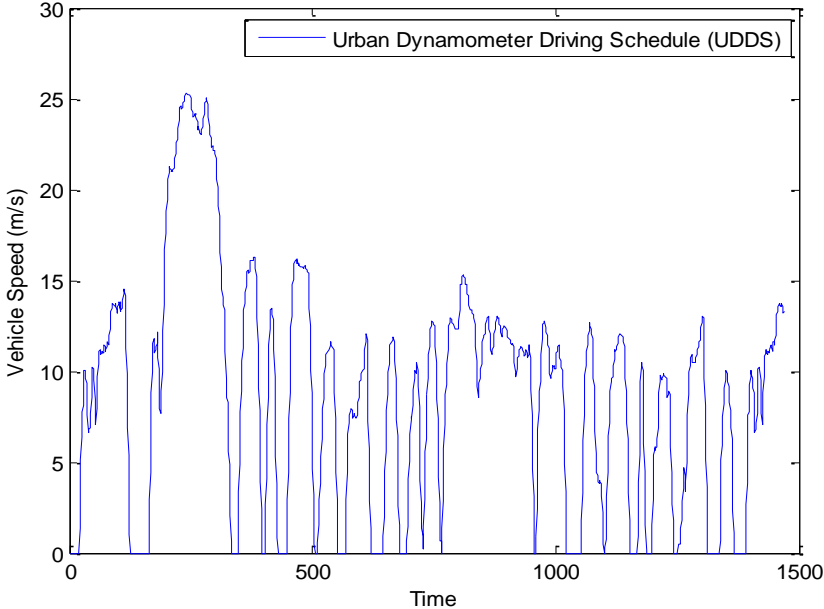# APPENDIX B   UDDS and HWFET Driving Cycles

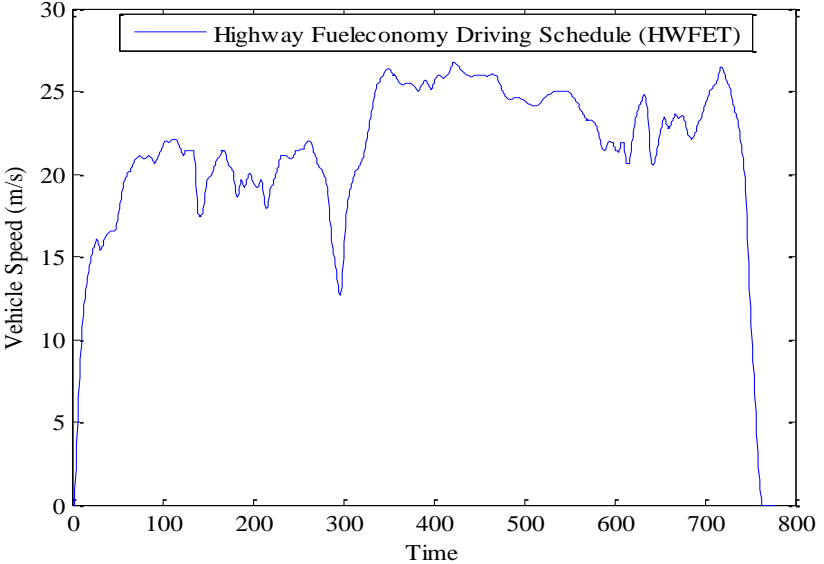Figure B.1. Urban dynamometer drive schedule (UDDS) driving cycle

Figure B.2. Highway fuel economy drive schedule (HWFET) driving cycle

Table B.1. Driving Cycles Specification

Driving cycle	UDDS	HWFET
Max. Speed (km/h)	91.24	96.39
Ave. Speed (km/h)	31.53	76.27
Distance (km)	11.99	16.51
Time (s)	1369	779

REFERENCES

1. U.S. Environmental Protection Agency, "INVENTORY OF U.S. GREENHOUSE GAS EMISSIONS AND SINKS: 1990 – 2009", EPA 430-R-11-005 APRIL 15, 2011

2. http://www.eia.gov/

3. D. Bennett, "Zero Emission Vehicles: The Air Pollution Messiah? Northeastern States Mandate ZEVs Without Considering the Alternatives or Consequences", Volume 20, William & Mary Environmental Law & Policy Review, 1996.

4. www.afdc.energy.gov/afdc/data/

5. http://www.afdc.energy.gov/

6. K.Morita, "Automotive power source in 21st century," *JSAE Review*, 2003, 24(1): 3-7

7. K. Okamoto, "Overview of current and future hybrid technology," *Proc of the Symposium on Advanced Automotive Powerplants and Energy Resources*, Beijing: China SAE, 2002. 89-94

8. C. Chan, "The state of the art of electric and hybrid vehicles," *Proc of IEEE*, 2002, 90(2): 247-275

9. A.Wyczalek, " Hybrid electric vehicles year 2000 status," *IEEE AES Systems Magazine*, 2001, 16(3): 15-19

10. W.G. Livezey, "Input-split-power, Output-split-power, Compound-split-power, Power Train," *US Patent* 3,470,769, issued Nov. 1969.

11. S. Abe, S. Sasaki, H. Matsui, K. Kubo, "Development of Hybrid System for Mass Productive Passenger Car," *JSAE Proc.* 9739543, pp. 21-24.

12. T. M. Grewe, B. M. Conlon, A. G. Holmes, "Defining the General Moto 2-Mode Hybrid Transmission," *SAE Paper* 2007-01-0273.

13. M. Schulz, "Circulating Mechnical Power in a Power-split Hybrid Electric Vehicle Transmission," *Proc. Instn Mech. Engrs*., Vol. 208, Part D: J. Automotive Engineering, 2004.

14. http://www.getrag.de/

15. J. M. Miller, "Hybrid Electric Vehicle Propulsion System Architectures of the e-CVT Type," *IEEE Transactions on Power Electronics,* Vol. 21, No. 3, May, 2006.

16. D. Zhang, J. Chen, T. Tsieh, J. Rancourt, M.R. Schmidt, "Dynamic Modeling and Simulation of Two-Mode Electric Variable Transmission," *Proc. of IMechE* Vol 215, pp. 1217-1223, 2001.

17. D. Rizoulis, J. Burl, and J. Beard, "Control Strategies for a Series-Parallel Hybrid Electric Vehicle," *SAE Paper* 2001-01-1354, 2001.

18. J. Liu, "Modelling, Configuration and Control Optimization of Power-split Hybrid Vehicles,"*Dissertation*, University of Michigan.

19. R. Zanasi, and F. Grossi, "Modeling and control of Power-split Hybrid electric Vehicle," *In Proc. Of IEEE Vehicle Power and Propulsion Conference (VPPC)*, Sept. 1-3, 2010

20. J. Wishart, Y. Zhou, Z. Dong, and F. Firmani, "Dynamic Modeling and Simulation of a multi-regime Hybrid Vehicle Powertrain Architecture," *Proc. Of International Journal of Electric and Hybrid Vehicles, Vol. 1 Page 188-219*, 2008

21. M. P. O'Keefe and T. Markel, "Dynamic programming applied to investigate energy management strategies for a plug-in HEV," National Renewable Energy Lab., CO, Report No. NREL/CP- 540-40376, 2006.

22. C.-C. Lin, H. Peng, and J. Grizzle, "A stochastic control strategy for hybrid electric vehicles," in Proceedings of the American Control Conference, 2004.

23. B. Bole, S. Coogan, C. Cubero-Ponce, D. Edwards, R. Melsert, D. Taylor, " Energy Management Control of a Hybrid Electric Vehicle with Two-Mode Electrically Variable Transmission," *EVS26 International Battery, Hybrid and Fuel Cell Electric Vehicle Symposium,* Los Angeles, California, May 6 - 9, 2012

24. S. Moura, H. Fathy, D. Callaway, J. Stein, "A Stochastic Optimal Control Approach for Power Management in Plug-In Hybrid Electric Vehicles" IEEE Trans. Contr. Sys. Techn. 19(3): 545-555, 2011

25. C-C. Lin, H. Peng, J.W. Grizzle, "Power management strategy for a parallel hybrid electric truck," IEEE Transactions on Control Systems Technology, 2003, 11 (6): 839-849

26. N. Kim S. Cha, and H. Peng, "Optimal Control of Hybrid Electric Vehicles Based on Pontryagin's Minimum Peinciple," *IEEE Transactions on Control System Technology*, Vol. 19, No. 5, 1279-1287, September 2011.

27. L. Serrao, G. Rizzoni, "Optimal Control of Power Split for a Hybrid Electric Refuse Vehicle," *in Proc. 2008 American Control Conf.*, Seattle, WA, 2008, pp 4498-4503.

28. G. Rousseau, D. Sinoquet, P. Rouchon, "Constrained Optimization of Energy Management for a Mild-Hybrid Vehicle," *Oil-Gas Science and Technology, IFP*, Vol. 62, No. 4, 2007, pp. 623-624.

29. X. Wei, L. Guzzella, V. I. Utkin, G. Rizzoni, "Model-Based Fuel Optimal Control of Hybrid Electric Vehicle Using of Hybrid Electric Vehicle Using Variable Structure Control Systems," *ASME J. Dynamic Syst., Meas., Control*, vol. 129, No. 1, January 2007, pp. 13-19.

30. C. Kim, E. NamGoong, and S. Lee, "Fuel Economy Optimization for Parallel Hybrid Vehicles with CVT," *SAE Paper* 1999-01-1148, 1999.

31. G. Paganelli, T.M. Guerra, S. Delprat, J.J. Santin, M. Delhom, E. Combes, "Simulation and Assessment of Power Control Strategies for a Parallel Hybrid Car," *J. Automobile Engineering, also in Proc. Of the Institution of Mechanical Engineers IMechE, SAE International*, 214, pp. 705-718, 2000.

32. G. Paganelli, G. Ercole, A. Brahma, Y. Guezennec, G. Rizzoni, "General Supervisory Control Policy for the Energy Optimization of Charge-Sustaining Hybrid Electric Vehicles," *JSAE Review*, Vol. 22, No. 4, pp. 511-518, 2001.

33. G. Paganelli, M. Tateno, A. Brahma, G. Rizzoni, and Y. Guezennec, "ContrDevelopment for a Hybrid-Electric Sport-Utility Vehicle: Strategy, Implementation and Field Test Results," *Proceedings of the American Control Conference*, Arlington, VA, 2001.

34. C. Musardo, G. Rizzoni, and B. Staccia, "A-ECMS: An Adaptive AlgoHybrid Electric Vehicle Energy Management," *Proc. of IEEE Conference on Decision and Control*, Seville, Spain, 2005.

35. H. Banvait, X. Lin, S. Anwar, and Y. Chen, "Plug-in Hybrid Electric Vehicle Energy Management System Using Particle Swarm Optimization," *World Electric Vehicle Journal*, Vol. 3 - ISSN 2032-6653, 2009.

36. J. Liu and H. Peng, "Modeling and Control of Power-split Hybrid Vehicle," *IEEE Transactions on Control System Technology*, Vol. 16, No. 6, November 2008.

37. J. Liu, and H. Peng, "Control Optimization for a Power-Split Hybrid Vehicle," *Proceedings of the 2006 American Control Conference*, Minneapolis, MN, 2006.

38. K. L. Butler, K. M. Stevens, M. Ehsani, "A versatile computer simulation tool for design and analysis of electric and hybrid drive trains," *SAE Paper 970199*, 1997.

39. M. R. Cuddy, K. B.Wipke, "Analysis of the fuel economy benefit of drivetrain hybridization," *SAE Paper 970289*, 1997.

40. K. B. Wipke, M. R. Cuddy, and S. D. Burch, "ADVISOR 2.1: A user-friendly advanced powertrain simulation using a combined backward/forward approach," *IEEE Trans. Vehicular Technol.*, vol. 48, no. 6, pp. 1751–1761, Nov. 1999.

41. T. Markel, A. Brooker, T. Hendricks, V. Johnson, K. Kelly, B. Kramer, M. O'Keefe, S. Sprik, and K.Wipke, "ADVISOR: A systems analysis tool for advanced vehicle modeling," *J. Power Sources*, vol. 110, no. 2, pp. 255–266, Aug. 2002.

42. "PSAT Training," *http://www.anl.gov/*

43. http://www.powersimtech.com/

44. http://vtb.engr.sc.edu/vtbwebsite/#/Overview

45. Won, J. S., Langari, R., and Ehsani, M., (2005), "An Energy Management and Charge Sustraining Strategy for a Parallel Hybrid Vehicle With CVT," *IEEE Transactions on Control System Technology*, Vol. 13, No. 2, pp. 313-320.

46. P. Pisu, G. Rizzoni, C. Musardo, and B. Staccia, "A Comparative Study of Su;ervisory Control Strategies for Hybrid Electric Vehicles," *Proc. Of International Mechanical Engineering Congress and Exposition*, Anaheim, CA, 2004.

47. R. Bellman, "Dynamic Programming," Princeton University Press, 1957.

48. C.-C. Lin, H. Peng, J. Grizzle, and J.-M. Kang, "Power management strategy for a parallel hybrid electric truck," IEEE Transactions on Control Systems Technology, vol. 11, no. 6, pp. 839–849, 2003.

49. *http://www.eia.doe.gov*

50. P. Rutquist, "Optimal control for the energy storage in a hybrid electric vehicle," *Proceedings of the 19th International Electric Vehicle Symposium*, Busan, Korea, 2002. 1133-1139

51. R. E. Larson, J. L. Casti, "Principles of dynamic programming. Part I: Basic analytic and computational methods," New York: Marcel Dekker, Inc. 1978

52. D. P. Bertsekas, *Dynamic Programming and Optimal Control*. Belmont, MA: Athena Scientific, 1995.

53. A. P. De Madrid, S. Dormido, F. Morilla, "Reduction of the dimensionality of dynamic programming: a case study," *Proc. American Control Conference*, San Diego, California, USA, 1999. 2852-2856

54. R. Luus, "Optimal control by dynamic programming using systematic reduction in grid size," *Int. Journal of Control*, 1990, 51(5): 995-1013

55. N. Jalil, A. Kheir and M. Salman, "A Rule-Based Energy Management Strategy for a series Hybrid Vehicle", *Proc. of American Control conference*, pp. 689-693, June 1997.

56. B. Harpreetsingh, S. Anwar, Y. Chen, "A Rule-based Energy Management Strategy for Plug-in Hybrid Electric Vehicle (PHEV),"in *Proc. of the American Control Conference,* St. Louis. USA, June 10-12, 2009.

57. V. Johnson, K. Wipke, D. Rausen, "HEV Control Strategy for Real-Time Optimization of Fuel Economy and Emissions", *SAE Technical Paper* 2000-01-1543, 2000.

58. D. Karboeski, A. Rousseau, B. Pagerit, and P. Sharer "Plug-in Vehicle Control Strategy: From Global Optimization to Real-time Application," in *Proc. of the EVS22,* October, 2004.

59. N. Schouten, M. Salman, N. Kheir, "Fuzzy logic control for parallel hybrid vehicles," *IEEE Transactions on Control Systems Technology*, 2002, 10(3): 460-468

60. A. Rousseau, S. Pagerit, and, D. Gao, "Plug-in Hybrid Electric Vehicle Control Strategy Parameter Optimization," *Journal of Asian Electric Vehicles,* Volume 6, December 2008.

61. S. Hiramatsu, Y. Nakayama, Y. Kikuchi, "Development of the battery ECU for the Toyota hybrid system." *Proceedings of the 15th International Electric Vehicle Symposium*, Brussels, Belgium, 1998

62. K. Kelly, A. Rajagopalan, "Benchmarking of OEM hybrid electric vehicles at NREL," *Technical Report* NREL/TP-540-31086, National Renewable Energy Laboratory, USA, 2001

63. Y. Zhu, Y. Chen, G. Tian, H. Wu, Q. Chen, "A Four-step Method to Design an Energy Management Strategy for Hybrid Vehicles", *Proceeding of the 2004 American Control Conference*, Boston, Massachusetts June 30 - July 2, 2004

64. R. Zhang, Y. Chen, "Control of Hybrid Dynamical Systems for Electrical Vehicles", *Proceeding of the 2004 American Control Conference*, pp. 2884-2889 Vol. 4, 2001

65. A. Piccolo, L. Ippolito, V. Galdi, A. Vaccaro, "Optimization of Energy Flow Management in Hybrid Electric Vehicles via Genetic Algorithm," *2001 IEEE /ASME International Conference on Advanced Intelligent Mechatronics Proceedings*, Como, Italy, July 2001.

66. C. Desai, S. Williamson, "Optimal design of a parallel Hybrid Electric Vehicle using multi-objective genetic algorithms." in *Proc. of the IEEE Vehicle Power and Propulsion Congress,* 2009.

67. A. Wang, W. Yang, "Design of Energy Management Strategy in Hybrid Electric Vehicles by Evolutionary Fuzzy System, Part II: Tuning Fuzzy Controller by Genetic Algorithms," *Proceedings of the 6th World Congress on Intelligent Control and Automation*, June 21 - 23, 2006, Dalian, China.

68. M. Jain, C. Desai, N. Kharma, and S. S. Williamson, "Optimal powertrain component sizing of a fuel cell plug-in hybrid electric vehicle using multi-objective genetic algorithm," in *Proc. IEEE Annual Conf. of the Industrial Electronics Society*, Porto, Portugal, Nov. 2009, pp. 3741-3746.

69. B. Huang, Z. Wang, Y, Xu, "Multi-Objective Genetic Algorithm for Hybrid Electric Vehicle Parameter Optimization," *Proceedings of the 2006 IEEE/RSJ International Conference on Intelligent Robots and Systems*, October 9 - 15, 2006, Beijing, China

70. N. Srinivas and K. Deb. "Multiobjective Optimization Using Nondominated Sorting in Genetic Algorithms." *Evolutionary Computation*, 2(3):221 - 248, 1994

71. K. Deb, A. Pratap, S. Agarwal, and T. Meyarivan, "A Fast Elitist Multi-objective Genetic Algorithm: NSGA-II," *IEEE Transactions on Evolutionary Computation*, 6(2):182 - 197, April 2002

72. Y. Yu, Y. Gao, H. Peng, Q. Wang, "Parametric Design of Power-split HEV Drive Train,"in *Proc. of the IEEE Vehicle Power and Prop. Congress,* 2009.

73. K. L. Cheong, P. Y. Li and T. R. Chase, "Optimal Design of Power-Split Transmissions for Hydraulic Hybrid Passenger Vehicles," *Proc. American Control Conference*, San Francisco, CA, USA, 2011

74. H.A. Borhan, A. Vahidi, A.M. Philips, M.L. Kuang, I.V. Kolmanovsky, "Predictive Energy Management of a Power-split Hybrid Electric Vehicle," *Proc. American Control Conference*, 2009, ACC '09, page 3970 – 3976.

75. F. Litvin and A. Fuentes, "Gear Geometry and Applied Theory", Cambridge University Press, 2004.

VITA AUCTORIS

Name;   Yanhe Li

Born: Zhuolu, China, 1968

Education: 2002-2006 Bachelor of Applies Science

               Department of Mechanical engineering, University of Windsor

               1990-1193 Master of Science

               Department of automotive engineering, Wuhan Institute of Technology

               (Now; Wuhan University of Technology)

               1986-1990 Bachelor of Applies Science

               Department of automotive engineering, Wuhan Institute of Technology

               (Now; Wuhan University of Technology